# ABSTRACT

Title of dissertation:     TRANSPORT IN POLYGONAL
BILLIARD SYSTEMS

Matthew L. Reames, Doctor of Philosophy, 2009

Dissertation directed by:     Professor J. Robert Dorfman
Department of Physics

The aim of this work is to explore the connections between chaos and diffusion by examining the properties of particle motion in non-chaotic systems. To this end, particle transport and diffusion are studied for point particles moving in systems with fixed polygonal scatterers of four types: (i) a periodic lattice containing many-sided polygonal scatterers; (ii) a periodic lattice containing few-sided polygonal scatterers; (iii) a periodic lattice containing randomly oriented polygonal scatterers; and (iv) a periodic lattice containing polygonal scatterers with irrational angles. The motion of a point particle in each of these system is non-chaotic, with Lyapunov exponents strictly equal to zero.

For many-sided polygons, greater than 100 sides, we present the results of our study that shows that the systems appear to be diffusive with a transport coefficient nearly equal to that of a periodic Lorentz gas with circular scatterers at the same density. The partial van Hove function for the polygonal system has, numerically, a fractal dimension equal to that of the partial van Hove function for the periodic

Lorentz gas with circular scatterers. Further, we show that a non-zero average Lyapunov exponent for the system can be defined, numerically, in spite of the fact that the actual Lyapunov exponent is zero. It is also possible to verify a relationship, valid for chaotic systems, between the diffusion coefficient, the average Lyapunov exponent, and the fractal dimension of the partial van Hove function.

We also report results of a study of the transport properties and dynamical properties of a system with few-sided polygons, of less than 100 sides. These systems always appear to be super-diffusive, and non-chaotic, with a value of zero for the Lyapunov exponent. The partial van Hove function has the same fractal dimension as that for a periodic Lorentz gas with circular scatterers.

For randomly oriented scatterers and scatterers with irrational angles, we construct a simple channel model that allows us to isolate individual features of the polygonal Lorentz gases and study their effects on transport properties. The systems have a value of zero for their Lyapunov exponents, and, depending on the orientation of the scatterers, the systems can appear to be either diffusive or super-diffusive.

Although there does not seem to be a direct link between mathematical chaos and ordinary diffusion in these models, the non-chaotic systems show that if any such connection exists, it must be very subtle. Even a weak form of random walk motion may result in ordinary diffusion.

# TRANSPORT IN POLYGONAL BILLIARD SYSTEMS

by

Matthew L. Reames

Dissertation submitted to the Faculty of the Graduate School of the
University of Maryland, College Park in partial fulfillment
of the requirements for the degree of
Doctor of Philosophy
2009

Advisory Committee:
Professor J. Robert Dorfman, Chair/Advisor
Professor Thomas Cohen
Professor Theodore Einstein
Professor Christopher Jarynski
Professor Rajarshi Roy

# Dedication

To my uncle Bill, for sparking my interest in physics and your constant encouragement.

# Acknowledgments

I owe my gratitude to all the people who have made this thesis possible and because of whom my graduate experience has been one that I will cherish forever.

First and foremost I'd like to thank my advisor, Professor Bob Dorfman for giving me an invaluable opportunity to work on challenging and extremely interesting project. He has always made himself available for help and advice and there has never been an occasion when I've knocked on his door and he hasn't given me time. It has been a pleasure to work with and learn from such an extraordinary individual.

I would also like to thank Sudhir Jain, whose discussions in Fractional Kinetic Equation and Frational Calculus were extremely thought provoking and helpful.

My colleagues at the University of Maryland have enriched my graduate life in many ways and deserve a special mention. Chad Galley and Willie Merrell for there friendship an many late night homework session. Arseni Goussev for his friendship, encouragement and help. Min-Young Kim and Hailu Gebremariam for their constant friendship and advice.

I would also like to acknowledge support from my co-workers at the Patent and Trademark Office. Bill Baumeister, Jerome Jackson, Hrayr Sayadian, Johanass Mondt, Jami Valentine, Jenny Wagner, Matthew Such and Earl Taylor for their encouragement.

I owe my deepest thanks to my family - my mother and father who have always stood by me and guided me through my career, and have pulled me through against

impossible odds at times. Words cannot express the gratitude I owe them.

My housemates and their family for their constant prayers and for being my second family.

Pastor Cho's family for their constant prayers and encouragement.

To everyone at Awana for their constant prayers and being my escape from real life on Wednesday nights, making it the best night of the week.

The University of Maryland, the Physics department and IPST for making my stay enjoyable and have a wonderful faculty and staff.

To the University of Vienna and the Technion in Haifa for their wonderful hospitality and to the NSF for their support.

It is impossible to remember all, and I apologize to those I've inadvertently left out.

Lastly, Thanks to God, for in Him all things are possible!

# Table of Contents

# List of Tables

# List of Figures

# Chapter 1

# Introduction

## 1.1  Macroscopic Diffusion

One of the fundamental problems of non-equilibrium statistical mechanics is to obtain expressions the transport properties, such as diffusion coefficients, viscosities, and so on, for a fluid in terms of the microscopic properties of its constituent particles [32, 81, 83, 84]. This problem has been the subject of study by physicists for almost two hundred years. For very dilute gases, that is, gases composed of particles whose mean free path is long compared to the size of a particle but small compared to some characteristic size of the macroscopic system, this problem has been solved in the context of the kinetic theory of gases and the Boltzmann transport equation. For dense gases and liquids this problem is still the subject of many studies. One of the main issues of interest to physicists is the question of how a time-reversible microscopic description of a fluid system, via the laws of mechanics, could give rise to a set of irreversible equations such as the Navier-Stokes equations of fluid dynamics. Most derivations of the equations of fluid dynamics use a stochastic assumption at some crucial point [81, 32]. This assumption typically takes the form of an assumption about the random-walk character of some quantity characterizing the transport. Examples include the assumption that a diffusing particle undergoes a random walk in the fluid caused by its collisions with other particles

in the fluid. These random walk assumptions lead to the *linear laws* of irreversible thermodynamics, which assert a direct proportionality between the fluxes of matter, momentum, or energy in a fluid and the gradients of mass density, momentum density, and energy density for the fluid. These linear laws are well known as Newton's law of friction, Fourier's law of heat conduction, Fick's law of diffusion, and so on. A somewhat more subtle stochastic assumption is embodied in the hypothesis of molecular chaos used in the derivation of the Boltzmann transport equation. Of course, the linear laws are not a re-writing of the laws of mechanics, either classical or quantum, since they are not time reversible [32].

## 1.2   Chaos

Over the past few decades it has become clear that dynamical systems theory might be able to provide a better resolution of the problem of irreversibility, at least for classical systems, by focusing on the chaotic nature of typical microscopic processes in atomic and molecular systems [4, 13, 19, 20, 26, 34, 38, 40, 42, 44, 63, 65, 77, 88, 91, 94, 108, 109] . Chaotic systems have the property that a small change in the initial conditions of the particles will lead to large changes in the state of the system some time later, so that infinite precision is needed to predict the trajectory of a chaotic, classical system with certainty [26, 32, 33, 42, 43, 45, 46, 47]. Chaotic systems can appear to behave stochastically and irreversibly even though they are deterministic and time reversible. The source of the irreversibility in such cases is to be found in the sensitivity to initial conditions leading to exponential

2

separations of, initially infinitesimally close, phase space trajectories [31, 48, 76, 93]. In such cases one can predict the behavior of an ensemble average, which typically shows an approach to thermodynamic equilibrium, even for an isolated system. In such cases the time reversed motion also shows an approach to equilibrium, due to the reversibility of the equations describing each member of the ensemble [33, 34, 43, 44, 45, 82]. In such cases one needs to argue that the ensemble average correctly describes the behavior of a typical system included in the average. This can be hard to demonstrate for physically interesting systems, but this assumption underlies much of statistical mechanics [40].

## 1.3  Moments of the Displacement of a Moving Particle

In order to understand the phenomenon of irreversibility and its application to non-equilibrium statistical mechanics, workers have turned to simple, low dimensional systems which exhibit transport and yet are analytically tractable. In this introduction we will give a brief overview of such systems and a more detailed discussion will follow in the following chapters. Among such systems one can include Lorentz gases of various types, both chaotic and non-chaotic [1, 8, 16, 28, 33, 35, 36, 37, 43, 45, 46, 47, 64, 65, 72, 79, 92, 98]. A Lorentz gas is a system of fixed scatterers and a collection of moving point particles that interact with the fixed scatterers but not with each other. Particularly useful models are those where the dynamics takes place in a plane. If the scatterers are hard disks/infinite sided polygons and the moving point particles make instantaneous, specular, elastic collisions

with them, the dynamics is known to be chaotic [43, 45, 65, 79]. The Ehrenfest wind-tree model is an example of a non-chaotic Lorentz gas [30, 38] . Here the scatterers, "trees", are oriented squares with diagonals along the $x$ and $y$ directions. The moving particles, "wind", have fixed speed and velocities along the $\pm x$ and $\pm y$ directions. This situation is preserved under the collisions of the moving particles with the scatterers, as illustrated in figures (1.1 and 1.2).
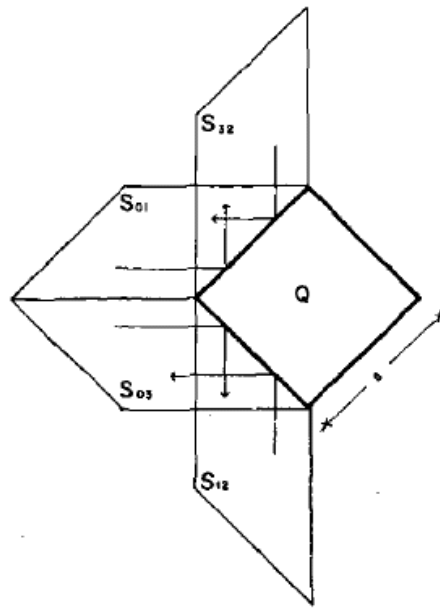


Figure 1.1: *An Ehrenfest "wind" scatterer. The scatterers' diagonals are oriented along the x and y axes. The particles move in the $\pm x$ or the $\pm y$ directions and change from one direction to the other upon collision with a scatterer [97].*

When the collection moving of point particles are considered as an ensemble one finds, for certain arrangements of scatterers, that the average motion of the particles is diffusive [30, 38, 65, 81]. In other words, for long times, the mean

4
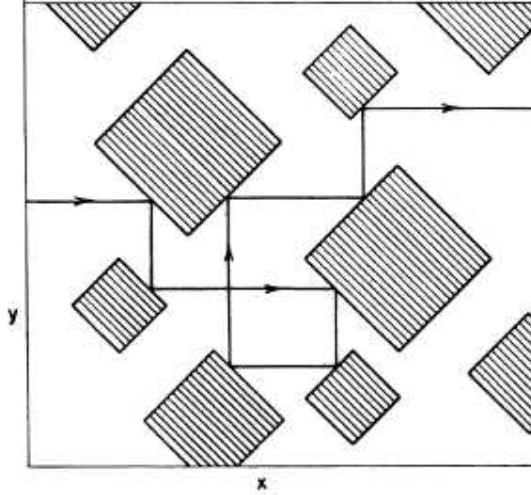
Figure 1.2: *An example of the Ehrenfest wind-tree gas. The particles are constrained to move either in the $\pm x$ or the $\pm y$ directions and switch directions when colliding with a scatterer [97].*

square displacement $< (x(t) - x(0))^2 >$ goes as:

$$< (x(t) - x(0))^2 >= 2Dt. \tag{1.1}$$

Here $x(t)$ denotes the $x$ coordinate of the moving particle at time $t$, the angular brackets denote an average over the ensemble of moving particles, and $D$ is the diffusion coefficient. We will have many occasions in this thesis to consider a more general situation where, for long times, the mean square displacement takes the form

$$< (x(t) - x(0))^2 >= At^\mu. \tag{1.2}$$

Here $\mu$ is called a transport exponent, which for ordinary diffusion is equal to one. In any case, in the absence of any external fields, the transport exponent, $\mu$, must be equal to or less than 2, since this value corresponds to free particle motion. The

phenomenon called *super-diffusion* corresponds to a transport exponent greater than 1 and less than or equal to 2, and *sub-diffusion* corresponds to a transport exponent with value between 0 and 1 [63, 88, 99, 103]. Such, anomolous diffusion has been extensively studied in the field Nonextensive statistics, Tsallis statistics [94].

The chaotic and transport properties of a Lorentz gas with circular scatterers placed at the vertices of a triangular lattice, have been studied in some detail. Sinai and Bunimovich have shown that this system is always chaotic and is also diffusive provided that the size of the scatterers is such that: (a) there are no closed regions; (b) that the particles can travel through the lattice; and (c) there are no infinite corridors where the particles can move without collisions for arbitrarily long distances [65]. Due to the spatial symmetries of the triangular Lorentz gas system the odd moments of the displacement are all zero [32, 12, 81]. However, the even moments are non-zero, the first of which is the mean square displacement.

### 1.3.1 The Van Hove Intermediate Scattering Function

To generate all of the moments (odd and even) of the motion of a moving particle we can use a generating function called the Van Hove intermediate scattering function. This function is defined by:

$$F(\mathbf{k}, \mathbf{t}) = \langle e^{i\mathbf{k} \cdot (\mathbf{r(t)} - \mathbf{r(0)})} \rangle, \tag{1.3}$$

where the angular brackets denote an equilibrium ensemble average. The importance of this function can be seen by expressing the probability, $P(\mathbf{r}, \mathbf{t})$ of finding a tagged

particle at point $\mathbf{r}$ at time $t$ in a fluid which is otherwise in equilibrium, in the form:

$$P(\mathbf{r}, t) = \frac{1}{V} \sum_{\mathbf{k}} e^{-i\mathbf{k}\cdot\mathbf{r}} W_{\mathbf{k}} F(\mathbf{k}, t), \qquad (1.4)$$

where $V$ is the volume of the container, the summation is over all the allowed values of the wave number in the Fourier expansion of functions defined inside the container with specified boundary conditions, $W_{\mathbf{k}}$ is a Fourier component of the initial probability distribution of the tagged particle,

$$W_{\mathbf{k}} = \int_{V} d\mathbf{r_1} e^{i\mathbf{k}\cdot\mathbf{r_1}} P(\mathbf{r_1}, t = 0), \qquad (1.5)$$

and $F(\mathbf{k}, \mathbf{t})$ is the Van Hove function, also known as the Van Hove intermediate scattering function, given above

The Van Hove intermediate scattering function is a "smooth" function of $\mathbf{k}$ due to the equilibrium average [12, 33, 43, 45]. However, for a chaotic system the chaotic motion causes a stretching and folding of functions defined in phase space. This stretching and folding will cause functions in phase space to evolve into very complex forms which typically are smooth is some directions in phase space and singular in other directions. These singular structures may be non-differentiable functions similar to Weierstrass functions, or may have zero derivatives almost everywhere but may have variations on sets of measure zero [43, 45, 99]. This and similar types of singular behavior characterize fractal functions.

## 1.3.2 The Incomplete Van Hove Function

For a chaotic Lorentz gas the microscopic displacement of a moving particle is a wildly varying function of the particles' initial position and velocity. This

7

wild variation is suppressed in the Van Hove function when the equilibrium average is carried out. However, it is useful to define a function that captures this wild behavior. Gaspard and Takagi defined such a function they called the incomplete Van Hove function in which partial averages are taken over some fraction of the available phase space [44, 45]. The incomplete Van Hove function for a chaotic Lorentz gas system turns out to be wildly varying and fractal, with a non-integer Hausdorff dimension. This dimension is one measure of the wildness of the variations of a fractal curve.

Gilbert, Gaspard, and Dorfman have shown that the incomplete Van Hove function is a fractal for a simple chaotic and diffusive model Lorentz gas-like system, called the multi-baker model [50, 51, 47]. Moreover they were able to derive a formula that relates the Hausdorff dimension of this fractal to the positive Lyapunov exponent and to the diffusion coefficient [52, 45]. The Lyapunov exponent is a characteristic property of chaotic systems which determines the rate of exponential separation of two infinitesimally close trajectories in phase space.

The Lyapunov exponent is defined by:

$$\lambda = \lim_{(\delta x(0) \to 0)} \lim_{t \to \infty} \frac{1}{t} \ln(\frac{\delta x(t)}{\delta x(0)}). \tag{1.6}$$

Here $\delta x(0)$ is the initial separation of two trajectories in phase space and $\delta x(t)$ is the separation of the two trajectories at time $t$ later. The $t \to \infty$ represents the fact that the trajectories have to be watched for long times in order to actually obtain a Lyapunov exponent. A positive Lyapunov exponent is a characteristic feature of most chaotic systems. The Lyapunov exponent is zero whenever the rate

8

of separation of nearby trajectories is algebraic [31, 48, 76, 93].

In the mid 1990's Claus, Gaspard, Gilbert and Dorfman expanded the validity of the dimension formula obtained for the multi-baker model by Gilbert *et al.* [45]. They derived the same relation for the incomplete Van Hove function for a diffusive, chaotic, two dimensional Lorentz gas. As mentioned above, they showed that the diffusion coefficient $D$ any chaotic diffusive system can be related to the Lyapunov exponent and fractal dimension of the partial Van Hove function, considered as a function of the wave number $k$ [43, 49, 50, 51]. This relation is:

$$D_H = 1 + \frac{D}{\lambda}k^2 + O(k^4).$$
(1.7)

A careful discussion of the incomplete Van Hove function and a derivation of the dimension formula will be presented in the next chapter. Suffice it to say, the relation gives a beautiful correspondence between the microscopic, chaotic properties and the macroscopic, diffusive properties of the system. For these chaotic systems one can derive information about transport from observations of the Lyapunov exponent and the Hausdorff dimension of the partial Van Hove function [50, 51, 45, 13].

However, the formula also raises a number of interesting questions. A major question arises when one considers non-chaotic systems that are at the same time, diffusive. What does the partial Van Hove function look like for a non-chaotic, diffusive system? Is the curve fractal, and if so, does there exist an analogous dimension formula consistent with the zero Lyapunov exponents for non-chaotic systems? One such system is the Ehrenfest wind tree model mentioned earlier. This is an old model defined by P. and T. Ehrenfest to illustrate and explain some

important features of the Boltzmann transport equation [1, 19, 30, 38, 55, 60, 96]. Its chaotic properties, or in fact, the lack of them, were studied within the past decade by Van Beijeren, Dettmann and Cohen [29], and later in more detail by Dettmann and Cohen [30]. They considered a number of different versions of the model, differing by the rules for placing the scatterers in the plane. We will briefly describe them now with a more detailed discussion to be presented in Chapter 3. One model consists of scatterers placed in space according to some specified rules with all diagonals oriented in the $x$ or $y$-directions. Dettmann and Cohen found that if the scatterers were placed on a periodic lattice, the motion of the particles became super-diffusive. However if the scatterers were placed randomly in space, that is in accordance with the original formulation of the Ehrenfest model, the system became diffusive.

However, Dettmann and Cohen also considered versions of the model where the diagonals of the scatterers can be rotated [30]. They found that if *small groups* of scatterers were rotated randomly as well as randomly positioned in space, forming a unit cell, and the unit cell is repeated periodically, then for certain periodicities the motion of the moving particle is diffusive. For example they found that if they used four scatterers per cell and randomized the scatterers within each cell and periodically repeated this cell, the motion is diffusive. It is important to mention here some differences between a Lorentz model with circular scatterers and the wind tree models mentioned above [30, 38, 65]. The Lorentz gas with circular scatterers is chaotic. A Lorentz gas of circular scatterers can be diffusive with any configuration of scatterers, periodic or not, provided that there are no regions that

confine the particles and no infinitely long corridors through which the particles can travel without collisions. The same cannot be said of wind-tree models with square scatterers. Since the sides of the trees are straight lines, the motion of the particles is not chaotic. Nearby trajectories separate algebraically rather than exponentially with time. It then appears that there are many possible behaviors, from sub through super-diffusion. However, *chaos is neither sufficient nor a neccessary condition for diffusion.* For example there exists a circular Lorentz gas which is not diffusive, the infinite horizon model, which will discuss in chapter 2. Also as previously noticed by Dettmann and Cohen, and as we will see again in this thesis, there are periodic arrangements of non-chaotic scatterers, trees, that exhibit normal diffusion. Here we shall endeavor to find some common features of the diffusive but non-chaotic Lorentz gases [30].

Another class of non-chaotic models that exhibit diffusion are wind tree models in which the squares are replaced by polygons. One may consider regular polygons or irregular polygons with irrational angles [66]. An interesting feature of these systems is that when all the angles are irrational the system is ergodic [89]. This is the analog for Lorentz gases of the well known result that the motion of a particle in a rectangle with non-commensurate sides is ergodic [56, 61, 87, 100, 96].

## 1.4   The Lorentz Channel

One system considered recently by Alonso and Ruiz is called a Lorentz channel [1, 2, 3, 47, 86]. A Lorentz channel is essentially a tube in two dimensions

with scatterers placed along the tube, the space available to the moving particles is unbounded in one direction and confined in another, as illustrated in figure (1.3).



Figure 1.3: *An example of a Lorentz channel. Transport occurs only along the horizontal, or x-direction[1].*

Alonso *et al* as well as a number of other authors (Sanders, Prosen Casati, etc.) [2, 3, 5, 6, 7, 8, 15, 16, 17, 18, 43, 57, 59, 86] considered motion of a particle in a Lorentz channel with triangular scatterers figure (1.4 and 1.5). The scatterers placed at the upper side of the channel were taken to be identical isosceles triangles, each with two angles $\phi_1$, that are irrational fractions of $\pi$. The scatterers placed on the lower side of the channel consisted of periodic repetitions of two isosceles triangles with the two equal angles $\phi_2$ equal to a rational fraction of $\pi$. Depending on $\phi_2$ the transport properties range from sub- diffusive to diffusive to super-diffusive. Both Alonso and Sanders provide some insights into these systems by showing that transport properties are determined by the presence or absence of *walking orbits* that exist whenever there are regions on both the top and bottom of the channel that are free of scatterers, and parallel to each other. If such regions exist the motion is super-diffusive. When the parallel sides are removed by an appropriate placement of the scatterers, one decreases the number of and magnitude of the contributions from walking orbits and the system becomes either diffusive or sub-diffusive. Furthermore, the fact that one row of triangles has angles that are

12
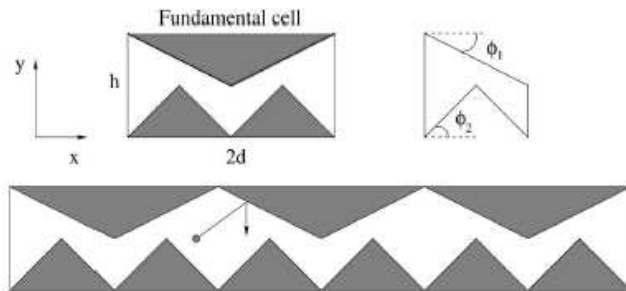
Figure 1.4: *The channel system studied by Alonso and Sanders. The system is a generalized Lorentz channel with triangular scatterers in place of circular scatterers.*
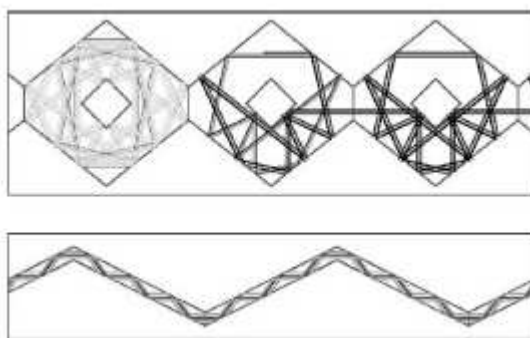


Figure 1.5: *Examples of the models studied by Alonso et al. and Sanders et al. showing the "walking orbits" in the system, one reason for super-diffusion in such systems [86].*

irrational fractions of $\pi$ appears to be responsible for the diffusive behavior of such systems [2, 3, 86]. These systems will be discussed in greater detail in chapter 5.

## 1.5 Polygons

So far most of the research on Lorentz gases in two dimensions has used either circular scatterers, which may be thought of as infinite sided, regular polygons, or

3 and 4 sided polygons, triangles, squares and rhombi [66]. Although the motion of particles in Lorentz gases is fairly complex, the dynamics is much simpler than hard disks. Further, as one considers polygonal scatterers with increasing numbers of sides, the dynamics becomes more and more complex. However, arbitrary $n$-gons offer a way to connect the dynamics of a Lorentz gas with circular scatterers to that with polygonal scatterers [23, 96]. The literature on arbitrary $n$-gons is noticeably sparse. Here we give a brief overview of the recent literature on such Lorentz gases.

In 1993, J. Vega, J. Ford and T. Uzer considered the motion of particles in a system of scatterers that are $n$-gons, with $n$ a large number so as to approximate circular scatterers [96]. As we discuss in the next chapter, Vega et al. showed that the trajectories of particles moving in such a system of $n$-gon scatterers can be characterized by an *effective Lyapunov exponent.* Therefore in some approximate sense such systems appear to be chaotic. In a similar spirit, T. Cheon and T. Cohen studied the quantum properties of a particle in a Richens-Berry billiard, which consists of particles outside scatterers that are basically squares but with small polygonal regions removed from one of the corners of the squares [23]. By removing more and more small polygons, one can make the corner of the scatterer approximate an arc of a circle, figure (1.6).

If this system were to be classically chaotic, the energy-level distribution would follow one of the random matrix ensembles, and not be a Poisson distribution typical of the energy-level distribution for systems that classically are simple and non-chaotic. Cheon and Cohen found that, for corners that have sufficiently large numbers of edges, the energy-level distributions were close to that of a Gaussian Or-
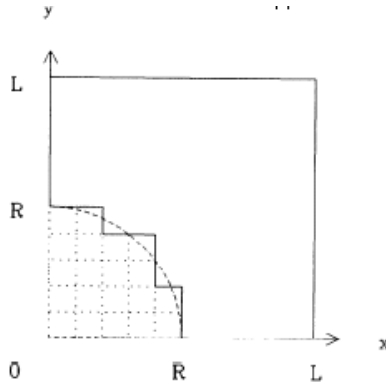
Figure 1.6: *The billiard model studied by Cheon and Cohen. The curved scatterer is successively approximated by an n-gon [23].*

thogonal Ensemble, time reveral invariant system with $\beta = 1$, generally indicative of a classical counterpart which is chaotic, instead of that of Poisson distribution which one would expect for a classical non-chaotic system. In fact as they added more and more sides by removing more and more pieces of the square, the distribution approximated more and more closely that of a Gaussian Orthogonal ensemble. Their results can be understood by considering the classical motion of a particle in a system of such scatterers. If one takes two trajectories that initially are close to each other, but not infinitesimally close, they can separate exponentially for an interval of time, even though the system is not actually chaotic. This occurs whenever the two trajectories encounter different sides of the same polygon. The angular separation of the two trajectories then jumps discontinuously, similar to what happens when the scatterers are circles. Since quantum systems are inherently coarse-grained at the level of the de Broglie wavelength, the energy level distribution should look something like the distribution for one of the Gaussian ensembles. The same mech-

15

anism is also responsible for the existence of an effective Lyapunov exponent for the systems studied by Vega, Uzer, and Ford.

A careful treatment of the transport properties for these systems has not been made. Of particular interest here is the study not only of the diffusive properties but also a study the partial Van Hove functions and a determination of their Hausdorff dimensions.

## 1.6   Outline of This Thesis

In this thesis we will compare the transport properties of chaotic Lorentz gases with those for purely non-chaotic, pseudo-chaotic systems. Here the term pseudo-chaotic system will be used for classical, non chaotic systems with complex dynamics, to be defined further on in this thesis. We will consider possible extensions of the dimension formula for the partial Van Hove functions to non-chaotic systems. An outline of this thesis is as follows:

In Chapter 2 we present a reasonably general discussion of the macroscopic and microscopic descriptions of particle diffusion in a Lorentz gas. Central to the macroscopic theory is the linear law of diffusion, known as Fick's law. This law states that the local flux of diffusing particles is directly proportional to the negative of the local density gradient. Fick's law, coupled with the macroscopic equation for the conservation of particles in the system leads directly to the diffusion equation. We then turn to a more microscopic picture, discuss the description of diffusion for dilute gases based upon the Boltzmann equation, and then consider a more

fundamental description, valid for all densities, that directly leads to the Van Hove function discussed above. At this point we define the *incomplete Van Hove function* and discuss its fractal properties for chaotic Lorentz gases as described by Gilbert *et al.*

In Chapter 3 we turn our attention to a class of periodic, non-chaotic Lorentz gases, where circular scatterers are replaced by regular, many-sided polygons with 100 or more sides. Our aim is to see if we can discover any indications that the system is not chaotic. We should point out that these systems, while not chaotic, are *pseudo-chaotic.* That is a system that has random dynamics with a zero Lyapunov exponent. For example, in the wind-tree model the dynamics provide a "random walk" behavior. However, the system has a zero Lyapunov exponent [102, 103, 104]. Thus, we would consider the system pseudo-chaotic. We will consider the dynamical behavior of these systems, as well as the transport properties. We will show that as one increases the number of sides of the system the transport properties of the system approaches that with a Lorentz gas with circular scatterers. Lastly, we will consider a coarse-grained dynamics of the system by adjusting the initial distances between nearby trajectories to be on the order of the length of a side of an $n$-gon. In this coarse grained regime we will look at the transport properties, define an effective Lyapunov exponent and calculate a partial Van Hove function. We will show that for many-sided $n$-gon scatterers, for sufficiently large $n$, the dimension formula is still valid if one uses the effective Lyapunov exponent.

In Chapter 4 we consider periodic arrangements of scatterers with few-sides. We will consider effective Lyapunov exponents and the transport properties of these

systems. We show that the transport properties of these systems are functionally related to the number of sides of the scatterers, and approach those for a diffusive system as the number of sides goes to infinity. However the transport properties approach those for ballistic motion as the number of sides goes to zero. In the latter case, these transport properties are measures in terms in the exponent $\mu$, as defined in Eq. (1.2) Further we will discuss a set of conjectures made by Zaslavsky that relate the various moments of the particles displacement to each other, for few-sided scatterers. We find that Zaslavsky's conjecture appears to be correct provided the number of sides of the scatterers is not too large.

In Chapter 5 we consider disordered placement of polygonal scatterers, along the lines of some of the work by Dettmann and Cohen. We attempt to estimate the minimum amount of disorder required for diffusive transport to occur. In order to shed some light on this question we construct a Lorentz channel model with the property that disorder can be introduced in a very simple way, and easily controlled. Finally, we consider another type of disorder produced by using periodic arrangements of polygonal scatterers with two irrational angles.

The main results of the research described in this thesis are:

1. We calculate the transport exponents for polygons ranging in size from 4 sides to over 100 sides.

2. We show that for many-sided polygons it is possible to coarse grain the dynamics, giving the system the appearance of diffusive system with a non-zero Lyapunov exponent.

3. In this coarse grained system we show that the dimension formula derived by Gilbert *et al.* for the Lorentz gas is valid.

4. We show that for few-sided polygons the first five even moments are related by the expression: $< x^{2n} >=< x^2 >^n$.

5. We provide a simple channel model that allows us to isolate individual features of the polygonal Lorentz gases and study their effects on transport properties.

Chapter 2

Diffusion and Chaotic Systems

## 2.1  Macroscopic Diffusion

This thesis is devoted to a study of diffusion of non-interacting particles in a two dimensional periodic array of fixed scatterers. Although the particles do not interact with each other, they are taken to make specular, elastic collisions with the fixed scatterers. This model is a simple version of a model first introduced by Lorentz in order to describe the conduction of electrons in metals  [65].

If there are no sources or sinks of particles in the system, then on a *macroscopic* scale, the density of moving particles, or the probability density for a single particle at a point $\mathbf{r}$ at time $t$ is governed by a *conservation law*, expressing the conservation of moving particles in the system:

$$\frac{\partial n(\mathbf{r}, t)}{\partial t} + \nabla \cdot \mathbf{J}(\mathbf{r}, t) = 0, \tag{2.1}$$

where $\mathbf{J}(\mathbf{r}, t)$ is the current of moving particles at $\mathbf{r}$ at time $t$  [81, 32]. This conservation law becomes useful when there is a *constitutive relation* connecting the current to the particle density. If there are no external forces, and the system is placed in a finite container, the density should approach a spatially uniform equilibrium state, described by a zero particle current. Further we assume that we are close enough to equilibrium that the density varies slowly over distances large compared to some

microscopic length of the system. The fact that the current is zero if the density of tagged particles is totally uniform suggests that the current and the density gradient should be related in a simple manner, since both the current and the gradient of the density are vectors. The simplest relation would be a direct proportionality of the form:

$$\mathbf{J}(\mathbf{r}, t) = -D\nabla n(\mathbf{r}, t). \tag{2.2}$$

The negative sign indicates that particles diffuse from regions of high density to low density. This is Fick's law. For the Lorentz gas, one can derive Fick's Law if the scatterers are arranged in such a way that there are no infinite straight paths for the moving particles. Here $D$ is taken to be a constant, as yet undetermined although possibly a slowly varying function of position, called the *diffusion coefficient* [81]. When these two relations are combined, one obtains an equation for the density alone called *the diffusion equation*, given by

$$\frac{\partial n(\mathbf{r}, t)}{\partial t} = \nabla \cdot [D\nabla n(\mathbf{r}, t)] = D\nabla^2 n(\mathbf{r}, t). \tag{2.3}$$

In the second equality on the right hand side of Eq. (2.3) we have made the usual, but not necessarily correct, assumption that $D$ is a constant, independent of position.

An important result for the work in this thesis is the Einstein formula, providing the connection between the mean square displacement of the moving particles and the diffusion coefficient. This follows immediately from the calculation of the Green's function for the diffusion equation [81, 32]. If we consider the mean square displacement given by $\langle \Delta \mathbf{r}^2 \rangle$, where $\Delta \mathbf{r} = \mathbf{r(t)} - \mathbf{r(0)}$, we obtain the following:

$$\langle \Delta \mathbf{r}^2 \rangle = 2Dtd \tag{2.4}$$

21

In this equation, the average is taken using the Green's function for the diffusion equation, considered as an equation for the probability density for finding at particle at point $\mathbf{r}$ at time $t$. The Einstein relation is extremely important when discussing diffusion since it relates the mean square displacement, a quantity easily calculated via simulations, to the diffusion coefficient.

## 2.2   Fick's Law

The purpose of this section is to provide a microscopic derivation of Fick's Law for some simple systems [81, 32]. As described above, Fick's law leads directly to the diffusion equation. We consider tagged particle diffusion in a Lorentz gas, although much of this discussion will be applicable to more general fluid systems. To start, consider one or more tagged particles moving among the scatterers. We assume the number of moving particles is constant in time. The microscopic expression for the number density of the tagged particle system is $n(\mathbf{r}, \mathbf{t})$, at point $\mathbf{r}$ at time $t$ is given by the following:

$$n(\mathbf{r}, t) = \sum_i \delta(\mathbf{r} - \mathbf{r}_i(t)), \qquad (2.5)$$

where $\mathbf{r}(t)$ is position of the particle at time $t$. and the index $i$ in the summation refers to one of the tagged particles, and all of them are included in the sum. It is understood that motion of the tagged particles is governed by classical mechanics. Since the number of tagged particles is conserved in the fluid, we can write a conservation equation which states that the local change in the number density in a small region of the fluid is caused only by a flow of particles into or out of the region as

described by a current. By differentiating Eq. (2.5) with respect to time, we obtain
the microscopic conservation law [81, 32]:

$$\frac{\partial n(\mathbf{r}, t)}{\partial t} + \nabla \cdot \mathbf{j}(\mathbf{r}, t) = 0,$$ (2.6)

where

$$\mathbf{j}(\mathbf{r}, t) = \sum_i \mathbf{v}_i(t)\delta(\mathbf{r} - \mathbf{r}_i(t)).$$ (2.7)

Here we have denoted the velocity of the tagged particles by $\mathbf{v}_i(t) = \dot{\mathbf{r}}_i(t)$. This
is as far as we can go without some further ingredients. In order to move from a
microscopic description to a macroscopic description of diffusion we will need to find
the average behavior of an ensemble of identical systems, and thus average these
expressions using an appropriate ensemble. Further, we need to find a useful way to
characterize the dynamical behavior of these systems and then to see if Fick's Law
is a natural consequence of the dynamics and the chosen ensemble.

## 2.2.1   The Lorentz-Boltzmann Equation

Our first approach to the derivation of Fick's Law is a traditional one that uses
the Lorentz-Boltzmann equation. The Lorentz-Boltzmann equation is a partial dif-
ferential integral equation for the moving-particle probability distribution function
$f(\mathbf{r}, \mathbf{v}, t)$ for the moving particles, such that $f d\mathbf{r} d\mathbf{v}$ is the probability of finding a
particle at point $\mathbf{r}$ with velocity $\mathbf{v}$ at time $t$  [22, 32, 81]. We consider the scatterers
to be circles of radius $a$, placed at random in a plane at low density - the mean
separation of scatterers is large compared to the radius $a$. The Lorentz- Boltzmann
equation describes the time rate of change of the distribution $f$ in this case, and is

23

given by

$$\frac{\partial f(\mathbf{r}, \mathbf{v}, t)}{\partial t} + \mathbf{v} \cdot \nabla f(\mathbf{r}, \mathbf{v}, t) =$$

$$= a \int_{\mathbf{v}\cdot\hat{\sigma}>0} d\hat{\sigma} |\hat{\sigma} \cdot \mathbf{v}| \left[ f(\mathbf{r}, \mathbf{v}', t) - f(\mathbf{r}, \mathbf{v}, t) \right]. \qquad (2.8)$$

Here the quantity $\mathbf{v}'$ is given by

$$\mathbf{v}' = \mathbf{v} - 2(\hat{\sigma} \cdot \mathbf{v})\hat{\sigma}. \qquad (2.9)$$

The time rate of change of the distribution function $f$ is given as a sum of three terms. The second term on the left hand side of Eq. (2.8) is simply the rate at which particles flow out of a small region $\delta\mathbf{r}\delta\mathbf{v}$ about the point $\mathbf{r}, \mathbf{v}$ due to the free motion of the particles. The first term on the right hand side represents the rate at which particles acquire the velocity $\mathbf{v}$ due to collisions with scatterers. The velocity $\mathbf{v}'$ is the velocity a moving particle must have when colliding with a scatterer with point of impact located by the unit vector $\hat{\sigma}$, where $\hat{\sigma}$ is a unit vector directed from the center of a scatterer to the point of impact of the collision. Finally, the second term on the right hand side of Eq. (2.8) represents the rate at which particles with velocity $\mathbf{v}$ are lost due to their collisions with the scatterers. Using the Lorentz-Boltzmann equation one can derive the diffusion equation for the moving particles together with an expression for the diffusion coefficient. The precise calculations can be found in the literature [81, 32]. Here we merely quote the results:

$$D = \frac{3v^2}{8\nu}, \qquad (2.10)$$

24

## 2.3 The Van Hove Function

where $\nu$ is the viscosity of fluid. An important generalization of the Einstein formula, applying to any system with diffusion of a tagged particle is provided by the Van Hove formalism [12]. Using standard methods of statistical mechanics, one can prove that the probability, $P(\mathbf{r}, \mathbf{t})$ of finding a tagged particle at point $\mathbf{r}$ at time $t$ in a fluid which is otherwise in equilibrium, is given by

$$P(\mathbf{r}, t) = \frac{1}{V} \sum_{\mathbf{k}} e^{-i\mathbf{k}\cdot\mathbf{r}} W_{\mathbf{k}} F(\mathbf{k}, t), \tag{2.11}$$

where $V$ is the volume of the container, the summation is over all the allowed values of the wave number in the Fourier expansion of functions defined inside the container with specified boundary conditions, $W_{\mathbf{k}}$ is a Fourier component of the initial probability distribution of the tagged particle [12],

$$W_{\mathbf{k}} = \int_{V} d\mathbf{r_1} e^{i\mathbf{k}\cdot\mathbf{r_1}} P(\mathbf{r_1}, t = 0), \tag{2.12}$$

and $F(\mathbf{k}, \mathbf{t})$ is the Van Hove function, also known as the Van Hove intermediate scattering function, given by

$$F(\mathbf{k}, t) = \langle e^{i\mathbf{k}\cdot(\mathbf{r}(t) - \mathbf{r}(0))} \rangle. \tag{2.13}$$

If we now compare expression Eq. (2.11) with the corresponding expression obtained by solving the macroscopic diffusion equation, we see that for normal diffusion the Van Hove function should have the form, for large times, and for small enough wave numbers,

$$F(\mathbf{k}, t) = e^{-Dk^2 t}. \tag{2.14}$$

Therefore we define a quantity $s_\mathbf{k}(t)$, a hydrodynamic frequency, which measures the decay rate of the Van Hove function by

$$s_\mathbf{k}(t) = \frac{1}{t} \ln < e^{i\mathbf{k}\cdot(\mathbf{r}(t)-\mathbf{r}(0))} > . \tag{2.15}$$

The hydrodynamic frequency can be related to the moments of the displacement of the tagged particle if we expand the exponential [12]. One has the following:

$$s_\mathbf{k}(t) = \frac{1}{t} \ln\langle 1 + i\mathbf{k}\cdot(\mathbf{r}(t)-\mathbf{r}(0)) - \frac{1}{2}(\mathbf{k}\cdot(\mathbf{r}(t)-\mathbf{r}(0)))^2/2 + O(k^3)\rangle. \tag{2.16}$$

One can take the average term by term so as to obtain

$$s_{\mathbf{k}(t)} = \frac{1}{t}(\ln\langle 1\rangle + i\langle\mathbf{k}\cdot(\mathbf{r}(t)-\mathbf{r}(0))\rangle - \frac{1}{2}\langle(\mathbf{k}\cdot(\mathbf{r}(t)-\mathbf{r}(0)))^2\rangle + O(k^3)). \tag{2.17}$$

We can further simplify the equation by considering a system that is spatially isotropic. In this case the coefficients of the odd powers of $k$ vanish, and the coefficient of the term of quadratic order in $k$ is the mean square displacement. To this order in wave number, the Van Hove function takes the form given by Eq. (2.14), where the diffusion coefficient is related to the mean-square displacement via the Einstein formula, Eq. (2.4). Now, by keeping terms of higher order in the wave number, beyond quadratic, and using the relation give in equation Eq. (2.4) we obtain an expression for the Van Hove function where the hydrodynamic frequency is given as a cumulant expansion [12]:

$$F_s(k,t) = \exp[-k^2\rho_1(t) + k^4\rho_2(t) - k^6\rho_3(t) + ...] \tag{2.18}$$

where the $\rho_i$ are the corresponding cumulants which are given by:

$$\rho_1(t) = (1/2!) < r^2(t) >, \tag{2.19}$$

$$\rho_2(t) = (1/4!)(< r^4(t) > -3 < r^2(t) >^2), \tag{2.20}$$

$$\rho_3(t) = (1/6!)(< r^6(t) > -10 < r^4(t) >< r^2(t) > +15 < r^2(t) >^3). \tag{2.21}$$

Having worked out a formal expression for the Van Hove function, we can now turn our attention to using the results in order to evaluate the various terms appearing in this function, and to considering a generalization that is important for a study of the chaotic and non-chaotic systems considered in this thesis.

## 2.3.1   The Lorentz Gas

The random Lorentz gas has been described previously. Here we turn our attention to a periodic Lorentz gas, shown figure (2.1), with hard disk scatterers in two dimensions [16, 47, 64, 65, 74, 79]. We consider the case where the scatterers are placed in a equilateral triangular array with a scatterer at each vertex of a triangle, as illustrated in figure (2.1). Depending on the density of scatterers, one can see super-diffusive behavior, ordinary diffusion or particles trapped in small regions of space. If the reduced density of the scatterers, $na^2$, is below $\frac{1}{12}$, then ordinary diffusion does not take place and the mean square displacement grows more rapidly than the first power of time, $t$ [43]. This is a consequence of the existence of corridors in the where particles can travel arbitrarily large distances without encountering a scatterer. For densities in the range $\frac{1}{12} < na^2 < \frac{1}{\sqrt{3}}$ the particle diffuses through the lattice, and at density $\frac{1}{\sqrt{3}}$ the particles become trapped in the small triangular

27

regions formed by three disks touching each other. In the infinite horizon case when the density is below $\frac{1}{12}$ there will exist regions wherein certain particles will travel freely for all times. This causes the system to exhibit a super-diffusive behavior [43, 74, 75]. In this thesis we will be using both the Lorentz channel and the two dimensional Lorentz gas [1]. The dynamics for both are identical; moreover, the two dimensional gas is easily obtain by tracking a winding number in along the $y - axis$.
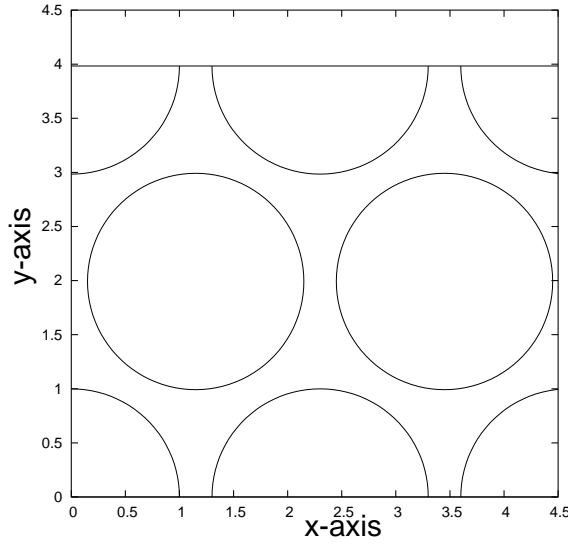


Figure 2.1: *A section of a periodic Lorentz gas with circular scatterers. The scatterers are equidistant from one another and centered at the vertices of equilateral triangles. The scatterers are also placed at high enough density so that no free, infinite trajectories exist in the system.*

One can computationally obtain the mean square displacement easily. To do this we set up the lattice on the computer, then we start $10^6$ particles around the circumference of one of the scatters as shown in fig. (2.2). Then one runs the system

for $10^5$ collisions.

As mentioned earlier, the Lorentz gas is chaotic, that is to say, it has a positive Lyapunov exponent [32, 65, 45]. The Lyapunov exponent measures the rate of separation of initially infinitesimally close trajectories from one another. Take, for example, two particles that start with infinitesimally close trajectories. Normally one would use trajectories, but since the particles in this system do not interact, two particles propagating simultaneously are equivalent to two trajectories. Suppose now that the time dependent coordinate is denoted by $x_1(t)$ for particle one and $x_2(t)$ for particle two. A measure of the distance between the two trajectories at a given time is given by [76]:

$$\|\delta x(t)\| = \|x_2(t) - x_1(t)\|. \tag{2.22}$$

Now if the particles separate at some exponential rate one now has:

$$\delta x(t) = \delta x(0)e^{\lambda t}, \tag{2.23}$$

where $\lambda$ is the Lyapunov exponent. Solving for $\lambda$ one has:

$$\lambda = \lim_{\delta x(0) \to 0} \lim_{t \to \infty} \frac{1}{t} \ln\left(\frac{\delta x(t)}{\delta x(0)}\right), \tag{2.24}$$

where we indicate the proper limits to be used when defining the Lyapunov exponent.

To see that the Lorentz gas is indeed chaotic consider two nearby trajectories. During specular collision with a scatterer particles momentums are reflected in slightly different directions. This is due to the *positive* curvature of the scatterers, as we illustrate in figure (2.2).

We will fix the energy by setting $v = 1$, $m = 1$. We will further fix the radii of the scatterers to $r_0 = 1$. This means at the lower limit of the density the

29
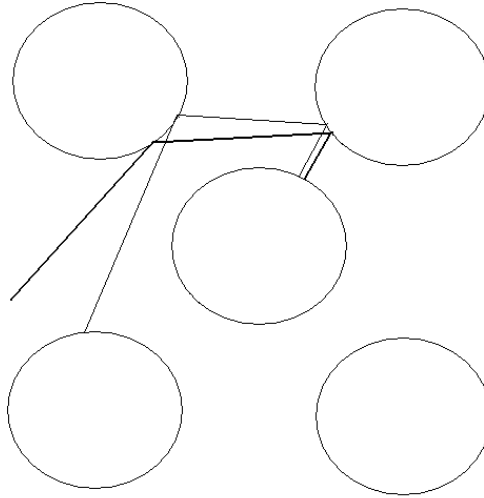
Figure 2.2: *An example of nearby particles with close initial conditions separating with time. This time varying separation is exponential and is characterized by a positive Lyapunov exponent.*

inter scatter spacing is about 2.3 in term of radii of the scatterers, and in one time step $t = 1$ the particles will traverse one radii. It can be shown numerically that the trajectories separate at an exponential rate, with the Lyapunov exponent thus becomes $\lambda = 1.76$, where is defined by [43, 44, 32, 45].

### 2.3.2 The Dimension Formula for Chaotic Systems

We have introduced the Van Hove function for a very specific reason. It can be used to derive an interesting and important relation connecting the microscopic dynamical quantities that characterize the chaotic dynamics of the system and the macroscopic diffusion coefficient [45, 51]. This derivation relies on an impor-

tant property of chaotic Hamiltonian systems, the existence of stable and unstable manifolds in phase space. Since Hamiltonian systems are measure-preserving, the exponential separation of trajectories mentioned above must be matched by an exponential approach of close trajectories as well. This structure of phase space for such systems is clearly described in text books on chaotic dynamical systems and we will not go into the details here. However, a consequence of this property is that fractal structures are very common in the physics of chaotic systems [32, 81]. The averaging that takes place in the partial Van Hove function does not reveal the fractal properties of the displacement function $\delta \mathbf{r}(t)$ [45, 93]. To exhibit the fractal properties we were to carefully examine the quantity $\exp[i\mathbf{k} \cdot \delta \mathbf{r}(t)]$ as a function of the initial position in phase space of the trajectory of the moving particle. This would be for large enough times $t$, a wildly oscillating function of the initial phase space point, since the displacement of the moving particle will change drastically as on changes the initial point in phase space [33, 45].

We can try to capture these wild oscillations by defining an *incomplete* Van Hove function [43, 45, 51]. Instead of integrating over the entire phase space as one does for the Van Hove function, one carries out only integrations over a part of phase space to define the incomplete function. Here we consider a simple case. We consider a set of initial points for the moving particle that are chosen in such a way as to simplify the definition of the incomplete Van Hove function. We consider one scatterer, and select the initial states of the moving particle whereby the particle starts at a point on the circumference of the scatterer with a velocity that is directed outward and normal to the disk. For such a choice, we define a cumulative function

31

by[45, 49, 50, 51]:

$$F_k(\theta) \equiv \lim_{t \to \infty} \frac{\int_0^\theta d\theta' \exp[(\mathbf{r}(t, \theta') - \mathbf{r}(0, \theta')) \cdot i\mathbf{k}]}{\int_0^{2\pi} d\theta' \exp[(\mathbf{r}(t, \theta') - \mathbf{r}(0, \theta')) \cdot i\mathbf{k}]}, \tag{2.25}$$

where the initial location on the circumference is a line parameterized by an angle $\theta$ where $\theta \in [0, 2\pi]$. We use the denominator to appropriately normalize the cumulative function such that $F_k(0) = 0$ and $F_k(2\pi) = 1$. We next construct a curve by plotting $(Re(F_k), Im(F_k))$. This curve is a fractal, for a chaotic system.

For small wave numbers, the Hausdorff dimension of this fractal curve has been shown to satisfy the relation [45]:

$$D_H = 1 + \frac{D}{\lambda} k^2 + O(k^4), \tag{2.26}$$

where $k^2$ goes a $1/length^2$, $\lambda$ goes as $1/time$ and $D_H$ is dimension less. We can also use Eq. (2.26) to obtain an expression for the diffusion coefficient in terms of the other quantities. This is

$$D = \lambda \lim_{k \to 0} \frac{D_H(k) - 1}{k^2}. \tag{2.27}$$

These equations express a connection between the microscopic Lyapunov exponent, the macroscopic diffusion coefficient, the wave number, and the Hausdorff dimension of the fractal curve constructed from the incomplete Van Hove function. They have been checked for a number of simple models [43, 44]. In order to calculate the fractals, we use a hexagonal cells shown fig. (2.3) [74].

Using the units previously discussed, we follow the system for about 15 time steps, then we coarse grain the final positions to the cell positions, since for long times the final position is roughly the cell position. We illustrate these ideas by
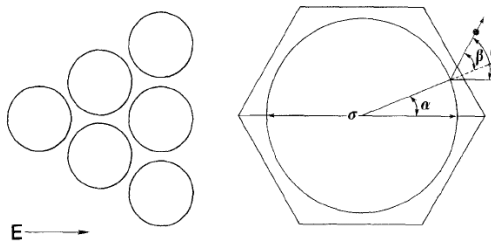
Figure 2.3: *A triangular Lorentz gas with circular scatterers. The figure also shows a hexagon as the unit cell of the gas.*

considering a periodic Lorentz gas with radius $r$ of the scatters equal to 1 and inter-disk distance $d = 2.3$. This places the system in a finite horizon regime, so that there are no free trajectories exist. We can the expression Eq. (2.26) by plotting the Hausdorff dimension versus $k^2$. The Lyapunov exponent is found to be $\lambda = 1.76$. The diffusion coefficient is obtained from the mean square displacement, and is $D = .25$.

### 2.3.3   The Hurst Exponent

For the Hausdorff dimension of the fractal curve, we use the Hurst exponent [93]. This equality holds for fractals that are compact and self similar. The Hurst Exponent is the tendency of a series to either regress or cluster in a direction. The Hurst exponent is defined by the scaling property of its structure:

$$S_q =<\mid g(x + \Delta)x - g(x) \mid^q>_{x_F}\sim (\Delta x)^{qH(q)}, \tag{2.28}$$

where $x_F >> \delta x$. The Hurst exponent is directly related to the fractal dimension by $D = 2 - H$. To test that the procedure returns the proper values we test the method for smooth functions $x^2$ and $\sin(x)$. The procedure returns a dimension of 1

for these function. We also test the procedure for several known fractals, the partial Van Hove for the multi-baker map discussed by Gilbert et al [49, 50, 51], and for the partial Van Hove for the finite horizon Lorentz gas with circular scatterers discussed by Gaspard et al [45]. Since the procedure returns the expected values in all the cases, we verify the procedure is working

In order to actually calculate the cumulative function for the Lorentz gas we follow $10^6$ particles. for a long time, roughly 15 or so collisions. We then plot the $Re(F(k))$ *vs.* $Im(F(k))$ to show the fractal nature of the function. The representative graphs of the cumulative function are given in figure (2.4). Further it is instructive to look at the physical location of each of the final positions $(x(t), y(t))$ for the particle which is shown in figure (2.5). The final postions show the particles diffuse in all directions equally.

## 2.4   Infinite Horizon Lorentz Gas

At this point it is important to note that chaos is not necessary nor is it a sufficient condition for diffusion. Take for example the infinite horizon Lorentz gas. In our example the circular scatterers are placed on an equilateral triangular lattice, as shown in figure (2.1). However, the scatterers are placed far enough apart that there can exist trajectories that never hit a scatterer. As a result for long times it takes on a $D \sim t \ln(t)$ representation [11].

The system is chaotic by nature of the circular scatterers. Moreover one can see that the $Re$ vs. $Im$ of partial Van Hove function is fractal. figure (2.6). The
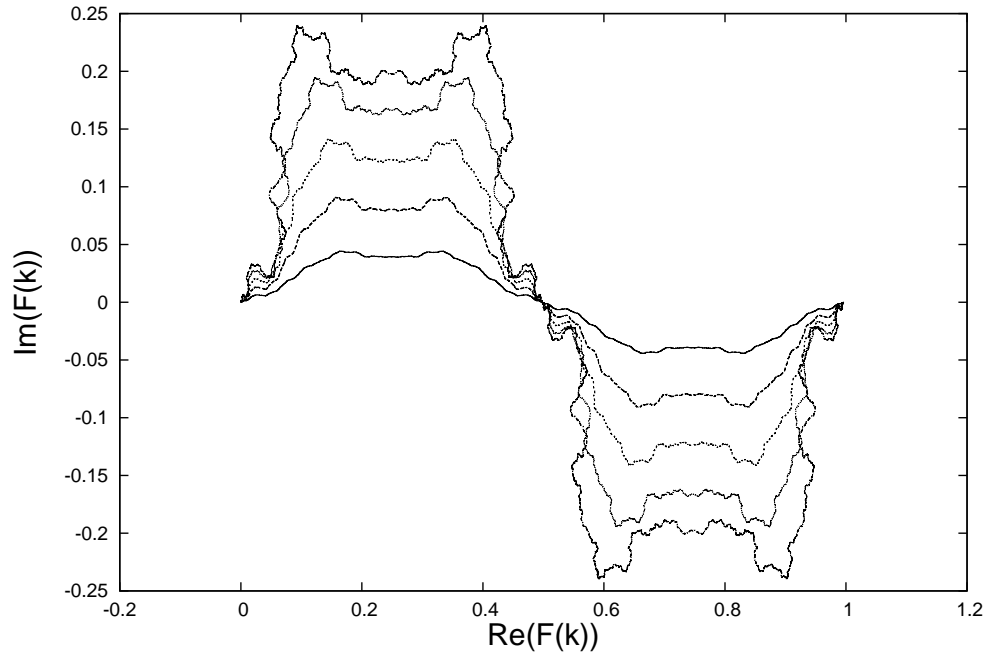
Figure 2.4: $Re(F(k))$ vs. $Im(F(k))$ a triangular Lorentz gas in the finite horizon regime, for k=0.2,k=0.4,k=0.6,k=0.8,k=1.0. The functions appear to be fractal with a non-integer Hausdorff dimension.

system has both a fractal partial Van Hove and a Lyapunov exponent; however, the system is super-diffusive. The relations given by Gilbert, the dimension equation 2.26, are not applicable for super-diffusive systems. As a result other methods need to be employed to relate the dynamics to the transport properties. We will discuss some of these method at the end of Chapter 4.

In this chapter we have observed that for certain diffusive systems that exhibit chaotic dynamics, there exists a simple relation between the dynamics and the transport coefficient. However, it is unclear if such a relation exists for non-chaotic systems. In the next chapter we will consider many-sided polygon scatterer and observe that if we coarse grain the initial condition, we obtain a transport exponent
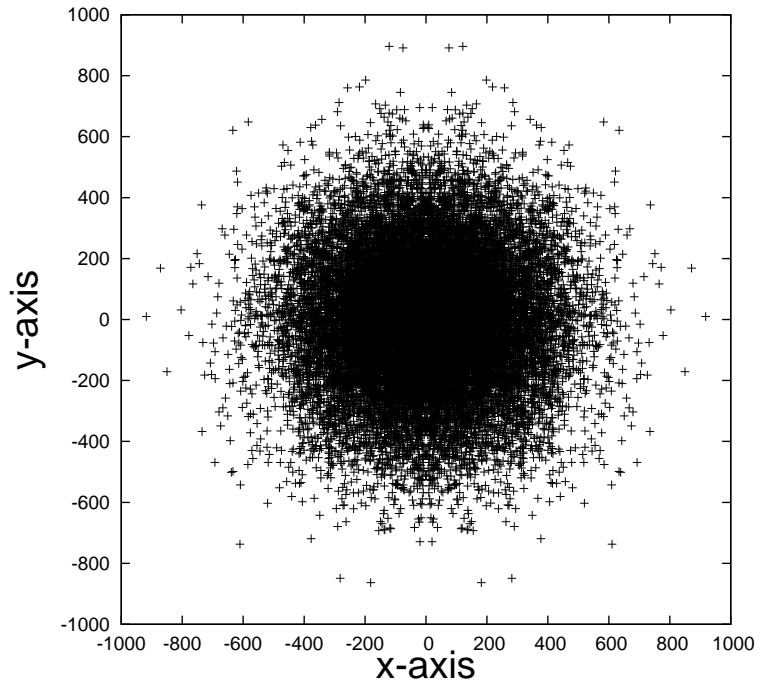
Figure 2.5: *The final position distribution for a triangular Lorentz gas with circular scatterers. The distribution shows transport in the system is isotropic.*

of 1 and an average Lyapunov exponent . Further, one can find a similar relation between for the diffusion coefficient in terms of fractal dimension and the Lyapunov exponent, if one uses an average Lyapunov exponent.
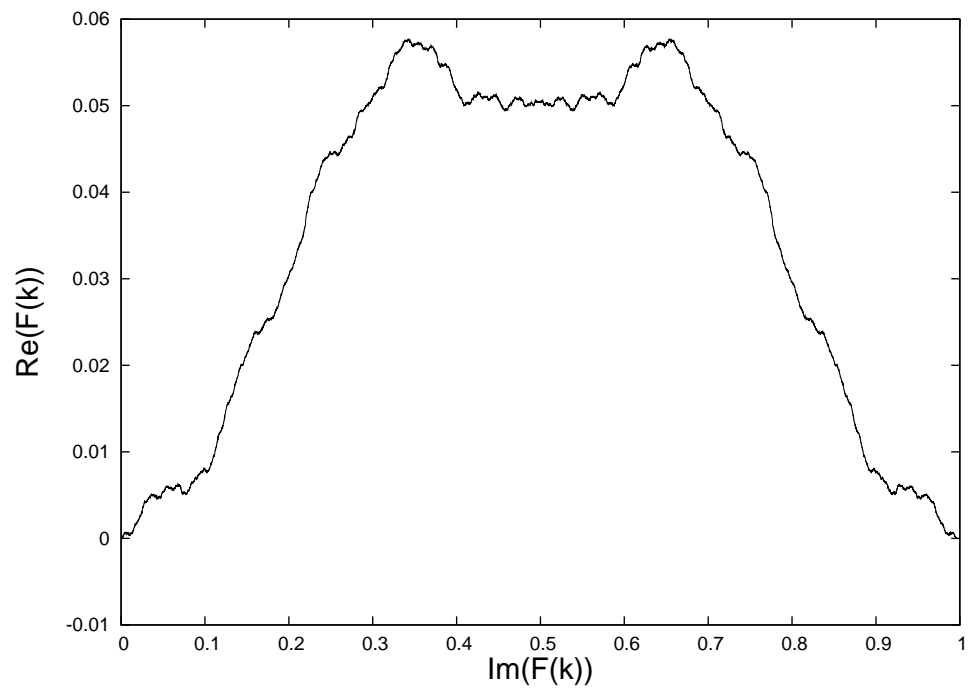
Figure 2.6: $Re(F(k))$ vs. $Im(F(k))$ using $k = 0.1$. The scatterers have a radius 1 and the distance between adjacent scatterers is 2.1. The values were obtained by running $10^6$ trajectories for 30 collisions.

Chapter 3

Transport in Many-Sided Polygonal Systems

## 3.1 Non-Chaotic Systems

In the preceding discussion we were able to relate the dynamical quantities for particle motion in a Lorentz gas of circular scatterers, namely, the Lyapunov exponent and the Hausdorff dimension, to the diffusion coefficient. However the theory breaks down if we replace a chaotic system by a non-chaotic one, that is, if we replace circular scatterers by squares, hexagons or, in general, polygonal scatters. Since the sides of the polygons are flat, the Lyapunov exponent is zero for particle trajectories, and the motion of the particle is no longer chaotic. As a result equations (2.26) and (2.27) make no sense since the diffusion coefficient would become undefined. In fact for many polygonal systems the diffusion coefficient might be either zero or infinite, since the particle's motion may, under various circumstances be sub- or super-diffusive, respectively [2, 3, 5, 6, 7, 38, 30, 57, 80, 23, 86, 87, 96, 100]. It is the goal of this section to consider the motion of a particle when the scatterers are flat-sided n-gons and to consider the rate at which nearby trajectories separate in such systems.

## 3.2 Polygonal Scatterers

Polygonal scatterers do not lead to chaotic dynamics for the moving particle because the flat sides of the polygons do not produce the defocusing needed for an exponential separation of trajectories. Instead two infinitesimally close trajectories will separate algebraically in time [30, 102, 103, 104, 105, 106]. Each scattering event is identical to the scattering of light when reflected by a plane mirror. This is shown in see Fig. (3.1). This is in contrast to reflection by a circular scatterer (or mirror), where there is a discontinuous change in the separation of trajectories at every collision with the scatterer. It is the discontinuous change which ultimately leads to a positive Lyapunov exponent.
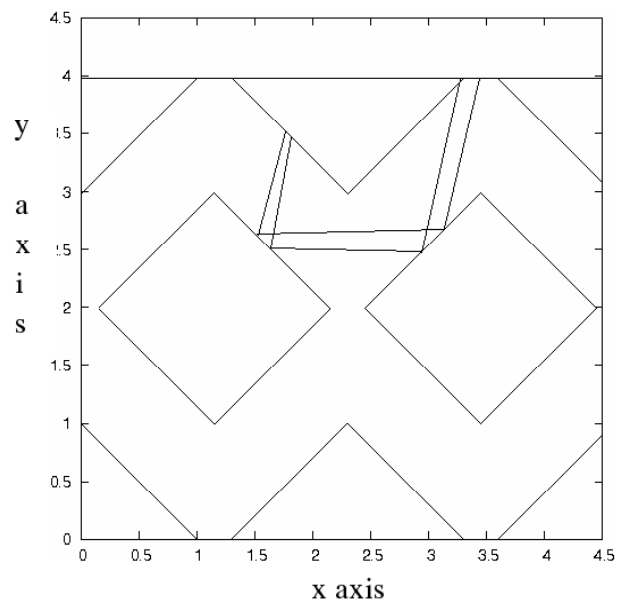


Figure 3.1: *The effect of nearby trajectories hitting the same sides of a scatterer when the scatterers are squares. The separation between nearby trajectories grows algebraically with time rather than exponentially.*

To understand the central question arising when the scatterers are polygons, we first consider in more detail computer simulations of motion with circular scatterers. Each circle is generated by sin and cos functions, which themselves are typically generated by $2^{64}$ straight lines. This means that in the simulations circles are actually many-sided polygons, so the systems that we are simulating are actually non-chaotic, in the strict mathematical sense of taking the limit when the two trajectories are infinitesimally close. This raises the question: Why do we obtain positive Lyapunov exponents in numerical studies of trajectory separations? The answer is quite simple: The Lyapunov exponents in the simulations are produced by nearby trajectories hitting different faces of the same scatterer. This is always the case in simulations since trajectories in the simulations are never close enough to hit the same face of a polygon of $2^{64}$ sides.

This observation led Ford, Vega, and Uzer, to try to define apparent Lyapunov exponents for polygonal scatterers with fewer sides than those used to simulate circular scatterers [96]. To do this these authors followed sets of trajectories pairs in a Bunimovich stadium. Whenever the trajectories hit the circular parts of the stadium scatterer that portion of the circle was replaced by two short, intersecting lines, i.e. a "corner", that would produce the same changes in direction of the trajectories. After $n$ collisions this procedure would generate 2n sides of a polygon. Moreover, for a given set of initial conditions, and up to the time of the last collision, the dynamics of a particle in the polygonal system would match, exactly, that of a particle pair moving in the stadium with the same initial conditions. For this reason they concluded that one might be able to define an apparent Lyapunov exponent for

motion of particles colliding with polygonal scatterers. In other words, as long as the two trajectories hit the same sides of the scatterer, there will be no de-focusing, but if the trajectories hit different sides, the two velocity directions will be rotated by different amounts, which is equivalent to a collision with chaos-producing scatterers, as illustrated in figure (3.2). This will cause an exponential separation of the trajectories as long as the two trajectories continue to hit different sides of the same scatterer. It is this hitting of different sides or "vertex splitting" that causes what appears to be chaotic behavior.
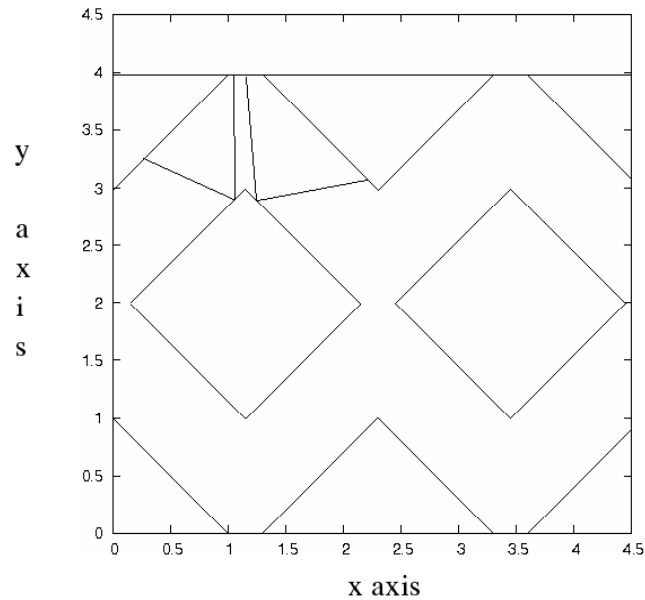


Figure 3.2: *The effect of nearby trajectories hitting different sides of a scatterer when the scatterers are squares. There is a jump in the separation of trajectories after particles the hit adjacent sides of the same scatterers.*

Ford *et al.* further noted that the mathematical definition of the Lyapunov

exponent requires an infinite time and zero trajectory separation limit. Both of these limits cannot strictly be achieved in a computer simulation. They suggested that the definition of chaos should changed to reflect this circumstance. Strictly speaking such polygonal systems are not chaotic, but motion among them may show a great amount of complexity, and might be characterized by an "effective" Lyapunov exponent, to be defined below.

Let us now return to our simulated circular scatterer and consider what is actually happening. Due to the finite memory size of a computer, variables are stored by different precisions. Two examples of these precisions are double precision which use $2^{64}$ bits and integer precision using $2^{32}$. During the simulation a circular scatterer is defined by two double precision functions, the *sin* and *cos* functions. As mentioned above, simulated circular scatters are not really circular at all, they are many-sided polygons. Now the number of initial conditions is necessarily finite. We generally only use about $10^4 - 10^6$ initial conditions. Therefore it is possible that numerically speaking, at least, mathematically non-chaotic systems may appear to be chaotic. This occurs whenever initial conditions are separated sufficiently far apart that during every collision with a scatterer 'vertex splitting' occurs. Further we insure that the trajectories are hitting the same scatterers otherwise the exponential behavior will be lost.

Now consider a situation for "simulated circles" where the number of initial conditions is of the same order or greater then the number of sides of each of the scatterer, $2^{64}$. This is theoretically possible but is impractical since it would take very long times to complete the simulations. However by doing this, we would

prevent the 'vertex splitting' of two trajectories. Now our system no longer appears to be chaotic, but, for finite horizons at least, it still appears to be diffusive, at least numerically. However in actuality the system may be sub or super-diffusive. This problem will arise again later in the chapter during our discussion of many-sided polygons.

To explore this situation in greater detail, we consider polygonal scatterers where the number of sides, $n$ is on the order of 100 sides or more. We consider periodic arrangements of scatterers as with the Lorentz gas illustrated in Figs. (2.1, 3.2, and 3.1). For such arrangements of scatterers we do not expect that a moving particle will undergo normal diffusion in the absence of chaotic motion. That is, if the dynamics is not chaotic, then there is no source of the randomness needed for diffusive motion, chaos provides a dynamical randomness that for periodic systems is necessary for normal diffusion. This is an issue which can be verified by means of numerical studies as discussed below.

First we consider the incomplete Van Hove function for a periodic system of non-chaotic scatterers. Here the scatterers will have a large number of sides and will approach circles as we allow the number of sides to approach infinity. Again we start all the trajectories at the surface of a scatterer with velocities normal to the surface. The initial conditions shall again be parameterized with the angle $\theta$. Further we shall use a very large set of initial conditions, $10^6$ particles or more. As for the Lorentz gas there are 4 degrees of freedom, two momentum components and two position coordinates. Because of energy conservation, there are only 3 degrees of freedom. However unlike the circular scatterers, there are no unstable

and stable directions in phase space for polygonal scatterers. Nevertheless, because of the vertex splitting of certain pairs of trajectories, there is some kind of instability in this system. As previously mentioned polygonal systems maybe sub-diffusive or super-diffsive. This is defined by a generalized transport exponent given by:

$$\langle (\mathbf{r}(t) - \mathbf{r}_0)^2 \rangle = Kt^\mu, \tag{3.1}$$

where the mean square displacement now is proportional to some arbitrary power of $t$. This power $\mu$ is be called the transport exponent, and it satisfies the condition that $0 \leq \mu \leq 2$. The case where $\mu = 1$ corresponds to normal diffusion, the range $1 < \mu \leq 2$ is called *super-diffusive motion*, and $0 \leq \mu < 1$ is called *sub-diffusive motion*.

The systems we are discussing in this chapter are periodic systems containing polygonal scatterers. We know that in the circular scatterer limit, and for scatterers' densities in the finite horizon range, the systems are both diffusive and chaotic. Further we know that for four- and six- sided polygon systems, the motion is super-diffusive and non-chaotic [87, 100, 104, 106]. The transport exponent for the four-sided system is greater than that for the corresponding six-sided system. This appears to indicate that the transport exponent may asymptotically approach 1 as one increases the numbers of sides. One expects that for a finite arbitrary number of sides that a periodic, polygonal system should be super-diffusive. The flat, parallel sides should allow the existence of "walking orbits" that lead to super-diffusion. If the orientation is randomized, the motion should look to be more diffusive. In the non-chaotic models mentioned in chapter 1 which were diffusive, there was some

44

instability or randomization inserted into the system that made the system diffusive [2, 3, 30, 86]. For example in the four sided scatterer systems studied by Dettmann and Cohen, the scatterers were randomized in both position and the orientation. In the triangular lattice systems studied by Alonso, the irrational angle for certain configurations appears to act to destabilize the dynamics enough to induce diffusion. We will discuss these systems in greater length in chapter 4.

## 3.3  Lyapunov Exponents and Transport in Lorentz Gases with Many-Sided Scatterers

For periodic systems with many-sided polygonal scatterers, we expect the system to be slightly super-diffusive. Moreover since the spacing between nearby initial trajectories is much smaller then the vertex separation, we expect a zero Lyapunov exponent. We can check both "effective" Lyapunov exponents and transport exponents for these systems by running the simulation as described above for several different n-gon scatters. In the table (3.1) we present results for the transport exponents and the Lyapunov exponents for periodic, polygonal systems with a range of sides.

The Lyapunov exponents are equal to zero within error bars for all the systems. The transport exponent however has an error is on the order of $\pm 0.01$, thus the systems are super-diffusive. As mentioned earlier we expect this type of behavior since our system is a periodic billiard (gas). However there are polygonal systems which are diffusive, which we will discuss in the following chapters. These systems

Table 3.1: *This table shows the variation in the transport exponents for different polygonal Lorentz gases. Each system uses n-gons as scatterers, for $100 \leq n \leq 264$. The table also shows that within the errors of the simulations, the Lyapunov exponent is zero for each of the systems.*

| number of sides | $\mu$ | $\lambda$ |
|---|---|---|
| 100 | 1.15 | 0.00179 |
| 112 | 1.14 | 0 |
| 120 | 1.12 | -0.0142 |
| 132 | 1.09 | 0.021 |
| 140 | 1.12 | 0.00717 |
| 156 | 1.10 | 0 |
| 168 | 1.08 | 0.0107 |
| 180 | 1.080 | -0.0036 |
| 192 | 1.079 | 0.0153 |
| 208 | 1.067 | .001064 |
| 220 | 1.066 | .01544 |
| 236 | 1.058 | 0.00537 |
| 248 | 1.052 | 0.01108 |
| 264 | 1.053 | 0.02337 |

use other methods to create the diffusive behavior and are typically not periodic. Since we are dealing with periodic arrangements of polygonal scatterers, we expect that the transport exponent as a function of number of sides should asymptotically

approach 1. A plot of the transport exponent *vs.* the number of sides, for 4 to 264 sides is shown figure (3.3) as well as a plot of the effective Lyapunov exponent as a function of the number of sides shown in figures (3.4-3.5).
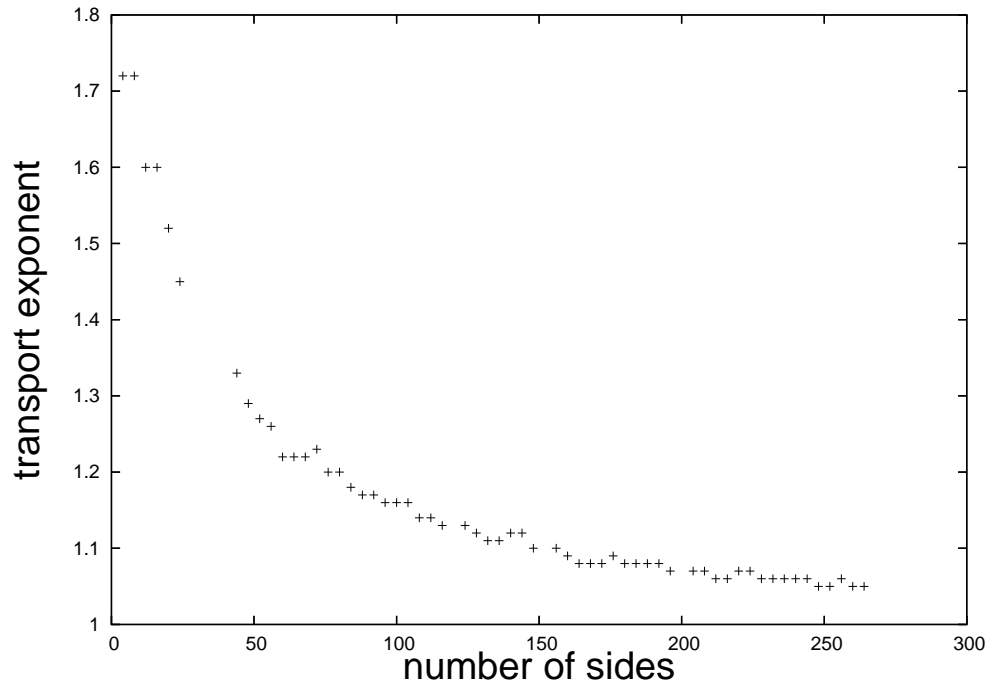


Figure 3.3: *Transport exponent vs. the number of sides, n, of a periodic billiard with n-gon as scatterers. The plot shows that the transport exponent, μ, appears to be a decreasing function of the number of sides.*

It is clear that the Lyapunov exponents are extremely close to zero for all number of sides, with very small deviations about zero. In a rigorous mathematical sense this is what one expects. However from a physical point of view it seems a bit odd, since we know in the large $n$ limit our polygons become circles. Figure (3.6) and the table (3.2) show that the Lyapunov exponent as a function of sides is a step function, equal to zero everywhere except at infinity. Now as one increases the number of sides, we expect larger and larger numbers of trajectory pairs to be split
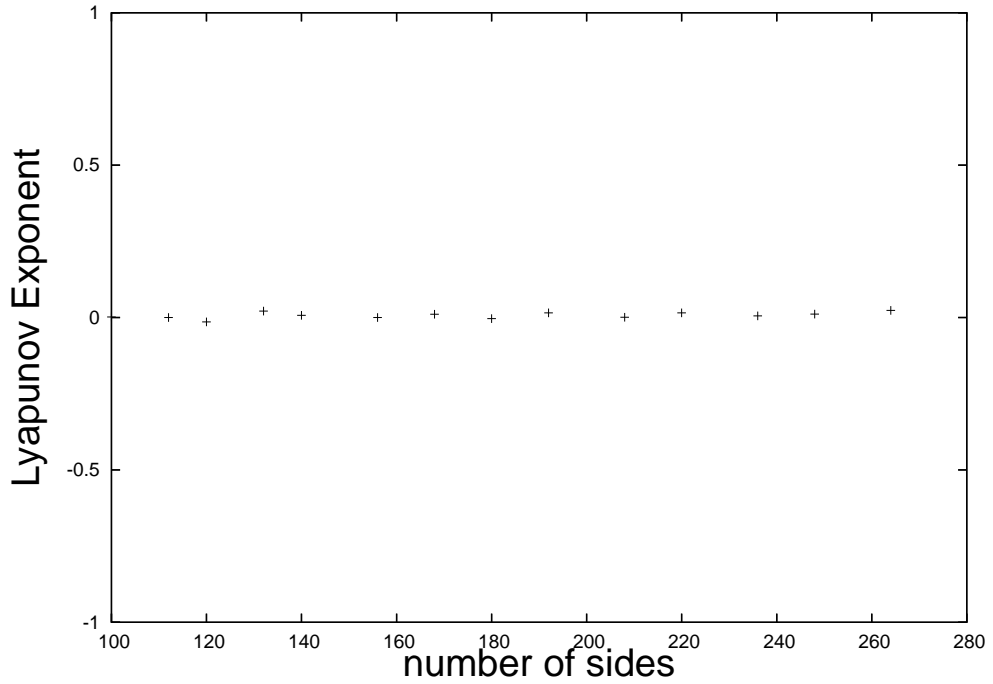
Figure 3.4: *Lyapunov exponent vs. the number of sides of a periodic billiard with n-gon as scatterers. The plot shows that the Lyapunov exponent is zero for each system, within errors.*

apart by these vertex splitting events. Our data show that the transport exponent seems to vary as the number of sides is increased, but the Lyapunov exponent remains zero over the range of sides used. However, from the work of Vega et al. there should exist a regime with a non-zero effective Lyapunov exponent. There exists a Lyapunov exponent in the limit as the number of sides goes to $2^{64}$, and therefore one might expect that there is some number of sides, perhaps accessible to computer simulations where one might find non-zero Lyapunov exponents. Below we show the results obtained with polygons of $10^3$ sides, figure (3.6). We still see evidence of diffusive behavior over the time scales studied.

The explanation of these results is that on these time scales the motion is
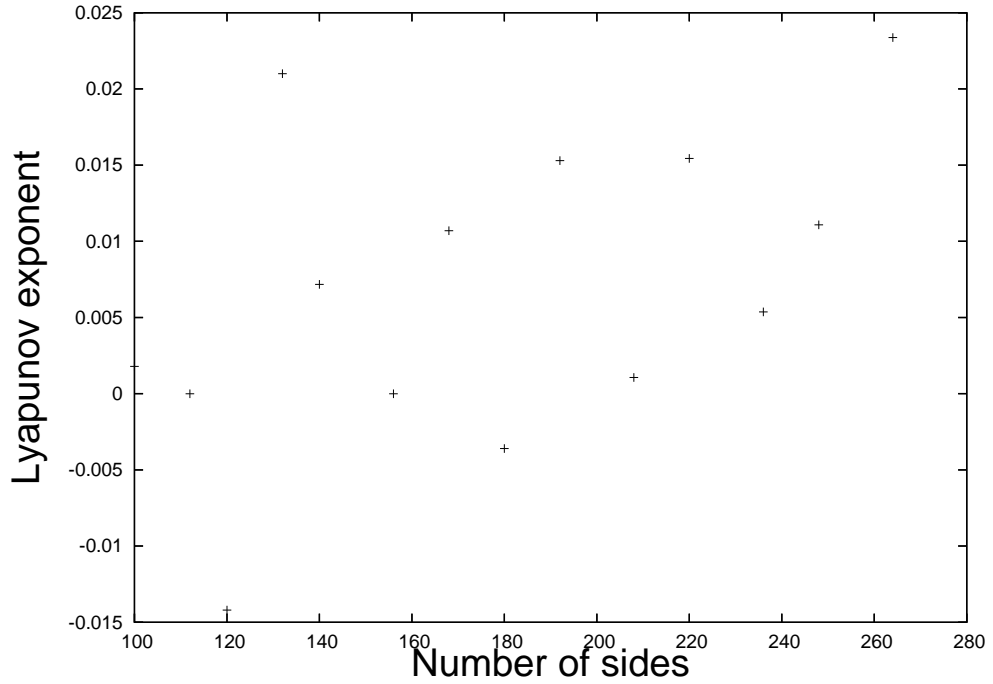
Figure 3.5: *An enlargment of figure (3.4), showing Lyapunov exponent vs. the number of sides of a periodic billiard with n-gon as scatterers. The Lyapunov exponents are zero to within the errors of the simulations.*

still not sufficiently chaotic-like. Many trajectory pairs separate algebraically with time unlike those for circular scatterers. Moreover, when we calculate the mean square displacement we are averaging over two types of trajectories, those close to "chaotic" trajectories, which shadow a similar trajectory that would be obtained for circular scatterers, and "non-chaotic" trajectories. These "non-chaotic" trajectories are responsible for the system being super-diffusive. If one considers our Lorentz gas made of $2^{64}$-sided polygonal scatterers, we notice that the initial conditions parameterized in such a manner that all trajectory pairs will undergo vertex splitting. This is due to the fact that our initial conditions vary on a much coarser scale then the scale for the number of sides. So in effect these initial conditions have removed the
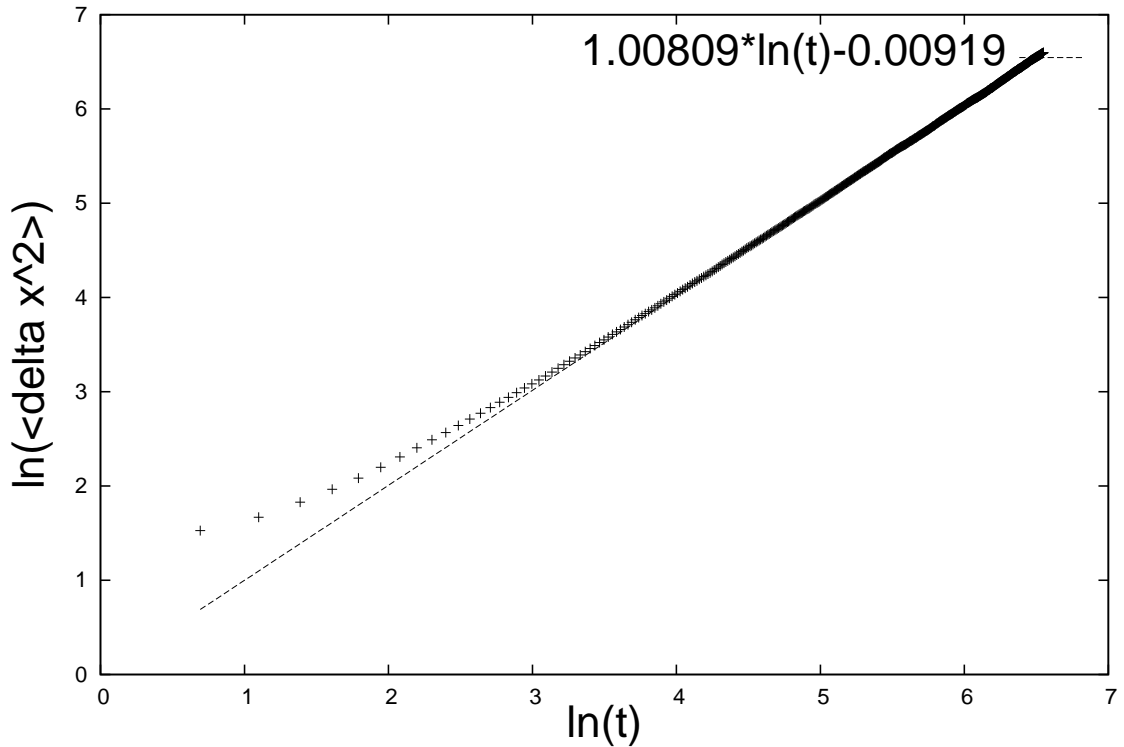
Figure 3.6: $\ln(\delta x^2)$ *vs.* $\ln(t)$ *of a periodic billiard with* 1000 *sided scatterers. The results show that the system appears to be slightly super-diffusive within errors. The best fit line is also shown as a gray line represented by the equation* $1.00809\ln(t) +$ 0.00919

"non-chaotic" trajectories from the averaging for both the Lyapunov exponent and the mean square displacement. In this system we see both a Lyapunov exponent and a transport exponent of 1. More over the system satisfies the relation of Claus, Gilbert, Gaspard and Dorfman [50, 51, 45]. This is in spite of the fact the system, in the strict mathematical sense, is not chaotic.

Now we can test to see if these non-chaotic trajectory pairs are indeed causing the super-diffusive behavior. To do this we will now consider a regime where our initial conditions are parameterized on a coarser scale then the number of sides.

Moreover to reduce any systematic effects we will choose them in a random fashion. This may seem objectionable at first since one will be disregarding large number of points, but one can justify it by considering the preceding arguments about the simulated Lorentz gas. Further we will restrict ourselves to fairly large numbers $n \geq 500$ of sides, in this manner we can insure that one can always take an adequate average. Below is a table of Lyapunov, table (3.2), exponents for a given separation distance, we have included polygons that are well below the 500 side limit to show that there is a Lyapunov exponent for separation distances on the order of 1/100 the vertex separation.

Table 3.2: *The table shows values of effective Lyapunov exponents for a Lorentz gas containing n-gons as scatterers, for $10^2 \leq n \leq 10^4$. As one increases the initial separation distance between neighboring trajectories, these systems appear to have positive Lyapunov exponents.*

| number of sides | separation distance | $\lambda$ |
|---|---|---|
| 100 | 0.0125 | 2.03 |
| 100 | 0.000628 | 1.29 |
| 200 | 0.0125 | 1.84 |
| 200 | 0.000628 | 1.41 |
| 300 | 0.0125 | 1.91 |
| Continued on next page | | |

Table 3.2 – continued from previous page

| number of sides | separation distance | $\lambda$ |
|---|---|---|
| 300 | 0.000628 | 1.38 |
| 400 | 0.0125 | 1.83 |
| 400 | 0.000628 | 1.64 |
| 500 | 0.0125 | 1.78 |
| 500 | 0.000625 | 1.50 |
| 600 | 0.0125 | 1.93 |
| 600 | 0.000628 | 1.63 |
| 700 | 0.0125 | 1.88 |
| 700 | 0.000628 | 1.33 |
| 800 | 0.0125 | 1.82 |
| 800 | 0.000628 | 1.68 |
| 900 | 0.0125 | 1.96 |
| 900 | 0.000628 | 1.46 |
| 1000 | 0.0125 | 1.88 |
| 1000 | 0.00628 | 1.59 |
| 2000 | 0.0125 | 1.86 |
| 2000 | 0.00628 | 1.52 |
| 3000 | 0.0125 | 1.93 |
| 3000 | 0.00628 | 1.63 |

Table 3.2 – continued from previous page

| number of sides | separation distance | $\lambda$ |
|---|---|---|
| 4000 | 0.0125 | 1.93 |
| 4000 | 0.00628 | 1.63 |
| 5000 | 0.0125 | 1.95 |
| 5000 | 0.000628 | 1.56 |
| 6000 | 0.0125 | 1.89 |
| 6000 | 0.000628 | 1.61 |
| 7000 | 0.0125 | 1.99 |
| 7000 | 0.000628 | 1.69 |
| 8000 | 0.0125 | 1.89 |
| 8000 | 0.000628 | 1.77 |
| 9000 | 0.0125 | 1.95 |
| 9000 | 0.000628 | 1.77 |
| 10000 | 0.0125 | 1.95 |
| 10000 | 000628 | 1.80 |

The Lyapunov exponents in this case are non-zero and are on the order of that of our Lorentz gas. What one actually finds is the Lyapunov exponent varies with the initial separation distance of our initial conditions.. For very small separation, we find Lyapunov exponents close to zero. As one increases the separation distance

53

the Lyapunov exponent asymptotically approaches some fixed value which is approximately equal to the Lyapunov exponent of a circular scatterer. This Lyapunov exponent *vs.* separation distance is shown in figure (3.7).
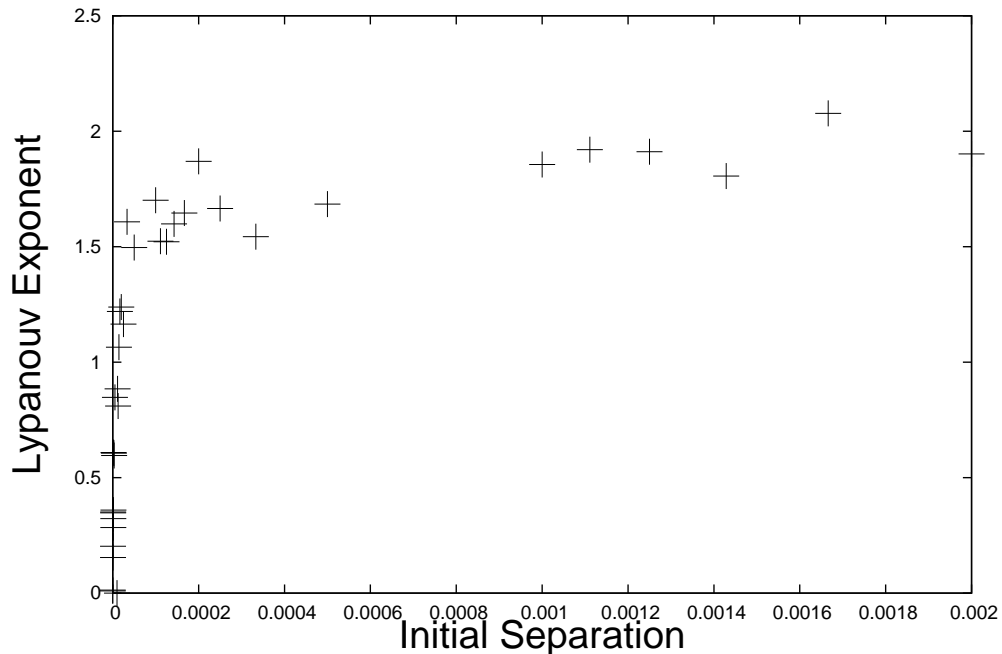


Figure 3.7: *Lyapunov Exponent vs. separation distance of a periodic billiard with 1000-sided scatterers. The plot show how the effective Lyapunov exponent varies with the separation distance between initial trajectories.*

The Lyapunov exponent for the poygonal system do not exactly equal the Lyapunov exponent for Lorentz gas. Moreover, the Lyapunov exponent varies depending on the separation distance as shown in table (3.2). However, these can be accounted for by error. The associated error increases for decreasing numbers of sides and increasing separartion distance.

If our system now appears chaotic this would imply that the system would be diffusive as well. We check this as described earlier, by parameterizing the initial

conditions on a coarser scale then the number of sides, and further by randomizing the conditions to insure that results are less likely a result of the initial conditions and are a result of the system dynamics. We find that for this regime the system is indeed diffusive for a 10000 sided polygon as shown in table (3.3).

Table 3.3: *This table shows the effective transport exponent and the effective diffusion coefficient, for n-gon Lorentz gas systems. Both values are, within errors, equivalent to that of a triangular Lorentz gas with circular scatterers.*

| number of point average | $\mu$ | diffusion coefficient |
| --- | --- | --- |
| 1000 | .9826 | .28 |
| 2000 | 1.0023 | 0.21 |
| 4000 | 1.01 | 0.23 |
| 6000 | 1.002 | 0.24 |

This seems to indicate that the trajectories which are removed when a larger separation distance is used, have a large impact on the transport properties of the system. It maybe that these trajectories tend to be "walking" orbits that have a super-diffusive behavior similar to that of a particle traveling down a pipe. Since the sides of the polygons are flat, these walking orbits are *stable*.

Due to the stability of these walking trajectories, there may be dense sets of them. Each of these orbits contributes to the mean square displacement giving the system it super-diffusive behavior. By coarse graining our trajectories we remove these dense sets, and the final result is a diffusive looking system, with chaotic trajectory pairs. We will return to this concept in the next chapter when we discuss

few-sided polygons

## 3.4 Partial Van Hove Functions for Lorentz Gases with Many-Sided Polygonal Scatterers

We shall now return to the dimension formula of Gilbert, Gaspard, and Dorfman. So far we have considered coarse graining a non-chaotic system to give the system the appearance of a chaotic diffusive system. We now consider the Hausdorff dimension for the partial Van Hove functions for the coarse grained trajectories. We expect that this Van Hove scattering function should be a fractal with a dimension proportional to $k^2$. This is easily verified. We plot the $Im(F(k))$ *vs.* $Re(F(k))$ for the coarse grained motion of a particle in a Lorentz channel with polygonal scatterers, and compare that with the corresponding curve for circular scatterers. An example of the partial Van Hove for a $10^4$ polygon is shown in figure (3.8).

By fitting the data for $10^4$ sided polygons to the relation $D_H = mk^2 + b$ we can verify that the dimension for $k = 0$ is unity and that the diffusion coefficient satisfies $D = lim_{k \to 0} \frac{D_H(k)-1}{k^2 \lambda}$, where $\lambda$ is the apparent Lyapunov exponent for the coarse grained trajectories. This raises the question of what does one find if one does not coarse grain the trajectories. It is not clear to us *a priori* what might be expected. Remarkably we find that for many-sided polygonal systems that the dimension as a function of $k$ still goes as $mk^2 + b$. The $m$ value is the same for the systems. The $b$ value for many-sided polygons is same as that for circular scatterers. We also find that as the number of sides decreases, the curve appears to be a fractal
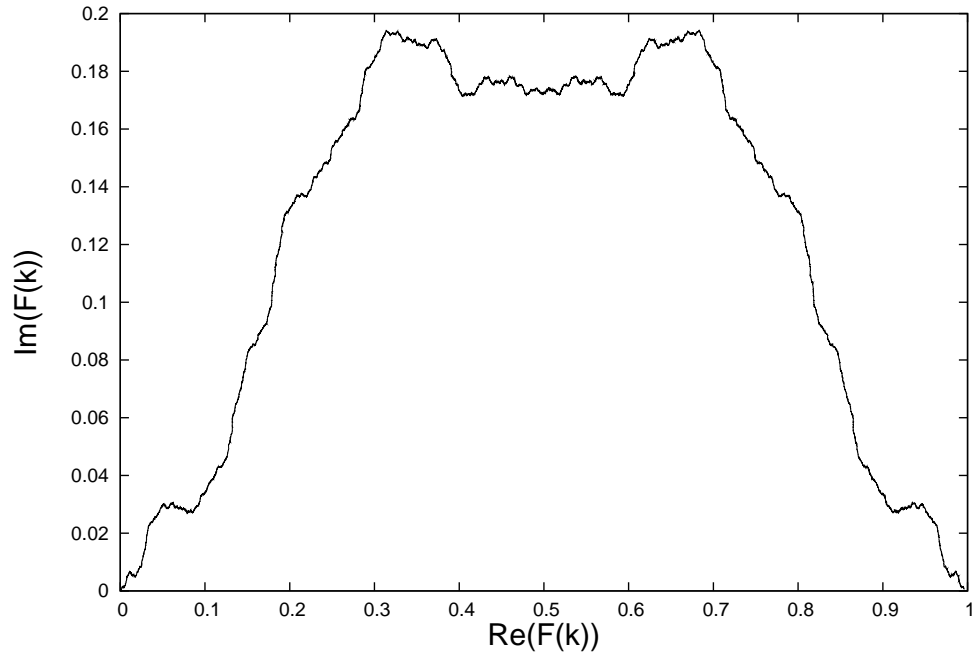
Figure 3.8: *An example of a plot of $Im(F(k))$ vs. $Re(F(k))$ of the partial Van Hove function for a triangular Lorentz gas with scatterers having $10^4$ sides.*

over smaller ranges of $k$ values. In other words for a 4 sided polygon the partial Van Hove function is fractal for $0 < k < 0.1$ while for $10^4$ sided polygons the Van Hove function is a fractal for $0 < k < 1$.

We find that the $k^2$ behavior of the Hausdorff dimension of these fractals is quite general, even without coarse graining. The "functionality" of the fractal seems however seems linked the dynamics of the system. For each imaginary value the partial Van Hove takes on multiple real values. As a result any self similar behavior is lost for large $k$ values. We will see this more clearly when we consider few-sided n-gon systems in the next chapter.

The last question we address about the partial Van Hove functions for polygonal system is whether these Van Hove functions are truly fractal, or only apparently

so on some scale. Consider the corresponding partial Van Hove function for a 4-sided polygon shown figure (3.10) and that of a circular Van Hove function shown in figure (3.9).
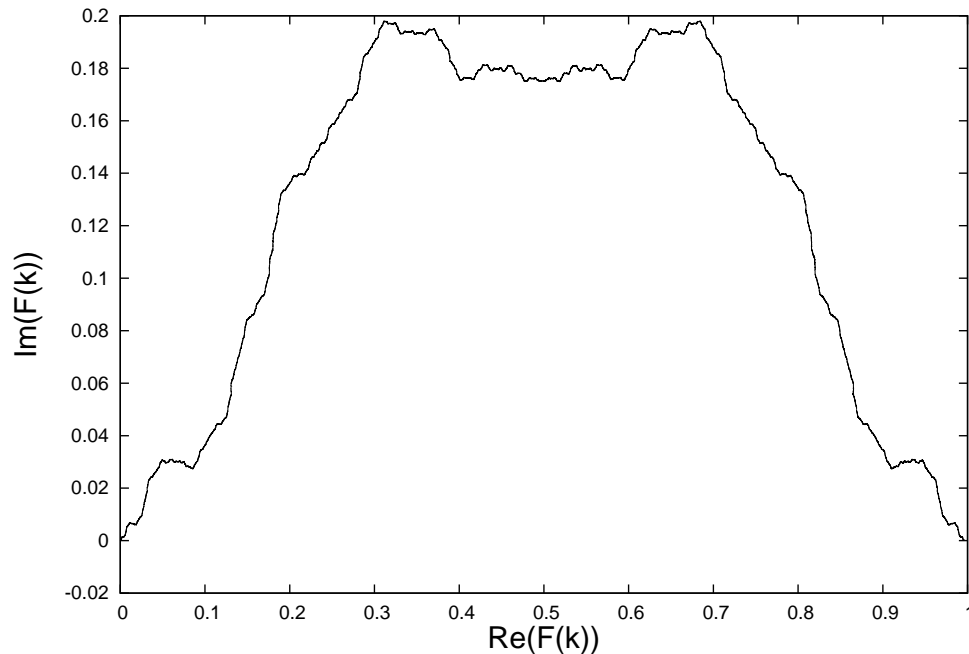


Figure 3.9: *A plot of $Im(F(k))$ vs. $Re(F(k))$ for the partial Van Hove function for a triangular Lorentz gas with circular scatterers. When compared with the $Im(F(k))$ vs. $Re(F(k))$ of a partial Van Hove function for a billiard with scatterers having $10^4$ sides there appears to be very little difference between the two curves.*

One sees that the circular system Van Hove function appears much more fractal. In fact the 4-sided polygon appears to be smooth except for a small region of $k$. Perhaps the partial Van Hove functions for 4 sided systems are not truly fractal. However, the behavior of the function may be sufficiently complex that the computer cannot distinguish the difference between this curve and a genuinely fractal curve. If one were to have infinite precision, the computer should eventually be able
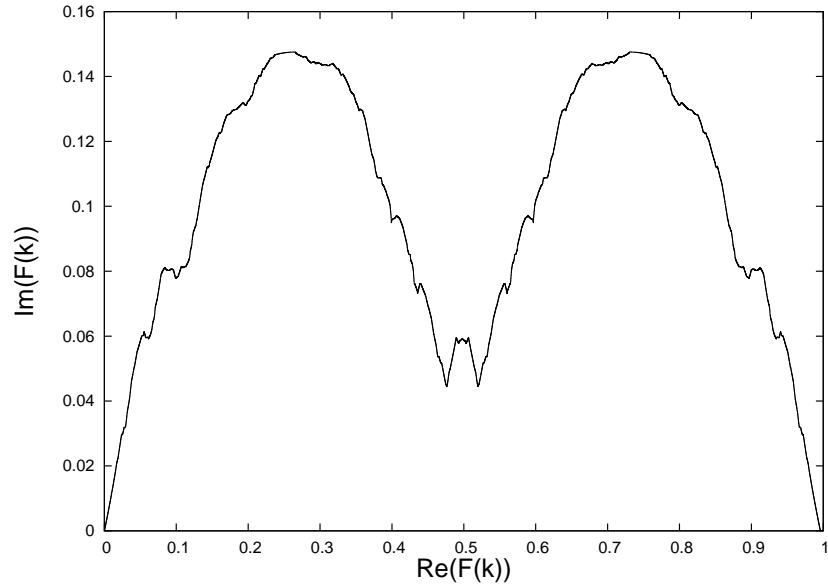
Figure 3.10: $Re(F(k))$ vs. $Im(F(k))$ of the partial Van Hove Function for a system of point particles moving on equilateral triangular lattice consisting of polygonal scatterers having 4 sides. The fractal dimension for this curve is the same as that for a Lorentz gas composed of circles obtained by circumscribing the squares.

to tell the difference for these curves, but as before with the many-sided polygons and the circles the computer cannot "see" the difference.

Our result shows, in agreement with the results of Ford, Vega, Uzer, [96], that in a "physical" setting, the rigorous mathematical limits required to define chaos are not always useful [53, 54]. We have shown that if one considers a coarse-grained system that one cannot effectively distinguish between chaotic and non-chaotic systems. We find that coarse grained systems can appear to be chaotic and diffusive, and that for them the dimension formula is satisfied. For gases with polygonal scatterers that at for regular polygons with 500 sides or more the formula holds.

Our work on many-sided polygons leaves many questions unanswered. For

example, why do the curves appear to be fractal even for the fine grained trajectories? Why is the fractal dimension proportional to $k^2$? What is the meaning of the coefficient of this term for a non-chaotic system? In next chapter we study few-sided n-gons where additional questions arise.

Chapter 4

Few-Sided Polygonal Systems

## 4.1  Transport in Few-Sided Polygonal Systems

In the previous chapter we saw that as one increases the number of sides of regular polygonal scatterers, the scattering of point particles by polygons approaches that by circular scatterers and the motion of the point particles approach a chaotic limit. Moreover, for a periodic system of polygonal scatterers with finite horizon, the motion of the point particles becomes diffusive in the circular limit, as one would expect. We also showed that if the number of sides is sufficiently large, a non-chaotic system with polygonal scatterers can be made to appear chaotic on a coarse grained scale. However, if the scatterers have only a few sides one can not make the system appear to be chaotic even on a coarse grained scale. Nevertheless, the trajectories are still extremely complex, so complex that these system are referred to as pseudo-chaotic systems. In this Chapter we shall examine the transport and related properties of some pseudo-chaotic systems.

We begin by considering the polygonal Lorentz gas described in the last chapter as show in figure (4.1). In this chapter we shall consider periodic arrangements of polygonal scatterers with small numbers of sides, less than $10^2$.

We expect these systems to be super-diffusive or, equivalently, the transport exponent will satisfy $\mu > 1$. However, we expect that if we were to increase the
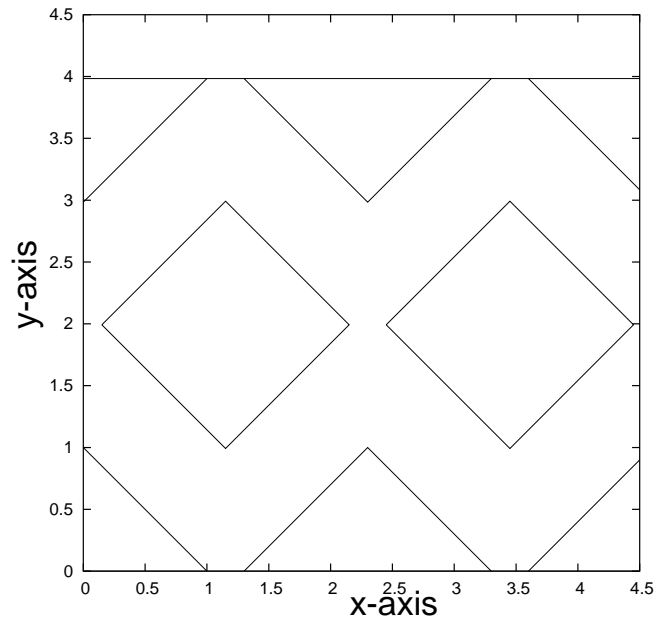
Figure 4.1: *A section of a polygonal periodic Lorentz gas, containing squares. The scatterers are equidistant from one another so that they form the vertices of equilateral triangles. The scatterers are also placed so that the system has a finite horizon. As a result no free trajectories exist in the system.*

number of sides, the motion of the particles would become more diffusive and the exponent $\mu$ would approach unity.

The difficulty with coarse graining these systems becomes apparent if one tries to define a coarse grained Lyapunov exponent for few-sided polygons as we did in the previous chapter for many-sided polygons. We find that the coarse grained scale one needs to use in order to see an effective Lyapunov exponent varies wildly depending on the initial conditions. Further, as expected, the actual Lyapunov exponent is zero for these systems. One still sees an exponential separation of

certain trajectory pairs. However for the system as a whole we can neither obtain a non-zero Lyapunov exponent nor define a coarse grained Lyapunov exponent. Trajectory pairs typically separate algebraically, generally linearly, with time. The vertex splitting of trajectories does not produce an overall exponential separation as can be seen in the chart below. Given the error bars of the simulations, the average Lyapunov exponent is zero as shown in table (4.1)..

Table 4.1: *The table shows the effective/average Lyapunov exponent for few-sided polygons with the associated error. As the number of sides decreases the associated error becomes on the order magnitude of the value of Lyapunov exponent*

| Number of Sides | Average Lyapnouv exponent | Error |
|---|---|---|
| 200 | 1.9 | $\pm 0.27$ |
| 150 | 2.00 | $\pm 0.31$ |
| 100 | 1.98 | $\pm 0.58$ |
| 80 | 2.07 | $\pm 0.42$ |
| 50 | 2.09 | $\pm 1.06$ |

For our systems of scatterers with very few sides, trajectory pairs begin to hit different scatterers even after the very first vertex splitting collision. This can be seen in a simple four'sided polygonal array shown in figures (4.1),(4.2), and (4.3). The discontinuity or jump between the nearby trajectories can be observed in figure (4.4).

The collision of a particle with a scatterer results in a rotation of the particle's momentum direction by $\pi/2$. So, in effect, two initially close trajectories lead to
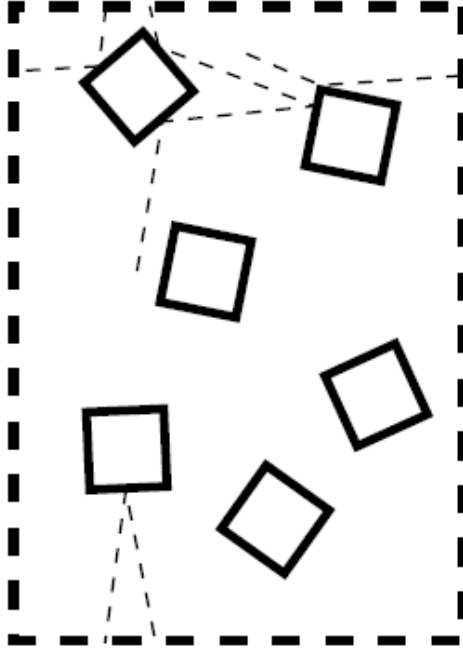
Figure 4.2: *An example of a pair of trajectories in a Lorentz gas with square scatterers. The trajectories split whenever each one collides with a different side of a scatterer.*

motion in opposite directions and the particles following these trajectories must hit different scatters, unless the dynamics is taking place on a torus. The striking of different sides causes a spike in the separation distance as shown for a four sided billiard with the initial separation at $\frac{\pi}{10}a$ where $a$ is the length of a side.

Since the Lyapunov exponent vanishes, and the motion of the particles is super-diffusive, we obviously do not expect the relation between the Lyapunov exponent, Hausdorff dimension and the diffusion coefficient, that characterizes the Van Hove function for a chaotic system, to apply to this case.
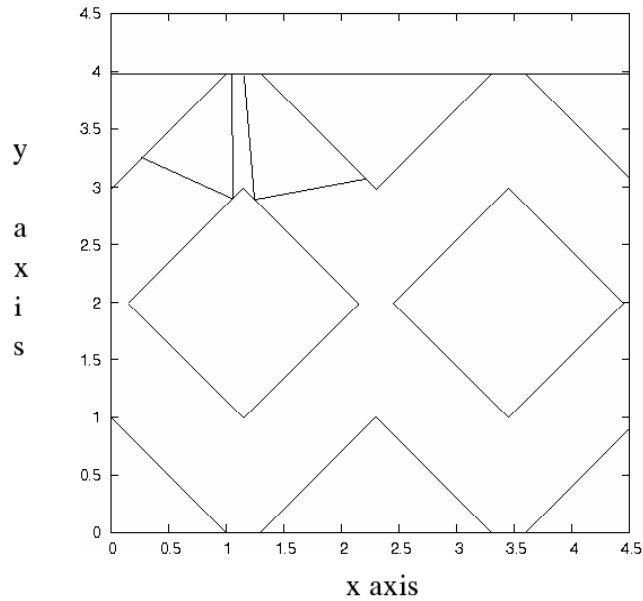
Figure 4.3: *Another example of a pair of trajectories in a system of periodically placed square scatterers. The trajectories split when they each collide with different sides of a scatterer.*

## 4.2 Super-Diffusive Motion in the Polygonal Lorentz Gas

We shall now consider transport in these systems. To start we shall consider a system composed of four-sided polygons. We know from the work of Dettmann and Cohen that transport is dependent on the lattice chosen. For example Dettmann and Cohen showed that the motion is super-diffusive for systems with periodic boundary conditions, but if the scatterers are randomly placed throughout space or randomly oriented the systems become diffusive [30]. Neither the randomly placed nor the randomly oriented systems are chaotic, but both appear to be diffusive. While it is not entirely clear what makes these systems diffusive, it may be linked to the absence of a type of motion called walking orbits [86]. Walking orbits are those
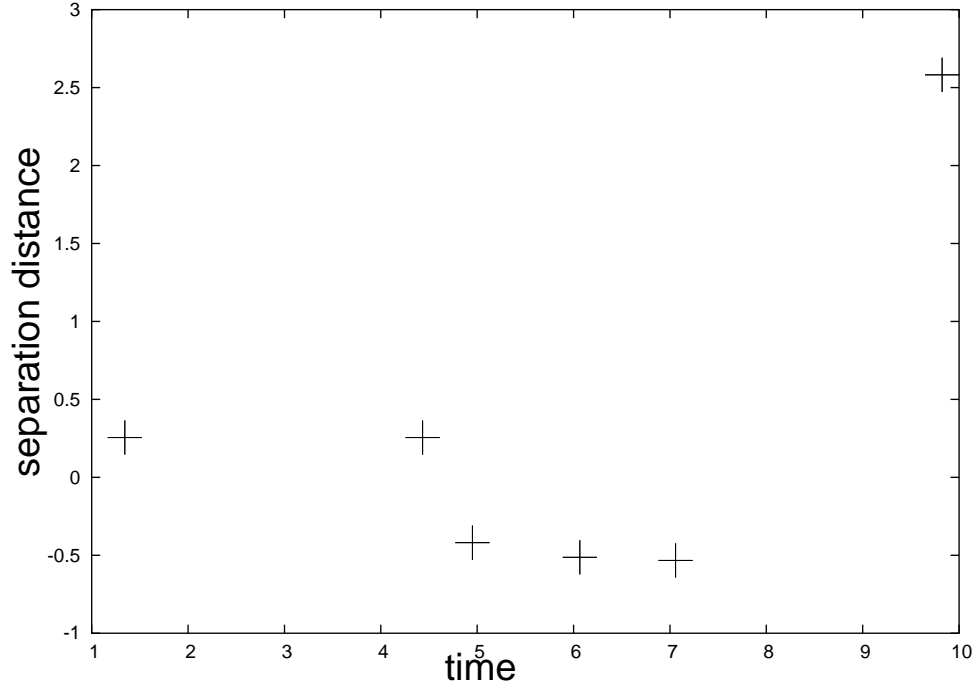
Figure 4.4: *Jump in separation caused by scattering from different sides of the same scatterer. The scatterer size is fixed so that the center to vertex distance is 1 and the length of each side is 1.701. The particles have an initial speed of 1 and are initially separated by a distance of 0.036, in these units. The last collision shows a very large change in the separation distance from about 0.05 to about 2.5. In the next collision (not shown) the particles hit different scatterers.*

sets of orbits that appear to be nearly free trajectories. Since these trajectories are nearly free we expect their square displacement to go as $t^2$. To see how this affects a system we shall return periodic lattice gas with four sided scatterers. First consider the dynamics of the lattice gas done on a torus or in a channel, figure (4.5).

The "walking orbits" are those orbits that appear because of the matching boundary conditions. For example if one were to form a torus by matching the boundary conditions of the cell there appears to be sets of trajectories which are
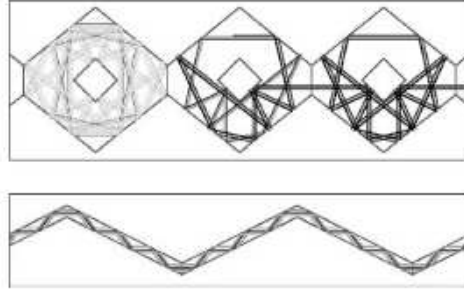
Figure 4.5: *Examples of walking orbits seen in studies of Lorentz channels by Sanders et al., for triangular scatterers placed along the upper and lower walls of the channel. These walking trajectories generally cause the motion of particles to be super-diffusive.*

periodic orbits. It is these orbits that are walking orbits on the full lattice. In a periodic gas these would travel very quickly through the system, effectively unhampered by the scatterers. One can see this by looking at the final distribution of points for a 4 (figure (4.6)), 12, (figure (4.7)), 20, (figure (4.8)), and 36 (figure (4.9)) sided polygons compared to that of circles figure (4.10).

The distributions of points for the four-sided systems appear to be very similar to that for circular scatterers except in four regions where the particle displacements are much greater than those for the rest of the distribution. These channel regions are similar to jets. It appears the trajectories in this region are traveling in a ballistic fashion. These are caused by sets of trajectories that bounce or walk between the sides of polygons without being substantially reflected as shown in figure (4.11). The walking trajectories occur because sides of different scatterers may be parallel, and because the system is periodic. The sides of the polygons act like the walls of a
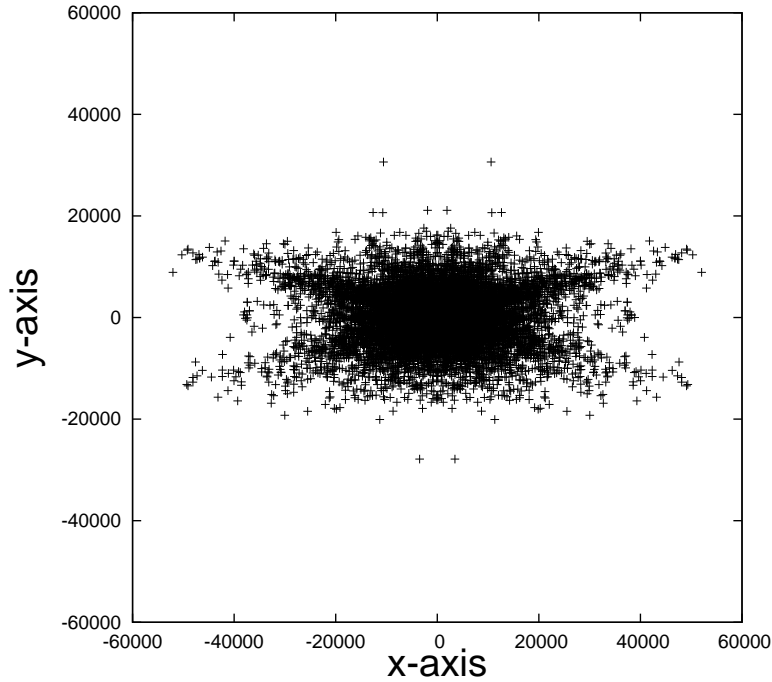
Figure 4.6: *Final distribution of positions for $10^4$ trajectories, after a time $10^5$ time units, for a system containing 4-sided scatterers. The scatterers are placed on an equilateral triangular lattice. The scatterer sizes and particle speed are as described in fig. (4.4). The inter-scatterer distance is of 3.64. The particles are started radially outward from a scatterer located at $(1.15, 1.15\sqrt{3})$ so that the angular separation between neighboring pairs of particles is $\frac{\pi}{5000}$. The "jets" are noticeable in the distribution.*

channel, or pipe, allowing the particles to travel ballistically. When we increase the number of sides of the polygonal scatterers we see that the "jets" for very long times as shown previously by Schmiedeberg for hexagons placed on honeycomb lattice [87].

As the number of sides increases the number of possible walking orbits in the system decreases. The decrease appears to be due to the fact that the walking orbits become less stable due to the additional number of vertices which cause
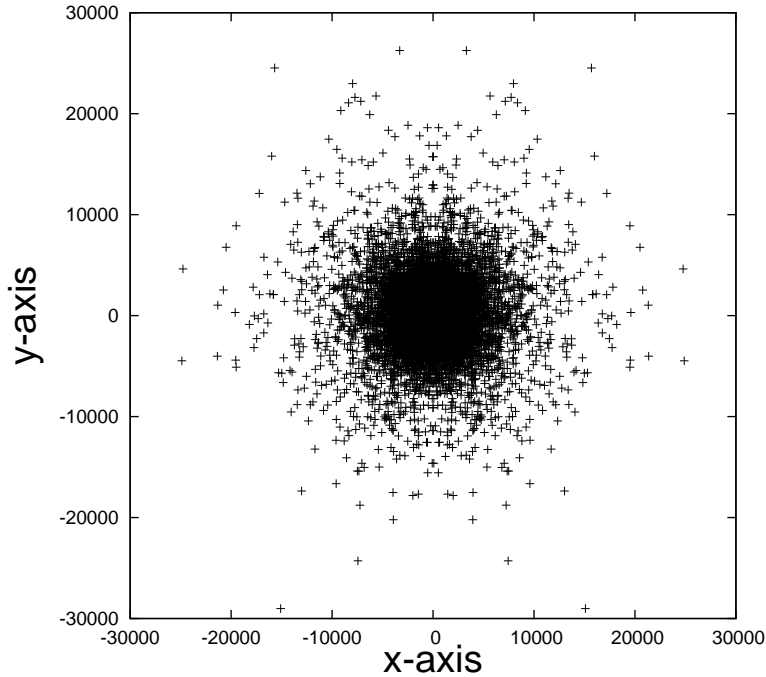
Figure 4.7: *Final distribution of positions for $10^4$ trajectories. after a time $10^5$ time units, for a system containing 12-sided scatterers. The scatterers are placed on an equilateral triangular lattice. The system parameters and angular separation of trajectories is as described in fig. (4.6).*

more trajectories to deviate from the walking orbits. As we introduce more sides more ballistic paths are blocked, until, in the limit of circular scatterers, where all trajectories are unstable and the ballistic trajectories occupy a set of measure zero in the space of all trajectories.

The reduction/blocking of walking trajectories would explain why certain non-chaotic systems exhibit diffusive behavior. In the instance of the randomly placed scatterers, the random placement of the scatterers blocks paths that lead to ballistic motion. In the case of the randomly oriented polygons the reduction of the number of parallel sides prevents trajectories from traveling in a ballistic fashion. In both

69
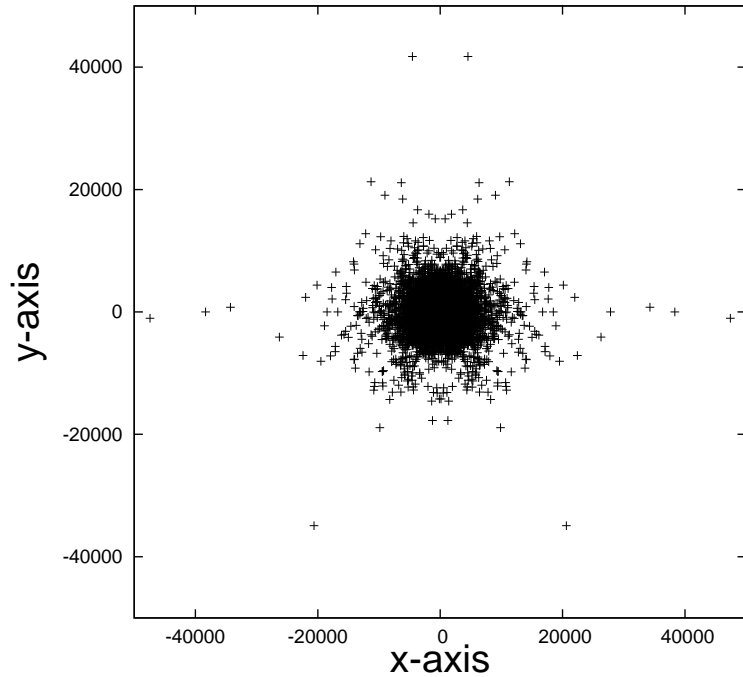
Figure 4.8: *Final distribution of positions for $10^4$ trajectories. after a time $10^5$ time units, for a system containing 20-sided scatterers. The scatterers are placed on an equilateral triangular lattice. The other parameters are as described in fig. (4.6).*

cases the systems appear diffusive on sufficiently long time scales [86].

Schmiedeberg and Stark find similar behavior for a honeycomb billiard [87], consisting of hexagonal scatterers shown in figure (4.12). Their results are shown in figure (4.13)

## 4.3  Transport Exponents

Let us once again look at our polygonal systems. If walking orbits do in fact affect transport, the transport exponent should change as the number of side changes. This is shown in fig. (4.14):

Here we consider the motion of a moving particle in a periodic system of polyg-

70
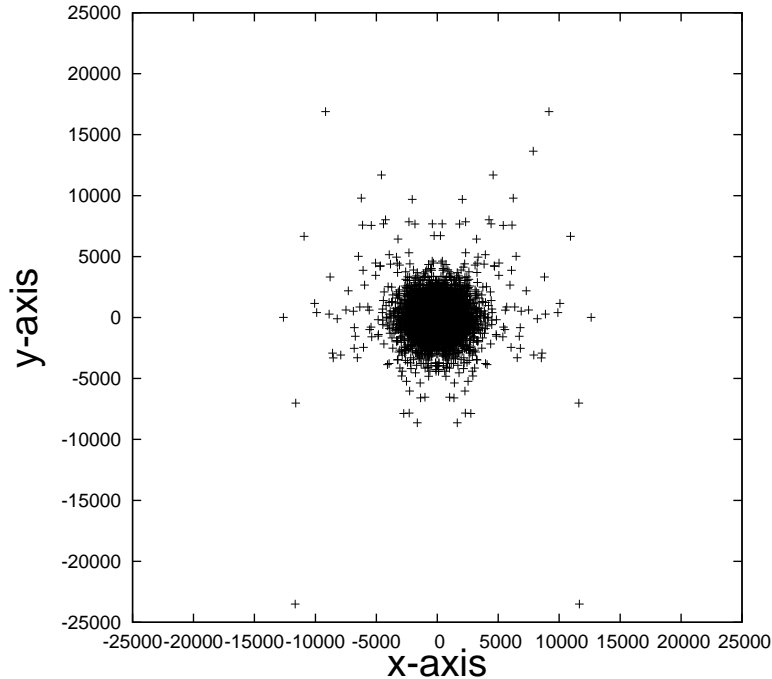
Figure 4.9: *Final distribution of positions for $10^4$ trajectories. after a time $10^5$ time units, for a system containing 36-sided scatterers. The scatterers are placed on an equilateral triangular lattice. The parameters are as described in fig. (4.6).*

onal scatterers. We recall that if the polygons were replaced by circles, the motion would be diffusive, while for the polygons it is super-diffusive with a transport exponent $\mu > 1$. Our numerical studies show that there appears to be a functional relationship between the number of sides and the transport exponent: We might try a functional relation of the form $\mu = 1/(n^y + 1) + 1$, since the transport exponent should asymptotically approach 1 as the number of sides goes to infinity. A possible functional relationship of this type is

$$\mu(n) = \frac{C}{(n+x)^y} + 1. \tag{4.1}$$

By fitting our numerical results to this form of $\mu(n) = \frac{C}{(n+x)^y} + 1$ we find that $C = 331.8, x = 48.7728, y = 1.532$. The best fit with error bars is shown in

71
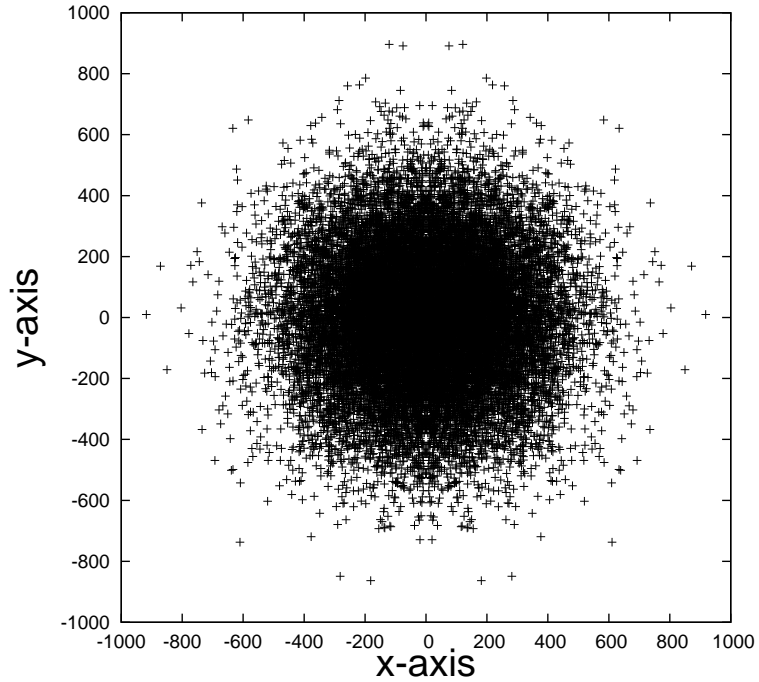
Figure 4.10: *Final Distribution represented for circular scatterers, with radius* 1, *on an equilateral triangular lattice. The inter-scatter distance, the initial conditions, and the final time are the same as those in fig. (4.1). For circular scatterers there do not appear to be any "jets."*

figure (4.15).

Of course this is only one of many possible forms and until a theoretical foundation is available, there is no way to decide among them.

## 4.4   Topology of Polygonal Billiards

In our previous discussions we have focused our attention on periodic, lattice systems in which point particles interact by colliding with polygonal scatterers. This type of system is known as an *external billiard* since all the interactions take place on the outside of the scatterer. Another type of billiard is called an *internal billiard*,
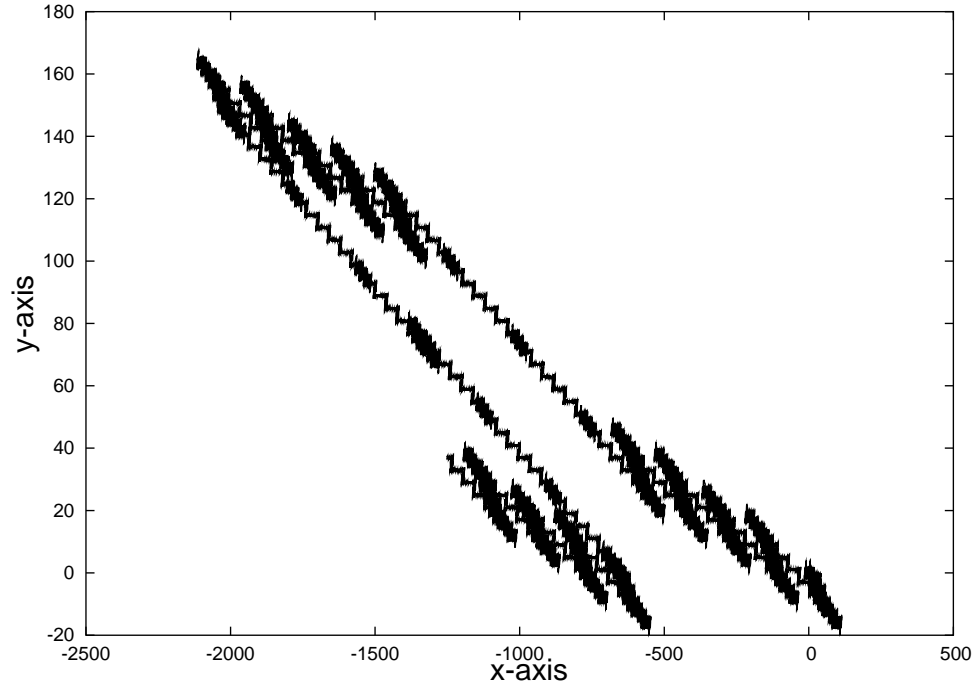
Figure 4.11: *A sample trajectory of a particle taken from the system shown in*

*fig. (4.1).*
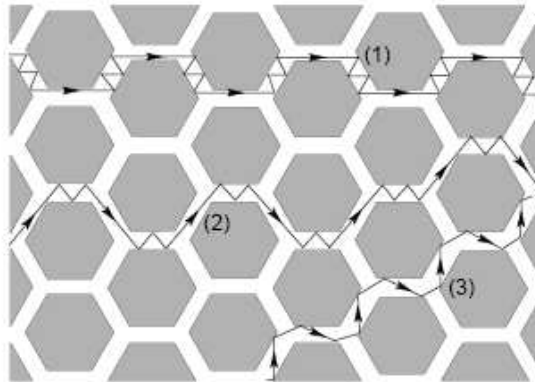


Figure 4.12: *The honeycomb billiard described in Schmiedeberg and Stark [87]. The*

*system consists of hexagonal scatterers on an equilateral triangular lattice. Also*

*shown are three examples of "walking orbits."*

where the particle motion takes place inside polygons or other shaped figures such

as a Bunimovich stadium [89]. Since the dynamics of internal billiards for simple
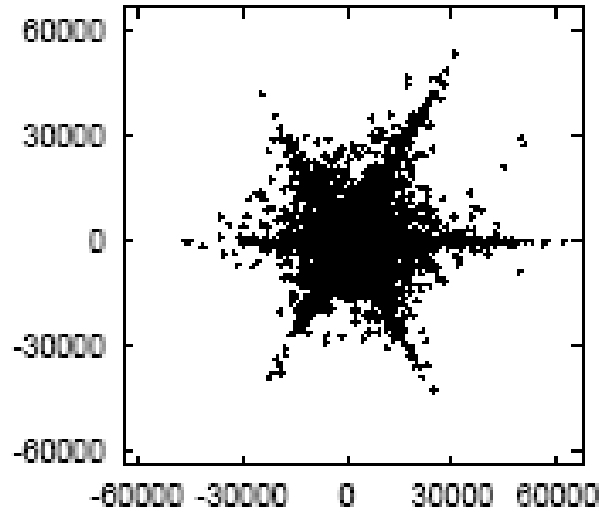
Figure 4.13: *Final Distribution of positions for a honeycomb billiard shown in fig. (4.12) [87]. The system consists hexagons with a radius (center to vertex distance) equal to 1 and the parallel sides of two adjacent scatterers forming corridors. The width of the corridors have a size 0.1 in terms of the radius. The systems is run with $10^4$ particles with velocity 1 are run for $10^5$ time units.*

polygons have been widely studied, it is useful to look at these systems to see if they can help us understand the dynamics of our external billiard systems.

The complexity of motion in an internal billiard drastically increases as one goes from motion inside simple polygons to motion in more complex arrangements [56, 89]. An example of an internal billiard widely studied is a rational, internal billiard which is a closed billiard table with internal angles that are rational fractions of $\pi$. The topological structure of the table in configuration space can be found by "tiling the plane" by using periodic reflection of cell [80, 89, 96]. An example of this tiling is a square billiard which yields a torus. This is the second simplest topological
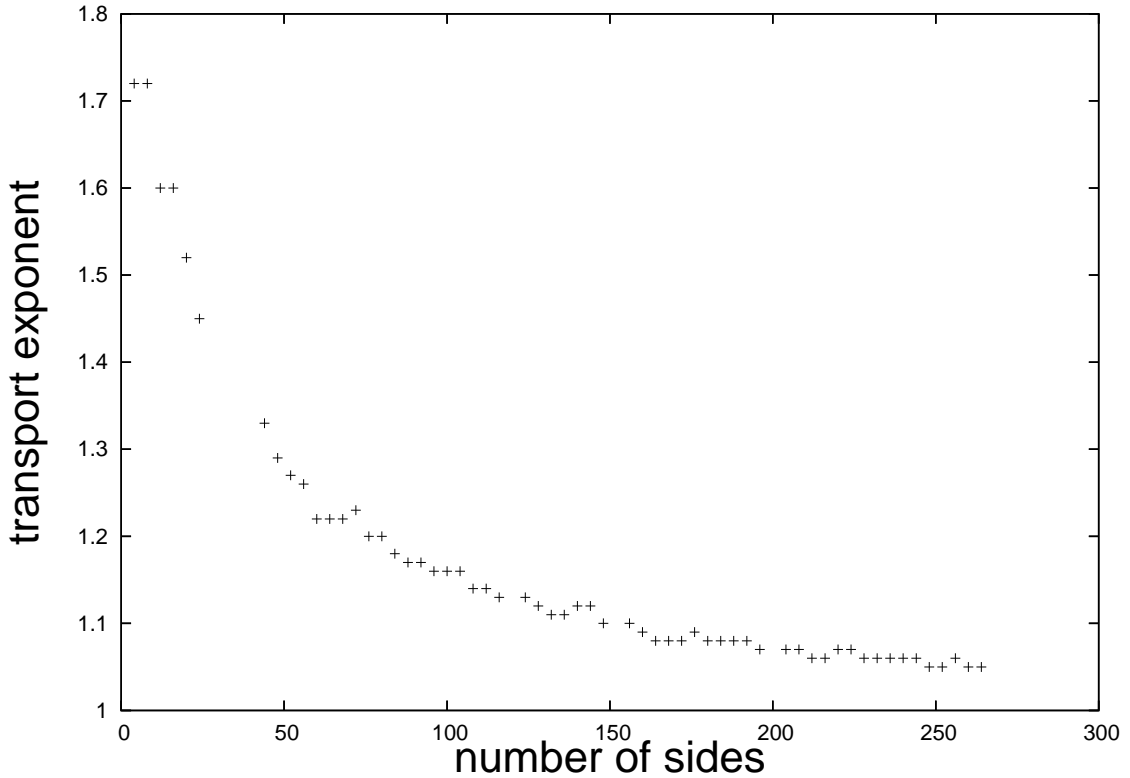
Figure 4.14: *Transport exponents as a function of the number of sides, for a system n-gon scatterers on an equilateral triangular lattice.*

genus with the first being a sphere[80, 56, 89]. If we put a scatterer inside the square, the topology changes. If we put a bar in the square [109, 57] the topology becomes that of two connected tori [101, 103, 104, 106]. If we replace the bar by a small square, the billiard is topologically equivalent to a five handled "pretzel" [80, 6]. Thus as we increase the number of scatterering surfaces the topology becomes more and more complex as show in figure (4.16 and 4.17). there also exist other more complex configurations as shown below:

As pointed out by Richens *et al.* Vega *et al.*, Gutkin, and Vivaldi *et al.* [80, 96, 56, 95], for genus larger than one there may exist isolated saddles which act like hyperbolic fixed points providing a "chaotic" type behavior. These would
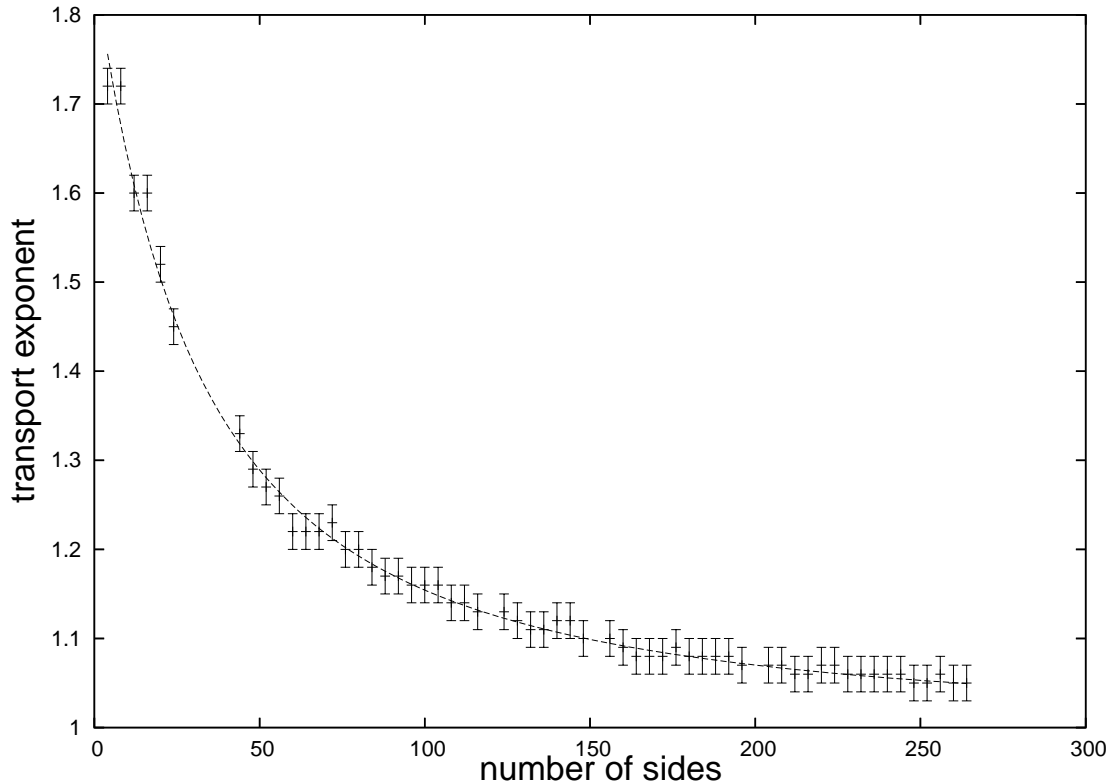
Figure 4.15: *Transport exponents as a function of the number of sides, for a system n-gon scatterers on an equilateral triangular lattice. Plot also shows the best fit for $C = 331.8, x = 48.7728, y = 1.532$ with error bars.*

correspond to the vertex splitting a polygonal billiard. These structures produce something like chaotic behavior for larger numbers of sides. This observation can be extended to include our external billiard system, where, as we have seen the vertex splitting provides a mechanism for the separation of trajectories. Thus even some trajectory pairs for systems of few-sided scatterers exhibit an effective non-zero Lyapunov exponent [96] as discussed in the previous chapter. Our models, which typically have algebraic separations of trajectories, are often said to display *weak chaos* [102, 39, 94, 7].
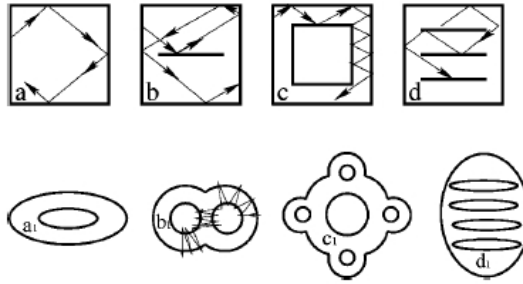
Figure 4.16: *Examples of simple internal billiards and their associated topologies. Motion of a point particle inside square cell, with specular collisions, is topologically equivalent to a torus. The addition a bar to the center of the cell yields two connected tori. Replacing the bar with square, one obtains a five handled pretzel as shown.*
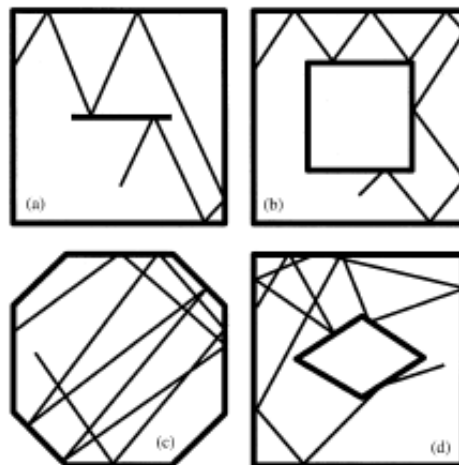


Figure 4.17: *Four examples of motion of a point particle inside boxes with bar scatterers and square scatterers.*

## 4.5 The Partial Van Hove Function

We next consider the partial Van Hove function for a periodic Lorentz gas with few-sided scatterers. When calculating the partial Van Hove functions we use

only small wave-numbers, $k$, since as $k$ grows the partial Van Hove function ceases to be a function and instead has the relevant curve shows self-intersections. That is, for every $Re(F_k(\mathbf{r},\mathbf{t}))$ there can exist several values of $Imk(\mathbf{r},\mathbf{t})$. In the last chapter we observed that the partial Van Hove function for large numbers of sides is stable. In other words, after 15 collisions the fractal appears the same and has the same dimension as an identical system run for $10^2$ collisions, or $10^3$ collisions or even $5 \times 10^3$ collisions. Therefore, it does not appear that these fractals change on time scales we can observe. We observe that for polygonal scatterers with a small number of sides, the partial Van Hove function changes its form over time, but for short times, on the order of tens of collisions, the curves still appear to be fractal. For longer times the curves develop self-intersections. Here we illustrate some of these curves for scatterers with different numbers of sides, starting with circular scatterers. For circular scatterers and for small $k$ values, the fractal dimension goes as $k^2$. As we decrease the number of sides from circles to polygons with $10^4$ sides fig. (4.18), to 500 fig. (4.19), to 100 fig. (4.20), to 60 fig. (4.21), to 20 fig. (4.22), and finally to squares fig. (4.23 4.24),and 4.25 and for $k = 0.1$, the partial Van Hove functions appear to be fractal, at least for short times.

It should be noted that at least for square scatterer the partial Van Hove appear relatively smooth. However, using the Hurst Exponent discussed in Chapter 2 we find the partial Van Hove function is fractal. I maybe a result of the computer not being able to distinguish the difference between a relatively rapidly varying function and a actual fractal. This would be computational limitations, and cannot be verified easily. Since, the Hurst exponent procedure returns the proper dimensions
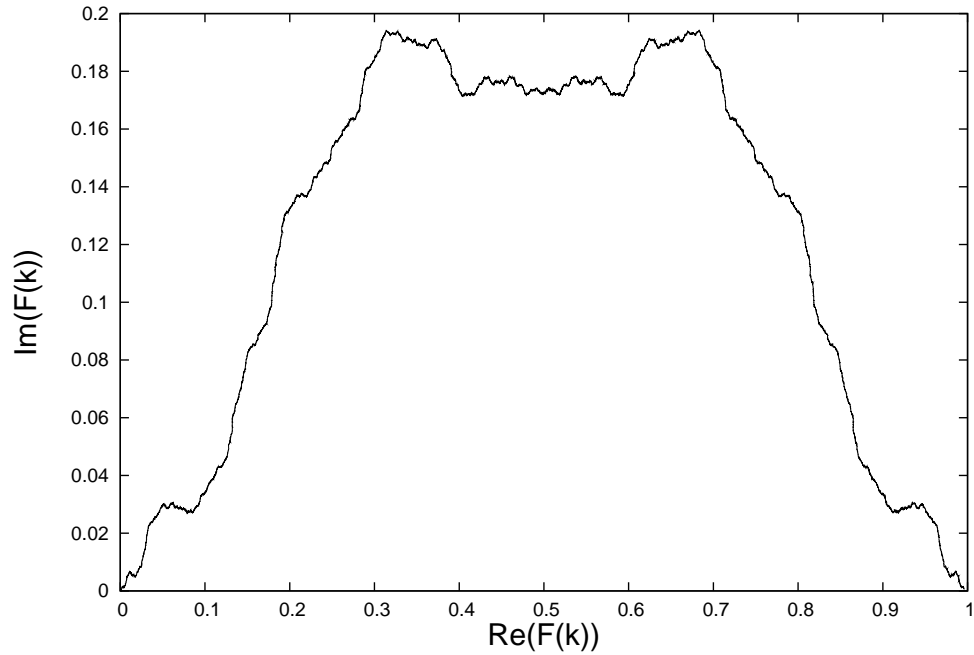
Figure 4.18: $Im(F(k))$ *vs.* $Re(F(k))$ *of the partial Van Hove Function for a system of point particles moving in a triangular Lorentz gas consisting of polygonal scatterers having* $10^4$ *sides.*

for smooth curves and known fractals, we shall say that the partial Van Hove for periodic Lorentz gas with square scatterers appears fractal.

The function changes appearance but for low $k$ and short times, the function appears to be a fractal. However, if we increase the time, the fractal ceases to exist. For example, one can see this for 4 sides as one increases the time to 40 collisions the graph develops self intersections as shown in figure (4.26). Likewise if one runs the trajectories for 200 collisions in a system of 40 sided polygons the partial Van Hove function develops self intersections as shown in figure 4.27). The range of $k$ values and time over which the partial Van Hove functions seem to be fractal depends on the number of sides of the polygons. For example for a square scatterer
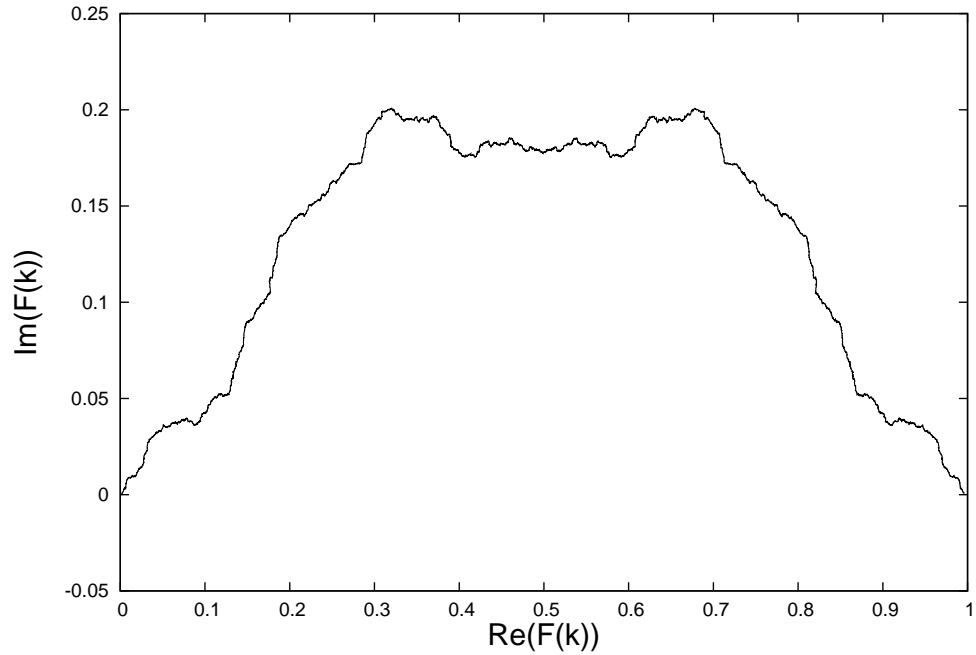
Figure 4.19: $Im(F(k))$ vs. $Re(F(k))$ of the partial Van Hove Function for a system of point particles moving in a triangular Lorentz gas consisting of polygonal scatterers having 500 sides. The fractal dimension for this curve is the same as that for circles approximated by the many-sided polygons.

system the range of $k$ values is $0 < k < 0.1$ and the upper limit of the time is less than 15 collisions. However, a $10^2$ sided scatterer system the range $k$ value is about $0 < k < 0.5$ and the time interval is about 50 collisions. These results indicate that these functions are not stable fractals, and one may not consider them fractals at all. The fractal structure exists only for short times. However for longer times the system loses its fractal structure and ceases to be a function as previously discussed. This perhaps gives one another test to check how "chaotic" a system is. One can consider the partial Van Hove function over time. The longer the partial Van Hove function exhibits fractal behavior the closer the system is to being a chaotic system.
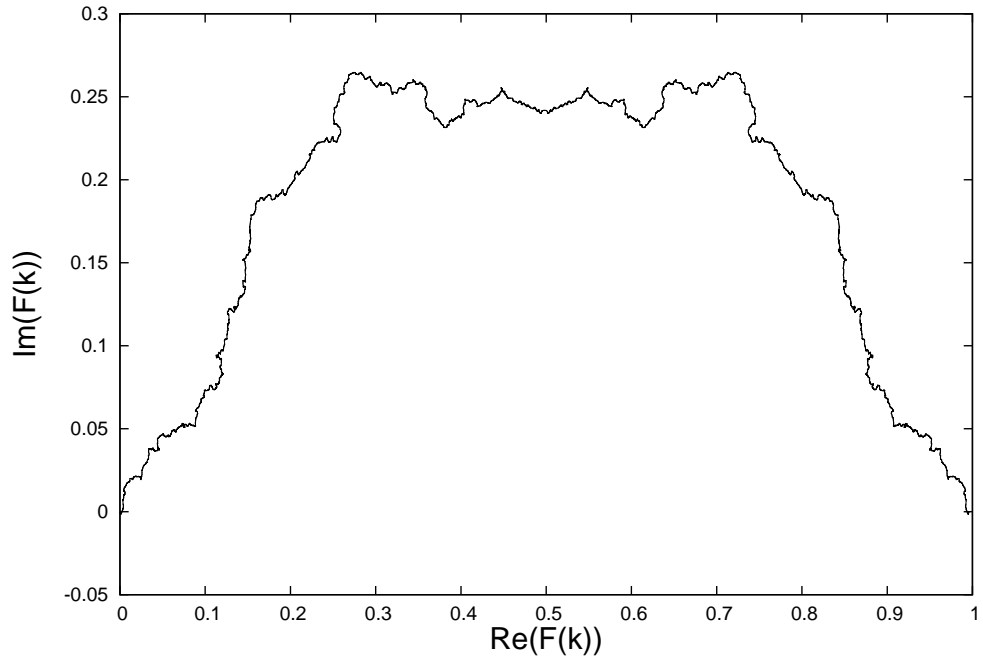
Figure 4.20: $Im(F(k))$ *vs.* $Re(F(k))$ *of the partial Van Hove Function for a particle moving in a triangular Lorentz gas consisting of polygons having* 100 *sides.*

So a system of $10^2$ sided scatterers would be more "chaotic" than a system of square scatterers. Recalling from the chapters 2 and 3 one observed the dimension of the partial Van Hove function want as $k^2$ [50, 51, 45]. We observe that for few-sided polygons, for short times, and for small $k$, the dimension of the partial Van Hove function goes a $k^2$. However, unlike the circular diffusive system the coefficient does not appear to have any significance because the system does not appear diffusive on any scale.

The existence of non-chaotic but diffusive models shows that chaos is not required for diffusion. As we saw in the previous section the generalized periodic Lorentz gas with few-sided polygonal scatterers are super-diffusive. One can change the system such that the system once again is diffusive. Thus, one can have few-sided
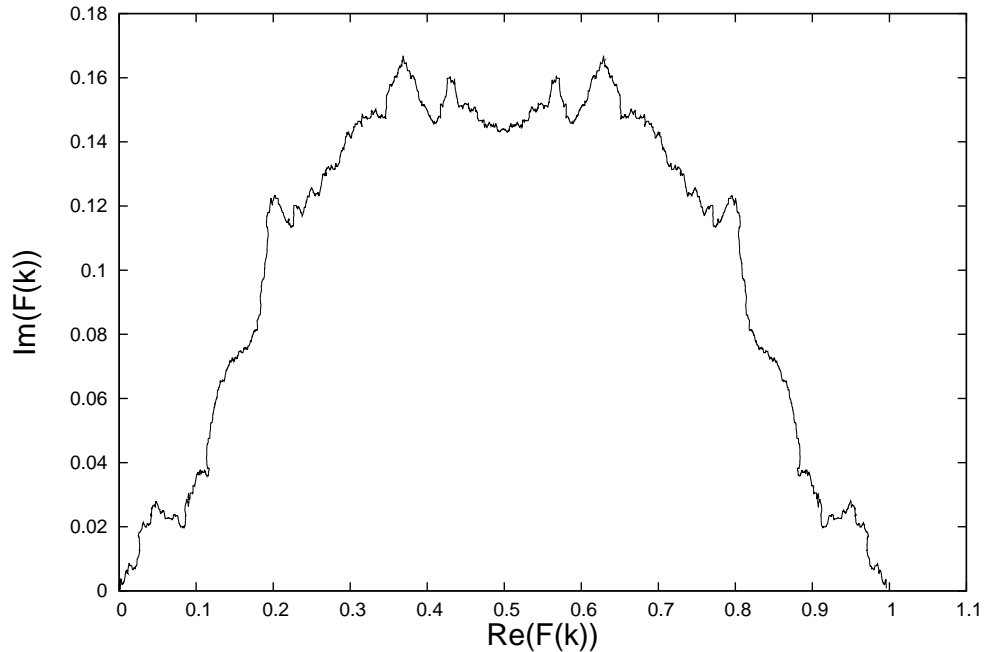
Figure 4.21: $Im(F(k))$ *vs.* $Re(F(k))$ *of the partial Van Hove Function for a system of point particles moving in a triangular Lorentz gas consisting of polygonal scatterers having* 60 *sides. The fractal dimension for this curve is the same as that for circumscribed circles as scatterers.*

(non-chaotic systems) which exhibit diffusion. Two such models were studied by Dettmann and Cohen [30]. The first is the standard Wind-tree model of Ehrenfest where the scatterers are placed randomly, and at low density. This system is diffusive [30, 38]. Dettmann and Cohen also considered cells containing randomly oriented scatterers (position and rotation) with 4 of scatterers per cell. The cells are put in a periodic array. This system was also found to be diffusive.

Dettmann and Cohen chose the size of squares to be $\sqrt{2}$ to keep their area equal to the area of the circles in a Lorentz gas, with a radius of $\sqrt{2/\pi}$. The number of scatterers $N$ per cell of length $L$ was set to be $N = L^2/4$. The velocity and the
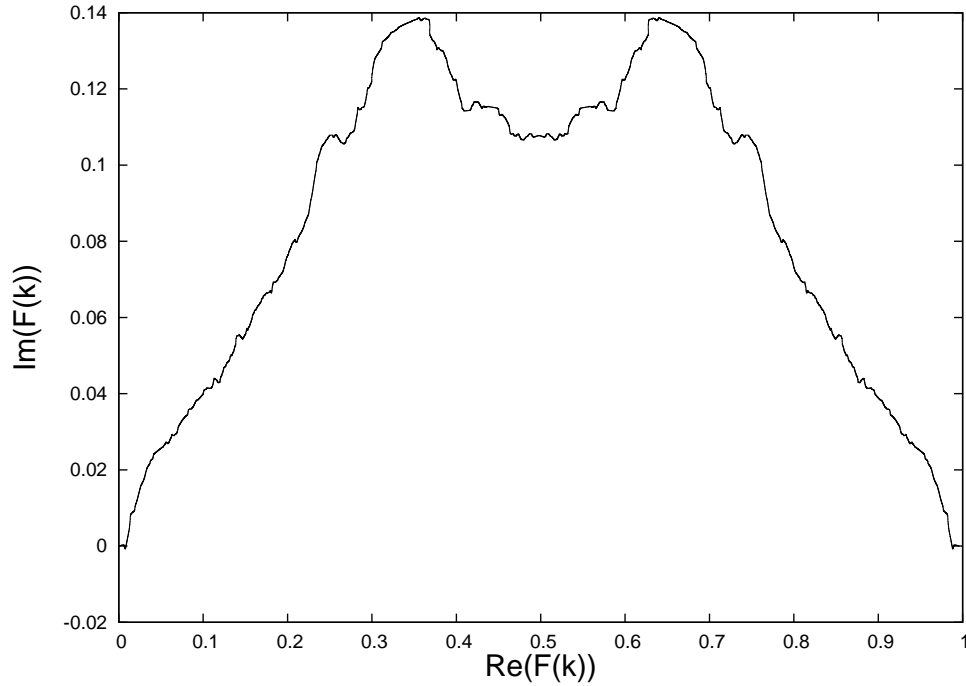
Figure 4.22: $Im(F(k))$ *vs.* $Ew(F(k))$ *of the partial Van Hove Function for a system of point particles moving in a triangular Lorentz gas polygonal scatterers having* 20 *sides. The fractal dimension for this curve is the same as that for circumscribed circles as scatterers.*

mass are set equal 1 . The diffusion constants for each of the system are listed in table (4.2).

Dettmann and Cohen considered 5 models that were diffusive. In this section we will consider three models that consist of scatterers placed in an effectively infinite plane. We also will look at the relationship found by Dettmann and Cohen between the diffusion coefficient and the number and types of periodic orbits [75]. The first infinite model Dettmann and Cohen considered was a system containing randomly placed squares/trees, a randomly placed wind-tree model. As previously described the sides of the trees to have a length of $\sqrt{2}$. The length of the cell was chosen to
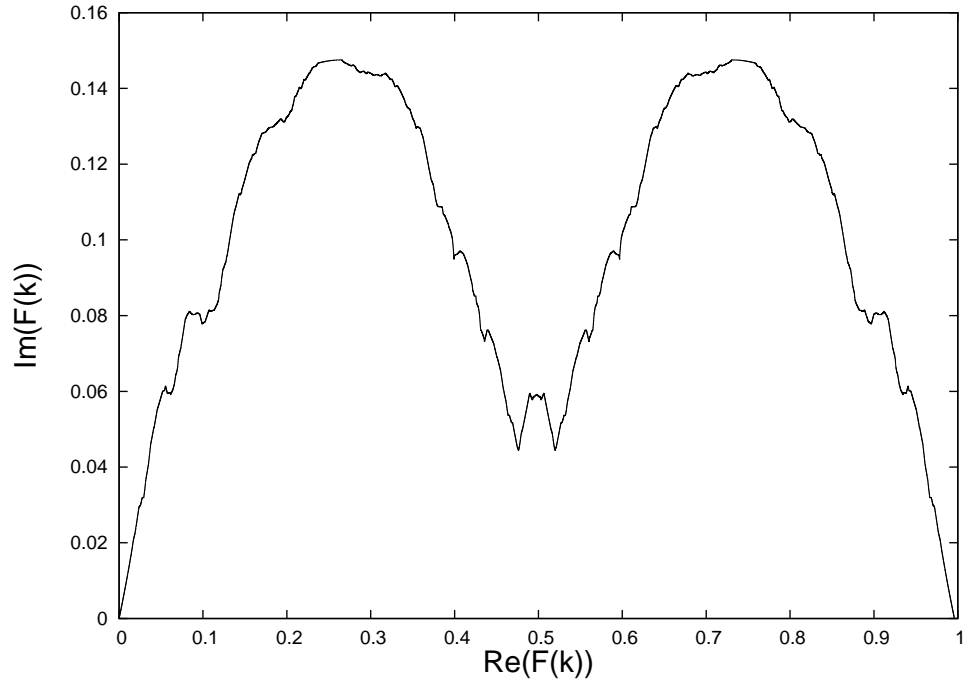
Figure 4.23: $Im(F(k))$ *vs.* $Re(F(k))$ *of the partial Van Hove Function for a system of point particles moving in a triangular Lorentz gas with square scatterers. The fractal dimension for this curve is the same as that for circumscribed circles as scatterers.*

be $L = 3500$ in units of scatterer's length. The number of scatterers was chosen to be $N = L^2/4$. These scatterers were randomly placed through out the cell, but they were not randomly oriented. The velocity and mass of the particles were set to be 1. The system was run for $t_f = 10^6$ time units which was sufficiently short that the particles never reached the edge of the cell. As a result the cell can be thought to have a length of $L = \infty$. They found the diffusion coefficient for this system to be $D = 0.44$, fig. (4.28).

The second infinite model they considered was a random Lorentz gas with circular scatterers. The radius of the scatterers was chosen to be $R = \sqrt{2/\pi}$.
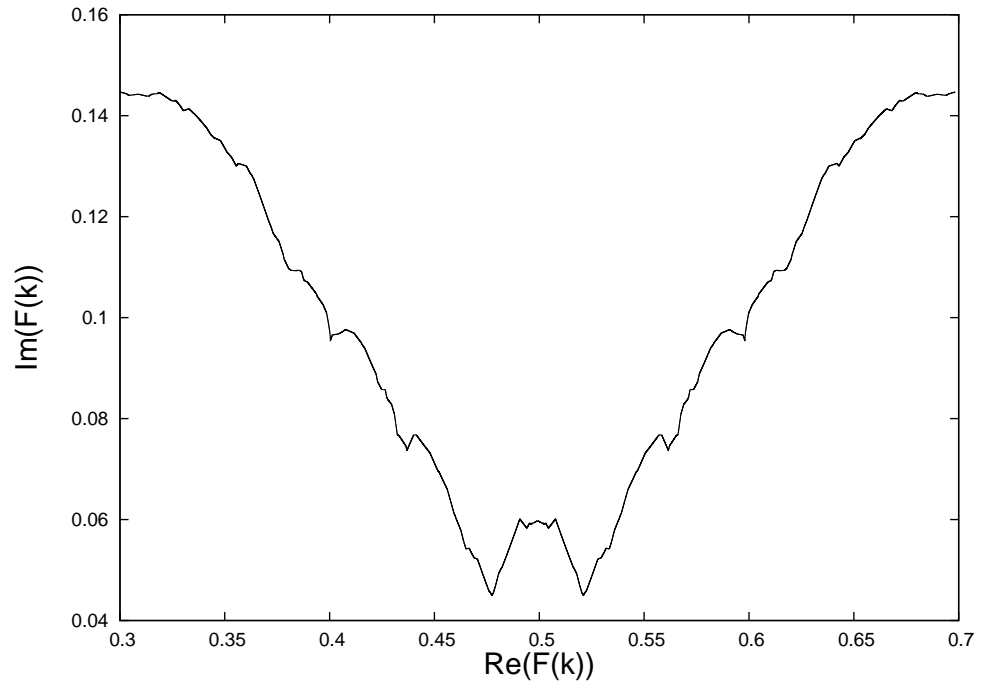
Figure 4.24: *A magnification of the partial Van Hove Function shown in Fig. (4.23), showing some of the fractal-like structure.*
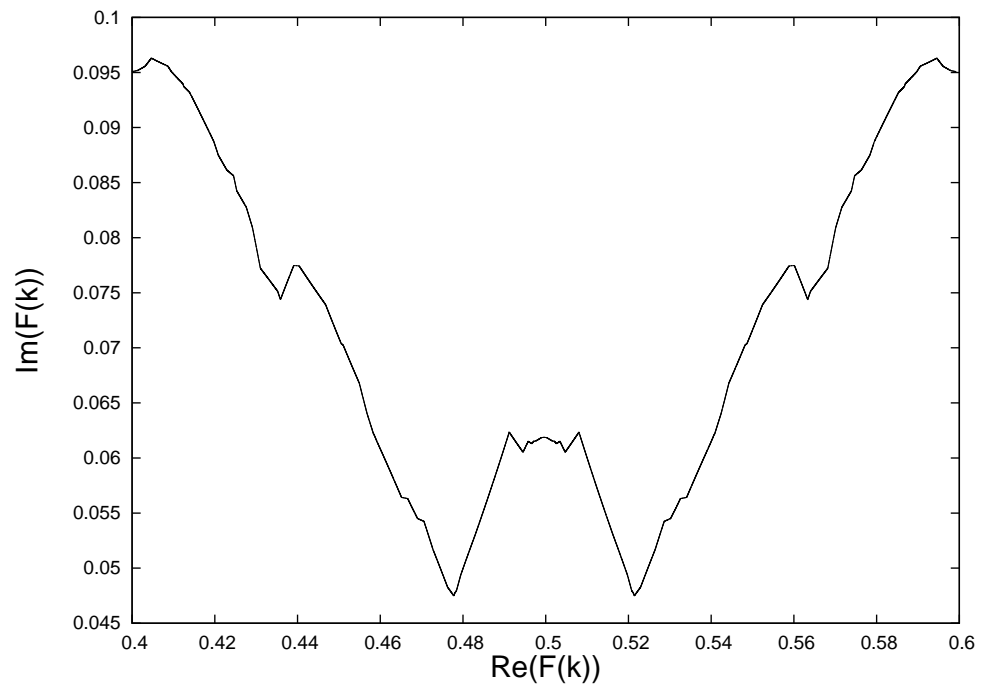


Figure 4.25: *A further magnification of the partial Van Hove Function shown in Fig. (4.24), showing some of the fractal-like structure.*
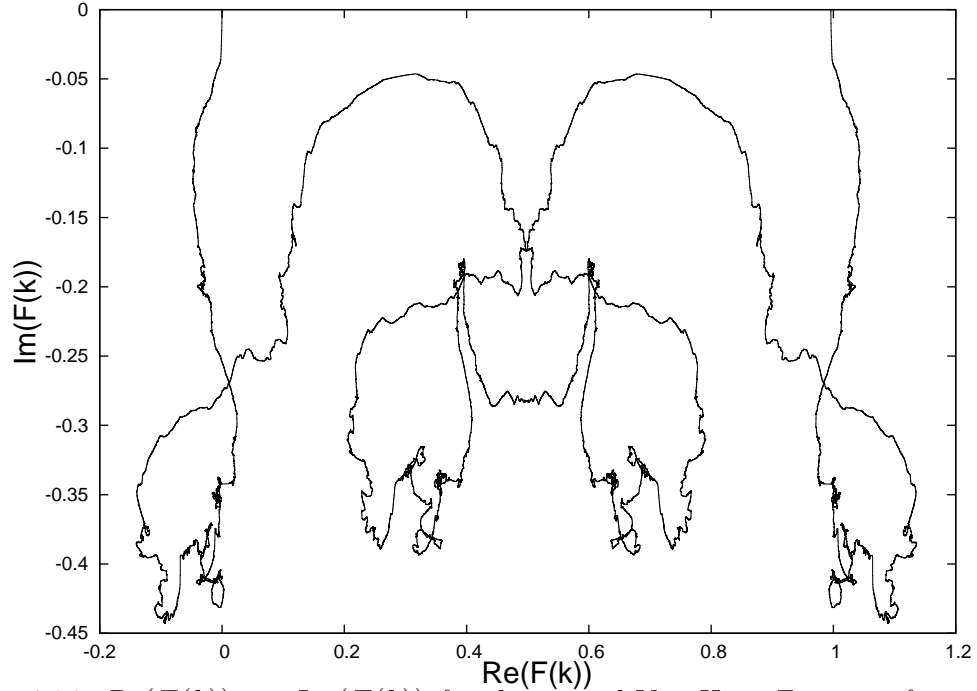
Figure 4.26: $Re(F(k))$ vs. $Im(F(k))$ for the partial Van Hove Function for a system with equilateral triangular lattice with square scatterers. The system is run for 40 collision times as opposed to 15 collisions used to obtain fig. (4.23).

The length of the cell and the number of scatterers were identical to the randomly placed wind-tree model. The scatterers were also randomly placed through out the cell. The velocity and mass of the particles were chosen to be 1. The system was run forthe same number of time steps, which was short enough that the particles never reached the edge of the cell. As with the randomly placed wind-tree model the system can be thought to have a length of $L = \infty$. They found the diffusion coefficient for this system to be $D = 0.27$, figure (4.29).

The last model was the randomly oriented wind-tree model. They chose the length of the sides of the trees so that their area would be the same as the circles mentioned above. The number and density of the scatterers were chosen to be the
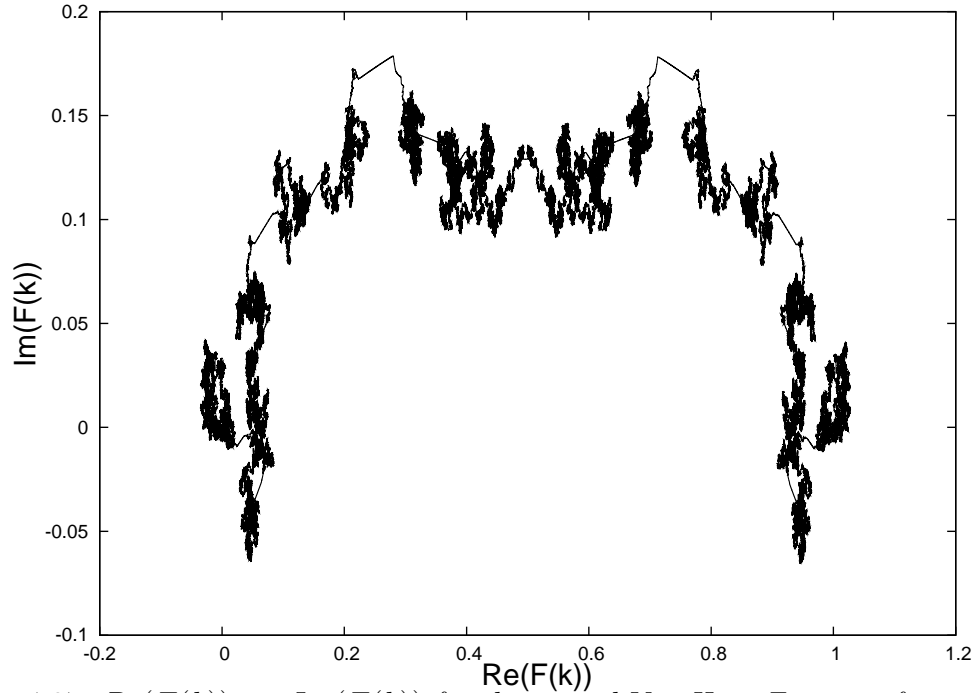
Figure 4.27: *Re(F(k)) vs. Im(F(k)) for the partial Van Hove Function for a particle in a triangular Lorentz gas with 40 sided scatters scatterers. The system is run for 200 collision times.*

same as the two models mentioned above, but they were rotated by some randomly chosen angle. Dettmann and Cohen found the diffusion coefficient for this system to be $D = 0.14$, figure (4.30).

Dettmann and Cohen argue that the differences in values of the diffusion coefficient were related to the number and type of periodic orbits. For the randomly placed wind-tree model, there exist no periodic orbits in the randomly placed model except for very rare special orientations of groups of scatterers. This follows from a result of Aarnes [30]. For the Lorentz gas with circular scatterers, there are an infinite number of unstable periodic orbits in the system. Lastly for the randomly oriented model, Dettmann and Cohen showed that a period 3 orbit can always be

Table 4.2: *Systems which were found to be diffusive by Dettmann and Cohen [30] with the associated diffusion coefficients.*

| System | D |
|---|---|
| Randomly oriented and placed squares | 0.14 |
| Randomly placed circles | 0.27 |
| Randomly placed squares | 0.41 |

found if the scatterers' sides outline an acute triangle as shown in fig. (4.31). The probability of these types of configurations in a randomly oriented wind-tree is non-zero. Further one can show that these orbits are quite stable. A sample of such a system is provided in fig. (4.31). As a result of these considerations Dettmann and Cohen argued that the comparatively high value of the diffusion coefficient for the randomly placed wind-tree model was a result of the lack of periodic orbits. Particles cannot get trapped for extended periods of times and diffuse quickly through the system. In the case of the circular Lorentz gas, trajectories close a periodic orbit, shadow the orbit for a short time then diverge from it. Thus the diffusion coefficient for the circular Lorentz gas has a diffusion coefficient comparatively smaller than the randomly placed wind-tree model. Lastly for the randomly oriented wind-tree model with stable periodic orbits, shadowing trajectories remain near the periodic orbit for extended period of time. As a result the randomly oriented wind-tree model had a comparatively smaller diffusion coefficient, suc a gas is shown in figures (4.28, 4.29, 4.30).

Other polygonal systems have been found to be diffusive as well. One such
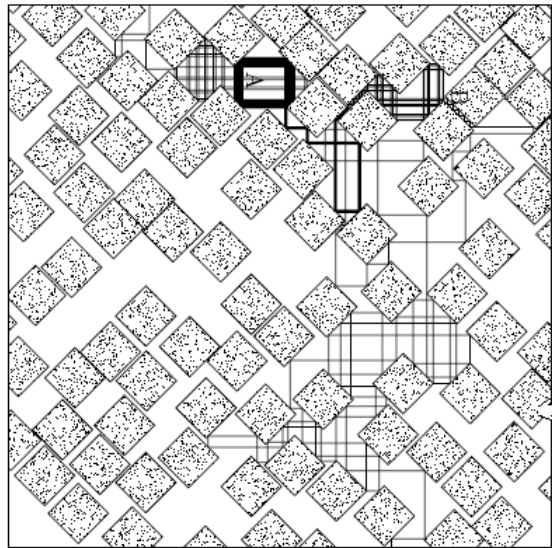
Figure 4.28: *A Lorentz gas with square scatterers, randomly placed. This model is found to be diffusive, and there are no periodic orbits [30].*
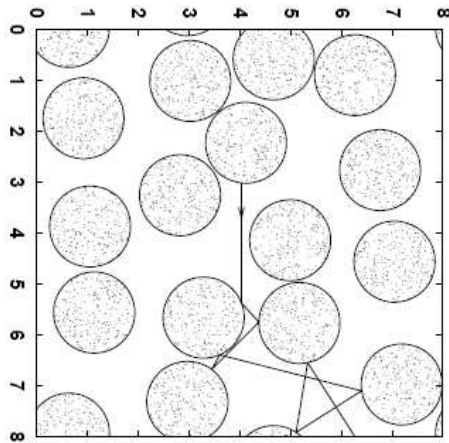


Figure 4.29: *A segment of a gas with randomly placed circular scatterers. This system is diffusive, and there are an infinite number of unstable periodic orbits [30].*

system is composed of rhombi with irrational angles [2, 3, 66]. In the next chapter we will discuss work of Alonso *et al.* who constructed models with the entire range of behavior - sub-diffusive, diffusive, to super-diffusive. We explore similar systems in the next chapter, where we consider polygonal scatterers with irrational angles, as opposed to the polygons with rational angles considered so far, and see how this change in angles affects the diffusive properties of the systems studied.
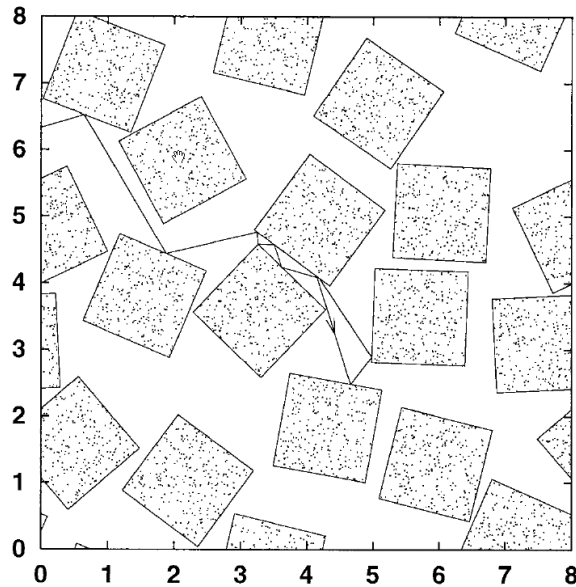


Figure 4.30: *A segment of a Lorentz gas with randomly placed and randomly oriented square scatterers. This system is found to be diffusive, and has a relatively low diffusion coefficient when compared to the other models illustrated in figs. (4.28) and (4.29). Dettmann and Cohen argue that this low value is due to stable periodic orbits in this system [30].*
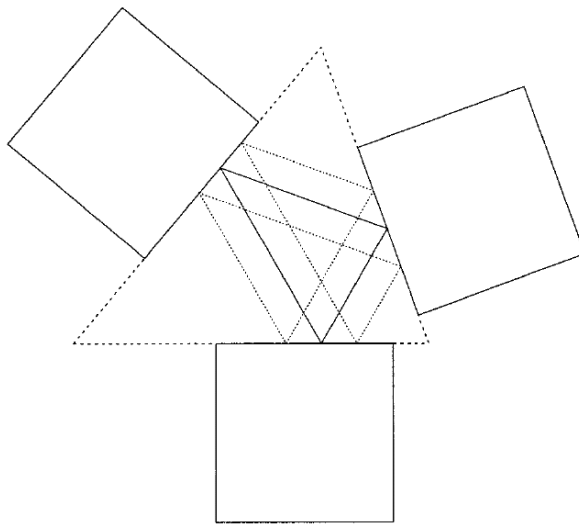
Figure 4.31: *Stable periodic orbits for an arrangement of square scatterers. These orbits appear to cause the diffusion coefficient to be smaller than those for other models studied by Dettmann and Cohen [30].*

## 4.6 Fractional Diffusion

### 4.6.1 Fractional Calculus

The remaining portion of this chapter will be devoted to the use of fractional diffusion equations for studying the properties of particle motion in pseudo-chaotic systems - non chaotic systems with complex dynamics. Pseudo-chaotic systems are systems with zero Lyapunov exponents, and with weakly mixing dynamics [39, 107]. Weak mixing is defined in terms of the time correlation function of two functions of the mechanical variables, $R_k$, given by:

$$R_k(f, g) = < f(T^k x)g(x) > - < f(x) >< g(x) > \tag{4.2}$$

where $T^n x$ shifts x to a new time $t_0 + nT$. The weak mixing property is that

$$\lim_{n \to \infty} \frac{1}{n} \sum_{k=0}^{n-1} R_k(f, g) = 0 \tag{4.3}$$

For example, the complex dynamics in wind-tree models provide a "random walk" behavior although these systems have zero Lyapunov exponents [102, 103, 104]. It is well known that a description of the properties of pseudo-chaotic systems requires a very sophisticated mathematical treatment [89, 106]. For example, we have already noted the fact that the motion of a particle in a periodic array of polygonal scatterers is equivalent to motion on a surface with holes specified by the genus number of the surface, determined by the number of sides of the polygons. For those systems that are super- or sub- diffusive, one would like to have a generalization of the diffusion equation with a corresponding Green's function that leads to the appropriate transport exponent, either greater or less than unity, in the same way

that the normal diffusion leads to the linear growth of the mean square displacement. Zaslavsky and co-workers have pioneered the use of the so-called *fractional calculus* to construct such generalized diffusion equations. For a detailed discussion of the fractional calculus see [99, 104, 106].

So far we have considered the rate of growth of nearby trajectories, the box counting dimension of the partial Van Hove function and the transport properties of pseudo-chaotic systems. We now describe how the methods of fractional calculus may be used to refine our understanding of the flow of particles in these systems. To do this we present here a brief overview of fractional dynamics and the predictions it makes for these polygonal billiard systems.

Most familiar physical phenomena are described mathematically by differential equations with integral powers of the various differential operators. For example, the equation relating force and momentum is one such equation, namely [99]:

$$\mathbf{F} = \frac{d\mathbf{p}}{dt}. \tag{4.4}$$

In this case the first time derivative of the momentum of a particle is the force on it. Normal Brownian motion is described by differential equations of first order in time and second order in space. However, there are a large number of physical systems that cannot be described easily by *integral*-order differential equations. These include the pseudo-chaotic systems discussed here when the mean square displacement grows as at non-integer power of time. Therefore it may be useful to find equations that describe these phenomena. Fractional calculus enables one to define any real power of a differential operator, and show that the definition has an integer form

that corresponds with the ordinary powers of these operators.

To develop the fractional calculus [99] we first consider an integral operator acting on some function, $f(t)$,

$$(Jf)(x) = \int_0^x f(t)dt. \tag{4.5}$$

If we repeat the integration we obtain:

$$(J^2 f)(x) = \int_0^x (Jf)(t)dt = \int_0^x \left( \int_0^t f(s)ds \right) dt. \tag{4.6}$$

By doing this an arbitrary number of times, we obtain the Cauchy formula:

$$(J^n f)(n) = \frac{1}{(n-1)!} \int_0^x (x-t)^{n-1} f(t)dt. \tag{4.7}$$

The fundamental observation needed for the development of fractional calculus is that one can extend the Cauchy formula to non-integer values of $n$ by replacing the integer $n$ by a real number, $\alpha$, and replacing the factorial by a Gamma function. We note that

$$n! = \Gamma(n+1). \tag{4.8}$$

A *fractional integral* of the function $f(t)$ may now be defined for arbitrary $\alpha$ as:

$$(J^\alpha f)(x) = \frac{1}{\Gamma(\alpha)} \int_0^t (x-t)^{\alpha-1} f(t)dt. \tag{4.9}$$

We extend this line of reasoning to define fractional derivatives. Consider the power series expansion of a function and examine the repeated derivative acting on one term of this expansion, $x^k$, say:

$$\frac{d^a}{dx^a}(x^k) = \frac{k!}{(k-a)!} x^{k-a}. \tag{4.10}$$

94

Now by replacing the factorials with Gamma functions we can define the fractional derivative of any power of $x$ and by extension, the fractional derivative of any function that can be represented by a power series. Thus

$$\frac{d^a}{dx^a}(x^k) = \frac{\Gamma(k+1)}{\Gamma(k-a+1)}x^{k-a}. \tag{4.11}$$

That is, to get the fractional derivative of a function one simply takes the fractional derivative of all terms in its power expansion [99].

## 4.6.2 The Fractional Diffusion Equation

Now, with the general ideas of fractional calculus we will once again consider a billiard trajectory where the scatterers are squares or a slit pattern as shown fig. (4.32), shown below:

We see that though the system is not chaotic, there is some indication that many of the trajectories may be self-similar. We can test this assumption using our data by means of the fractional calculus using an argument of Zaslavsky. The Zaslavsky form of the fractional diffusion equation for the probability $P(y,t)$ of finding the moving particle at a distance $|y|$ from the origin at time $t$ is [104, 106]:

$$\frac{\partial^\beta P(y,t)}{\partial t^\beta} = D_f \frac{\partial^\alpha P(y,t)}{\partial |y|^\alpha}. \tag{4.12}$$

Here $D_f$ is a constant that plays the role of the diffusion coefficient in the fractional diffusion equation. It is left unspecified here.

One can relate the exponents $\alpha$ and $\beta$ in Eq. (4.12) to the transport exponent $\mu$ by constructing solutions to this equation. In this way one finds

$$\mu = 2\frac{\beta}{\alpha}. \tag{4.13}$$

Note that for $\beta = 1$ and $\alpha = 2$ one obtains both the ordinary diffusion equation as well as the usual form of the transport exponent, $\mu = 1$! One possible solution of this equation satisfies the scaling relation

$$P(|y|, t) \sim t^{-\mu/2} P_0(\frac{|y|}{t^{\mu/2}}), \tag{4.14}$$

where $\mu = 2\beta/\alpha$. The fact that the solution satisfies a scaling relation implies that there may be a renormalization group treatment of the motion of the moving particle in much the same way as ordinary Brownian motion can be analyzed using renormalization group methods [27]. This is discussed in detail by Zaslavsky and co-workers [10, 104, 106]. We wish to use our simulations to check the scaling law, Eq. (4.14).

Assuming that Eq. (4.14) applies to out system, we can easily show that the moments of the displacement can be written in the following form:

$$\langle |y|^{2m} \rangle = const * t^{m\mu}. \tag{4.15}$$

We can use our data to check this expression in two separate ways.

1. We can fix the number of sides of a polygon and vary the values of $m$ in the scaling equations for the moments, Eq. (4.15), and

2. We can repeat this procedure by varying the number of sides of the polygons.

If the trajectories appear to have a self-similar structure - namely that they look roughly the same if we change the scale of observation - then we can expect that the scaling law should be satisfied to some degree. Below we present some sample

96

trajectories for a systems containing 4 sided scatterers in fig. (4.33) and 36 sided scatterers in fig. (4.34).
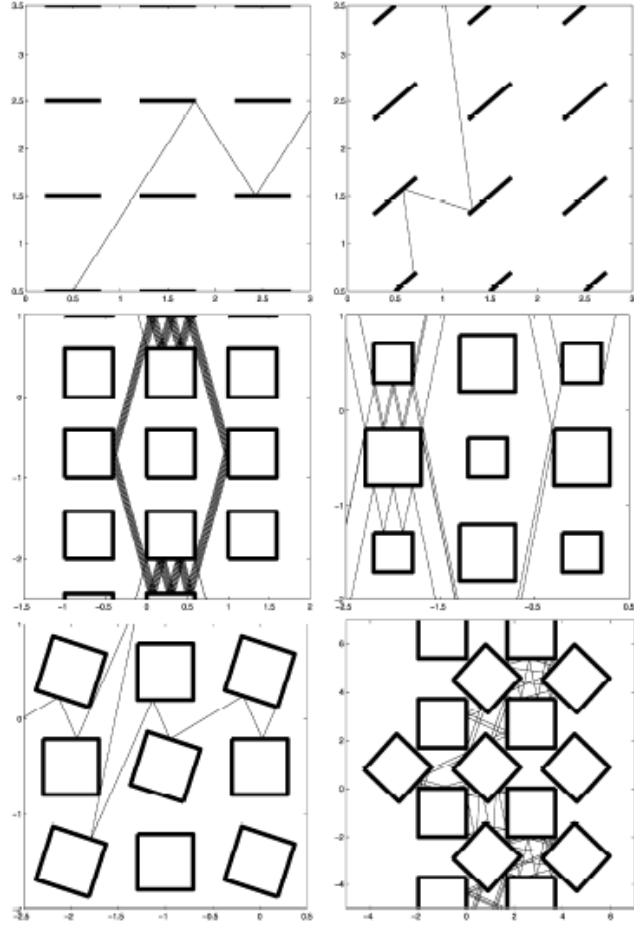


Figure 4.32: *Particle trajectories in Lorentz gases with four-sided or with bar scatterers.*

If we consider other nonzero moments of the system $< x^{2m} >$ for $2m = 4, 6, 8, 10..$ we find that the transport exponent scales as given in Eq. (4.16),

$$\langle |y|^{2m} \rangle = d(n, m) t^{m\mu(n)} \tag{4.16}$$

where $n$ denotes the number of sides of the polygons, $d(n, m)$ is a constant that depends upon the number of sides and the moment of the displacement, and $\mu(n)$
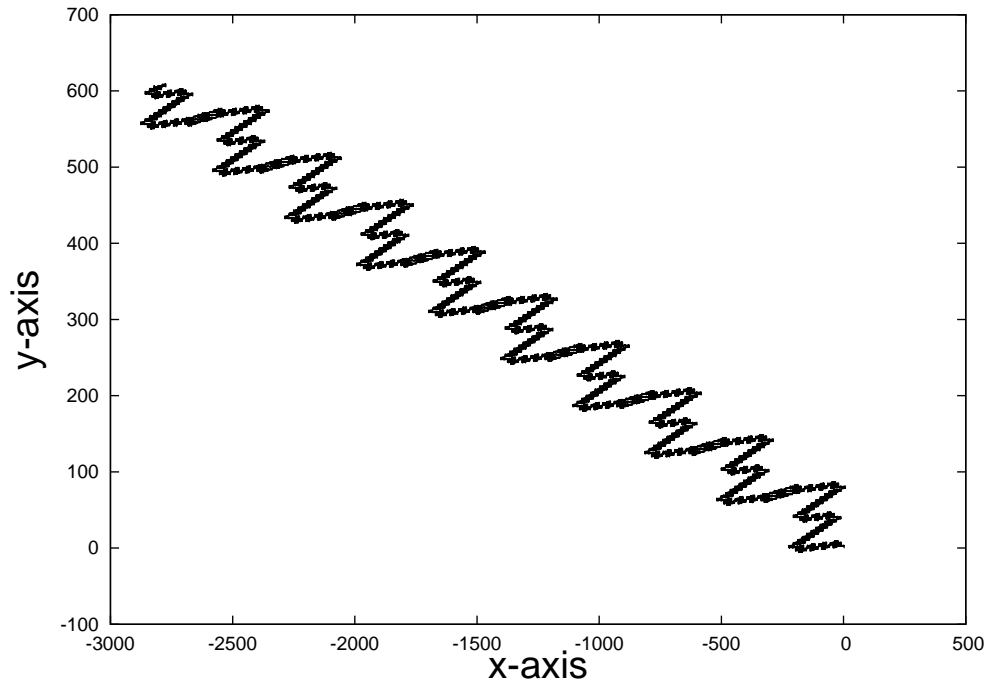
Figure 4.33: *An example of a particle trajectory in a system containing square scat-terers.*
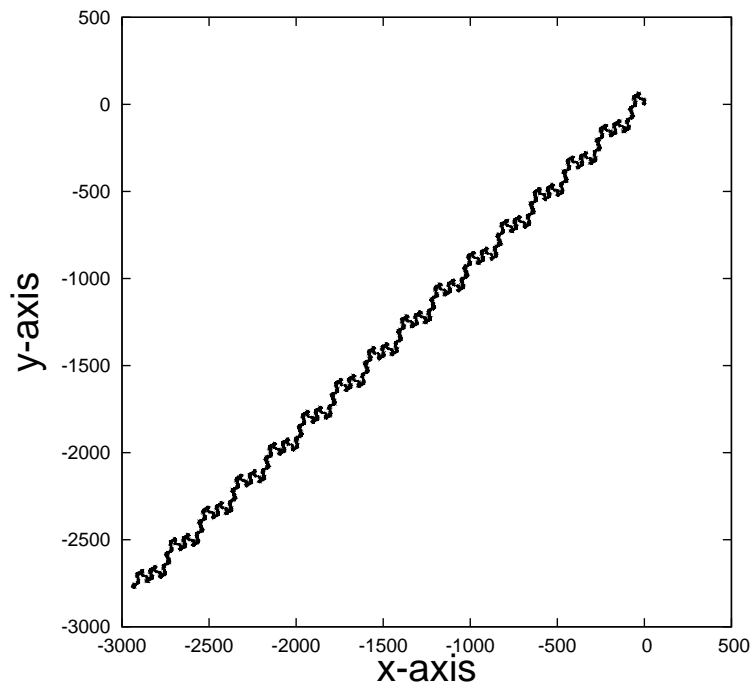


Figure 4.34: *An example of a particle trajectory in a system containing 36 sided scatterers.*

is the transport exponent for the mean square displacement in an arrangement of $n$-sided polygons. Our numerical results verify the scaling relations for a wide range of sides and values of the moments. Moreover we find that there is a scaling relation for the coefficients $d(n, m)$

$$d(n, m) = (d(n, 2))^m. \qquad (4.17)$$

For polygons with few numbers of sides as shown in table (4.3). For simplicity we will write

$$a(n, m) = \ln d(n, m). \qquad (4.18)$$

Table 4.3: *Values of the mth transport exponent and the mth transport coefficient for a system consisting* $n = 4, 8, 12, 16, 20, 24, 44, 48$ *and* 52 *sided polygons on a triangular lattice. According to the scaling formula,* $\mu(n, 2m) = m\mu(n, 2)$, *and* $a(n, 2m) = ma(n, 2)$.

| n | $\mu(n, 2)$ | $a(n, 2)$ | $\mu(n, 4)$ | $a(n, 4)$ | $\mu(n, 6)$ | $a(n, 6)$ | $\mu(n, 8)$ | $a(n, 8)$ |
|---|---|---|---|---|---|---|---|---|
| 4 | 1.71 | -1.148 | 3.566 | -2.385 | 5.482 | -3.586 | 7.423 | -4.769 |
| 8 | 1.73 | -1.32 | 3.56 | -2.79 | 5.48 | -4.20 | 7.43 | -5.59 |
| 12 | 1.60 | -1.860 | 3.39 | -3.773 | 5.21 | -5.148 | 6.94 | -5.31 |
| 16 | 1.592 | -1.550 | 3.4712 | -3.801 | 5.736 | -7.280 | 7.884 | -9.457 |
| 20 | 1.522 | -1.274 | 3.254 | -2.812 | 5.096 | -3.977 | 7.086 | -5.509 |
| 24 | 1.44 | -1.023 | 3.168 | -2.578 | 5.089 | -4.071 | 7.028 | -4.946 |
| 44 | 1.327 | -0.917 | 3.059 | -3.081 | 4.954 | -4.580 | 6.746 | -4.613 |
| 48 | 1.285 | -1.072 | 2.868 | -2.594 | 4.941 | -5.566 | 7.020 | -7.702 |
| 52 | 1.27 | -0.855 | 2.946 | -3.103 | 4.880 | -5.271 | 7.210 | -8.494 |

We will plot and fit the moments to a linear represented by the equation $\mu(m) = a * m$ to check the validity of Zaslavsky relation in figs. (4.35), (4.36), and (4.37) for the n=8, 20 and 48. We also check the coefficients in Figs. (4.38)-(4.40).
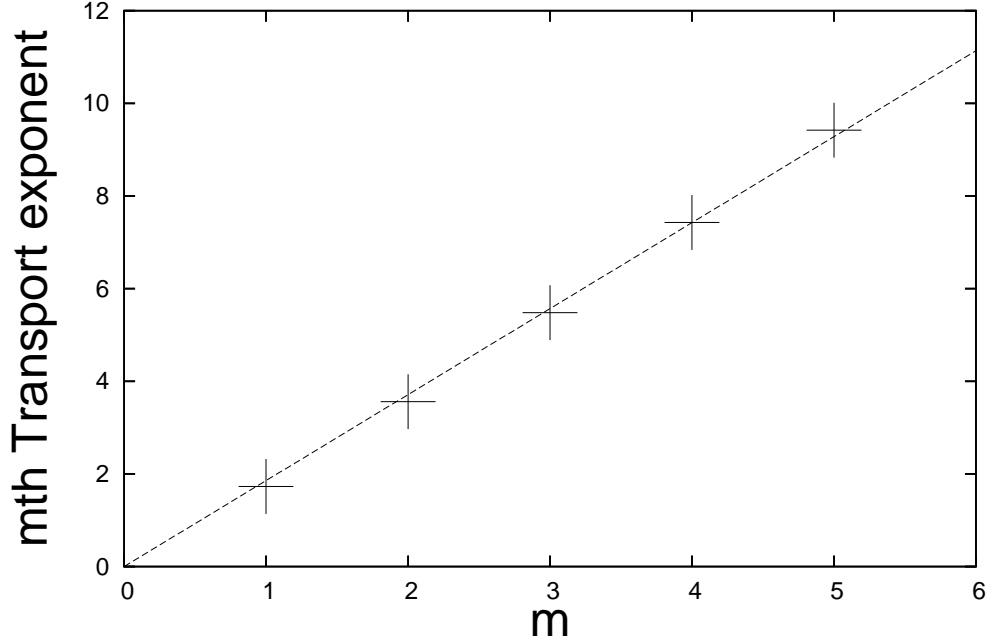


Figure 4.35: *The transport exponent for m=1,2,3,4, and 5 for a system containing 8 sided polygons. The best fit line shows a linear relationship as predicted by Zaslavsky.*

The results shown in figs. (4.38), (4.39), and (4.40) are certainly consistent with the scaling formula

$$\langle |y|^{2m} \rangle = d(n, m) t^{m\mu(n)}, \tag{4.19}$$

for few-sided polygons. The results of Zaslavsky provide us with a useful tool for analyzing motion in periodic, polygonal systems. We find that the moments of the displacement satisfy scaling relations and are self similar. These results add further support to the idea that the super-diffusive motion in these systems is due to walking
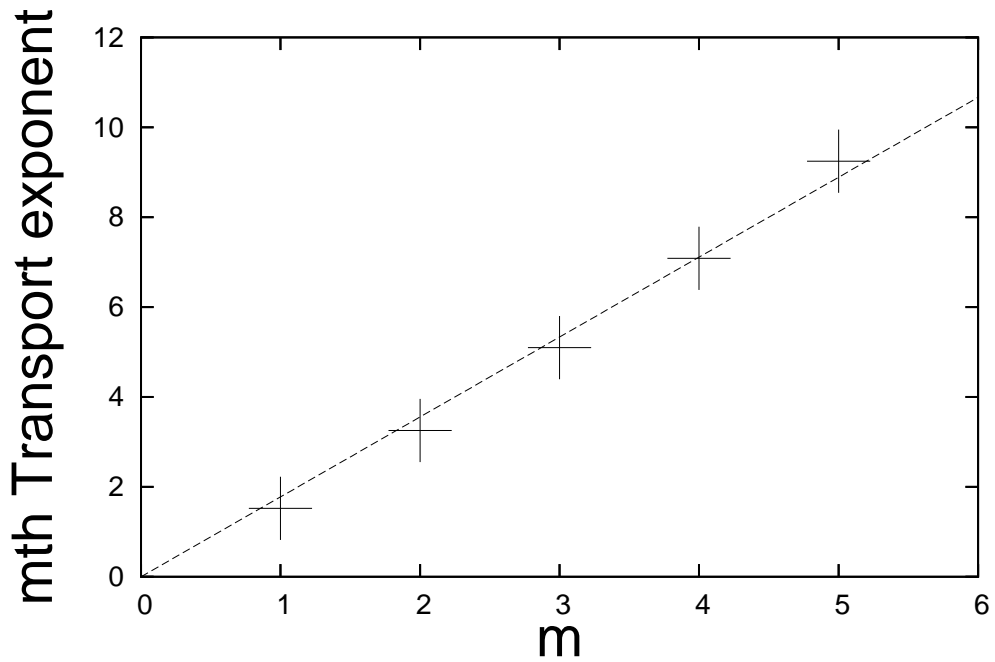
Figure 4.36: *The transport exponent for m=1,2,3,4, and 5 for a system containing* 20 *sided polygons. The best fit line is shown showing a linear relationship as predicted by Zaslavsky.*

orbits that travel across the system in a systematic, rather than random, way. The motion of a Brownian particle also satisfies a scaling property but one must look at the trajectories on a very coarse scale to see self similar properties, otherwise the motion looks very random [27].
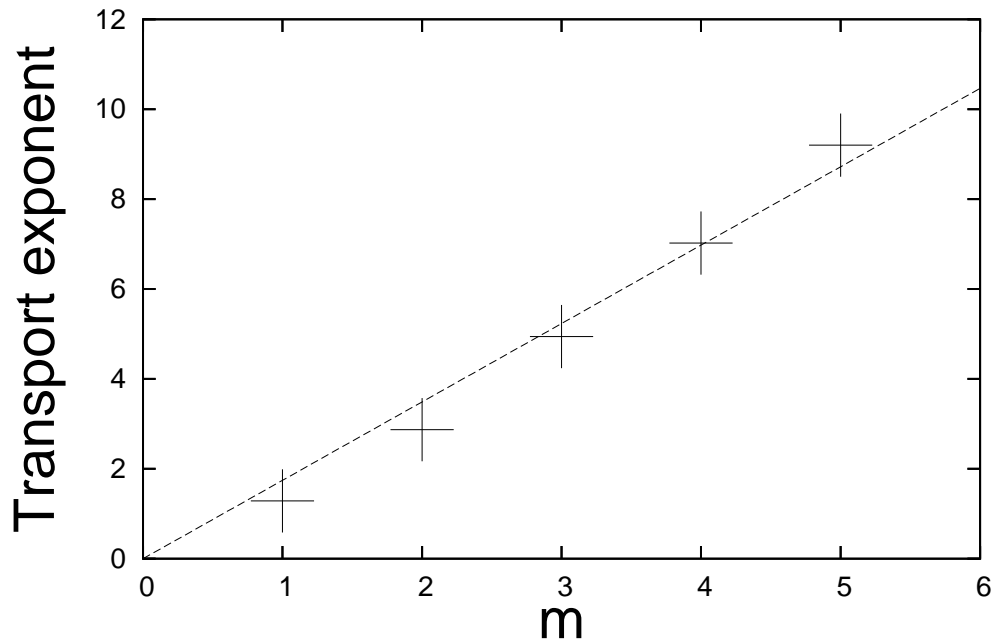
Figure 4.37: *The transport exponent for m=1,2,3,4, and 5 for a system containing 48 sided polygons. The best fit line shows a linear relationship as predicted by Zaslavsky.*
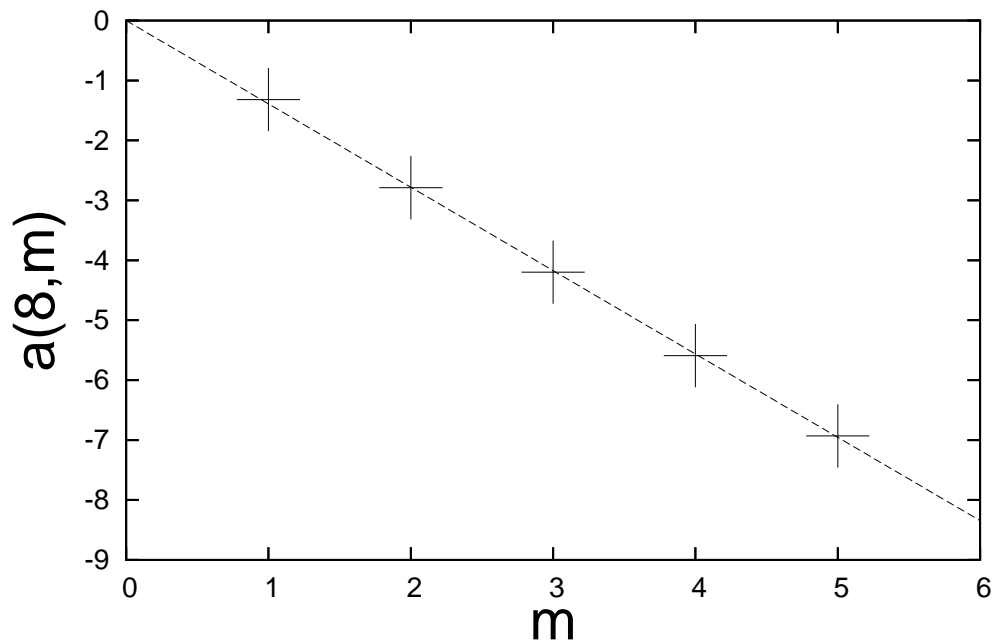


Figure 4.38: *The coefficients $a(n,m) = \ln d(n,m)$ for m=1,2,3,4,5 for a system containing 8-sided polygons. The best fit line is consistent with the scaling relation, $a(n,2m) = ma(n,2)$.*
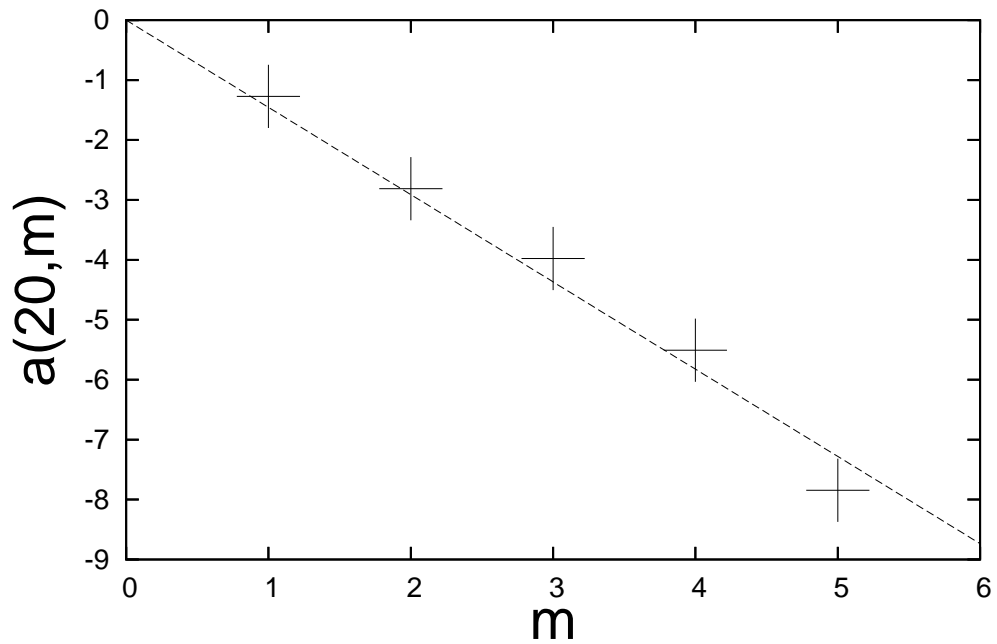
Figure 4.39: *The $a(n, m)$ for m=1,2,3,4,5 for a system containing $m = 20$ sided polygons. The results are consistent with the scaling relation, $a(n, 2m) = ma(n, 2)$.*
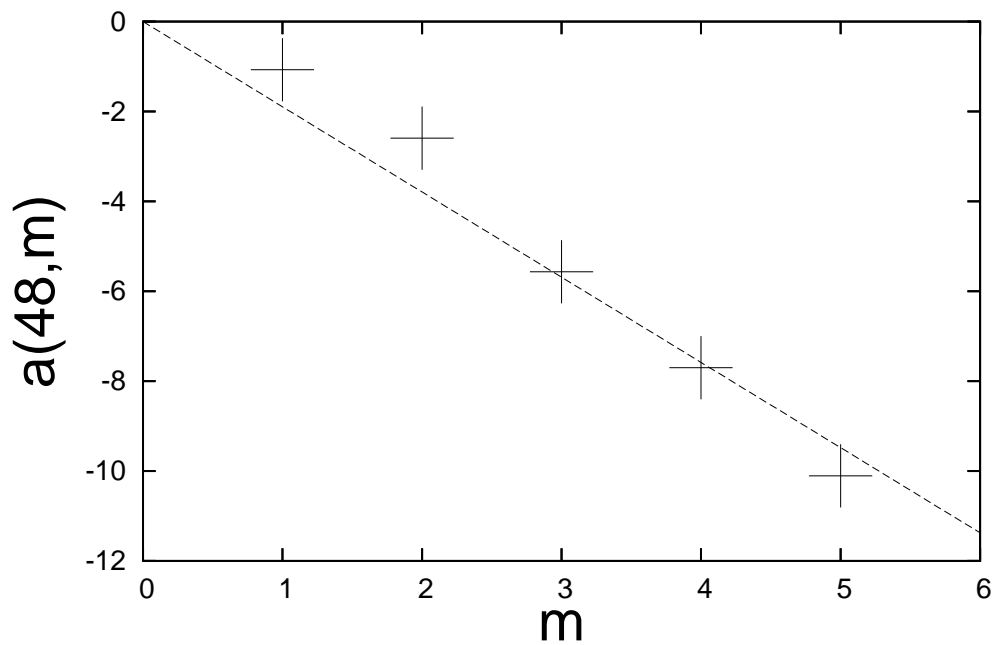


Figure 4.40: *The $a(n, m)$ and the best fit line for m=1,2,3,4,5 for a system containing $m = 48$ sided polygons.*

Chapter 5

Random Systems and Irrational Scatterers

## 5.1   Particle Transport in Randomized Polygonal Billiards

In the preceding chapters we considered circular, chapter 2, and polygonal, chapters 3-4, Lorentz gases, as in figures (5.1).
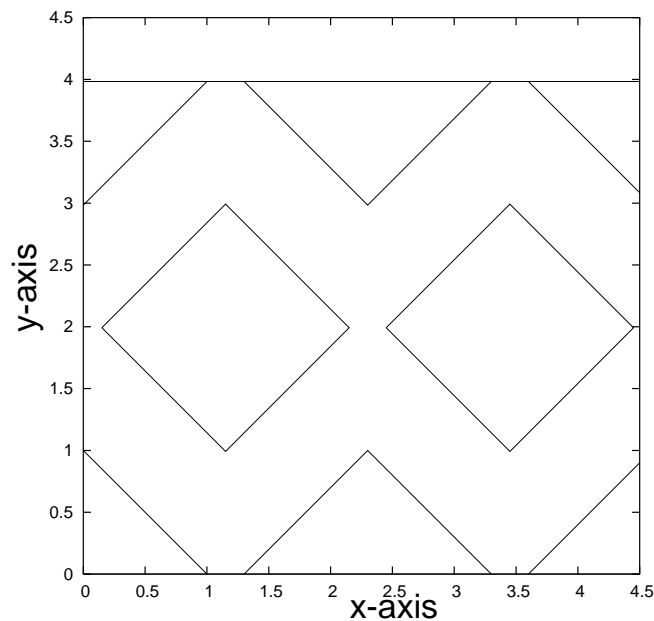


Figure 5.1: *A section of a polygonal periodic Lorentz gas, containing squares. The scatterers are equidistant from one another and placed at the vertices of equilateral triangles. The scatterers are also placed so that there are no unbounded trajectories exist in the system.*

We observed that for certain polygonal systems, with large numbers of sides, one can coarse grain the initial starting conditions so transport behavior of the system appears diffusive, although the system is probably slightly super-diffusive. We have also observed that periodic, polygonal Lorentz gases, with polygons of fewer than 100 sides are certainly not diffusive. Moreover the system cannot be coarse grained to have appearance of a diffusive system. However, we know from Dettmann and Cohen's work that certain randomized systems of square scatterers as well as some periodic arrangements of scatterers, are diffusive [30]. The systems considered by Dettmann and Cohen are shown in figs. (5.2)-(5.5).

However, from Dettmann and Cohen's studies it is unclear what makes certain systems diffusive and other systems super-diffusive. Further Dettmann and Cohen limited their research to square scatterers. In this section we construct a simple diffusive model with as few randomized scatterers as possible. We will first start by examining periodic systems, non-random systems, and consider the dynamics of these systems which might cause them to be super-diffusive behavior. We will then consider how one might randomize such systems to make them diffusive. Lastly we will consider a periodic pseudo-one dimensional channel systems with randomly oriented scatterers [2, 3, 16, 18, 37, 67, 69, 70, 73, 78, 86]. We will see that such systems have wide variety of transport behaviors, including normal diffusion; moreover, we will see that the orientation of the scatterers affects the transport behavior.

We recall that a polygonal gas with scatterers with few sides placed on a periodic lattice was found to be super-diffusive. When simulating a periodic system, one

105
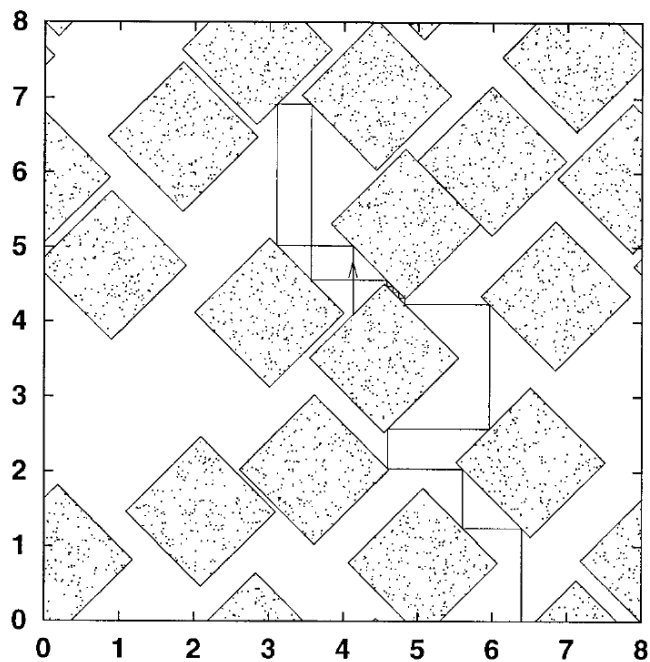
Figure 5.2: *One unit cell in a periodic version of the Ehrenfest wind-tree model. The scatterers are squares (trees) with diagonals oriented along the x and y axes. The trees are randomly placed within the unit cell and the entire cell is then repeated periodically covering the infinite plane. Particle transport in this system is super-diffusive [30].*

places a unit cell on a torus. When a trajectory crosses one the specified "boundary lines" on the cell, we increase or decrease a corresponding winding number by one unit. Then due the symmetry of the system, we consider the particle to be in the next unit cell and we continue to follow its motion.

On a torus or in a channel such as that illustrated in fig. (5.6), but with periodic boundary conditions, there appear to be sets of trajectories which are periodic orbits, but correspond to walking orbits on the full lattice.

These types of trajectories would add a ballistic component to the mean square
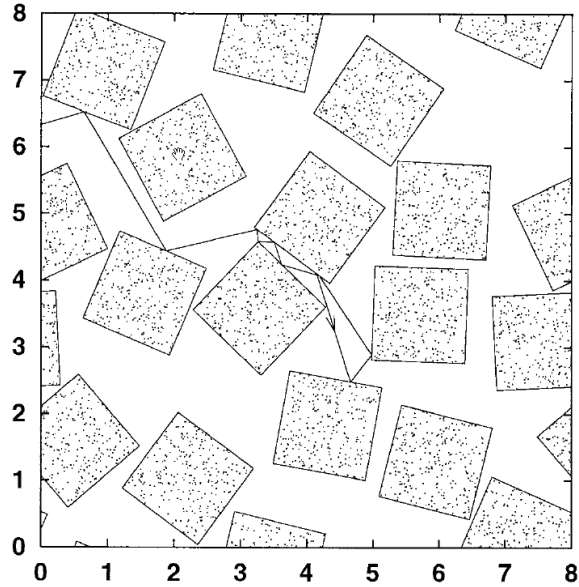
Figure 5.3: *A periodic system similar to that illustrated in fig. (5.2). Here the scatterers are both randomly placed and randomly oriented. Dettmann and Cohen found that this system is diffusive [30].*

displacement. Moreover, due to the flat sides of the polygons the orbits are stable. As a result there exists a set of sub-trajectories about the trajectory that also follow a similar path as the main trajectory. Systems containing large numbers of these quickly-moving trajectories tend to be super-diffusive [86]. If there are no infinite corridors allowing for arbitrarily long free motions, parallel sides of nearby scatterers are responsible for these ballistic-like motions. One can see this clearly in simulations, both those presented here as well as those described by Zaslavsky [104]. Examples are given in figs. (5.6)-(5.7) which show trajectories for a particle moving in an array of triangles

One can see that parallel sides of different scatterers are responsible for the

107
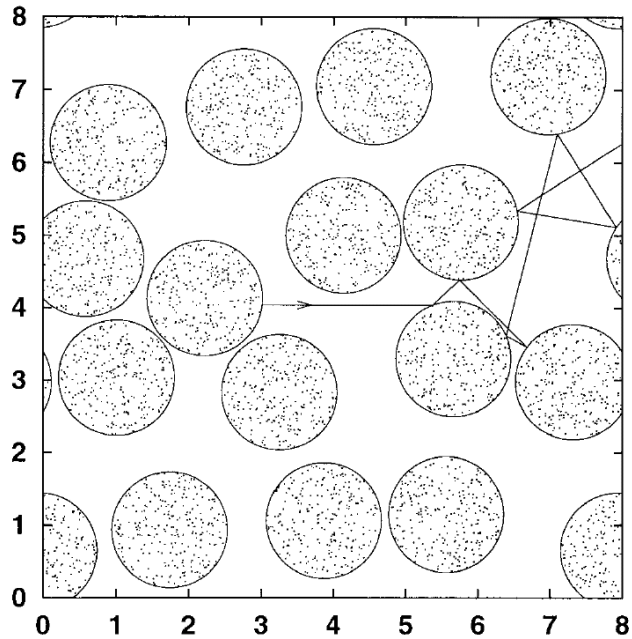
Figure 5.4: *The Lorentz gas with circular disk scatterers, placed at random in the plane. This system is diffusive [30].*

particle traveling nearly unhindered through system.

One way to destroy these periodic orbits is to place all the scatterers at random in the plane and, in the case of the original Ehrenfest model, to restrict the number of velocity directions. Hauge and Cohen were able to show that even the Ehrenfest model has some surprising properties. In this case, arrangements of scatterers can form mirrors that reflect trajectories back on themselves. If one allows the scatterers to overlap, the contribution of mirror scattering becomes large enough to make the system sub-diffusive [58]. In general, random placement of scatterers and the absence of overlapping configurations lead to normal diffusion even for few-sided scatterers. However, the infinite randomness is a burden computationally since simulating such systems potentially requires large amounts of memory. Thus, one would prefer to
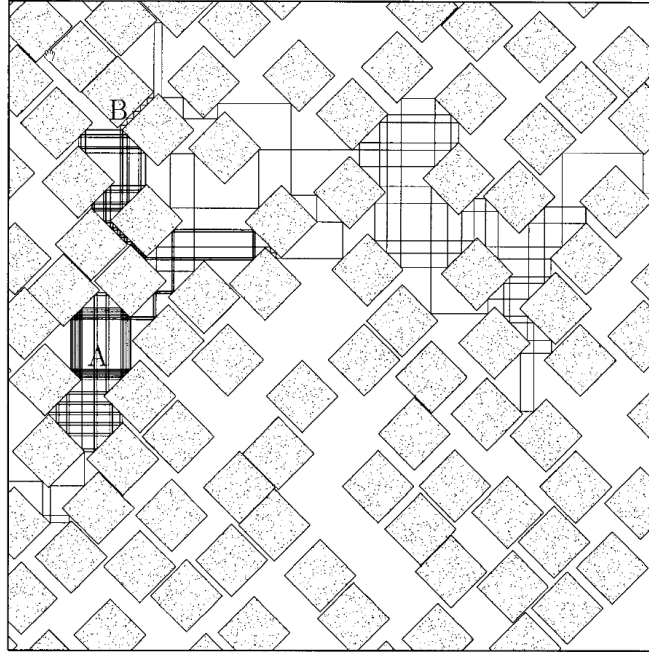
Figure 5.5: *The Ehrenfest wind-tree model where scatterers are randomly placed in the infinite plane. The system is diffusive, providing that the trees do not overlap [30, 58].*
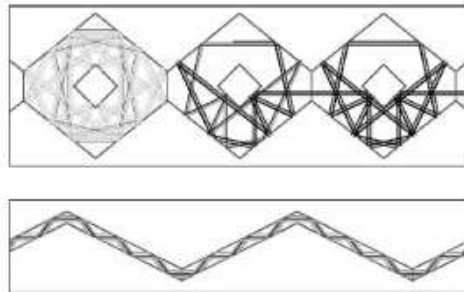


Figure 5.6: *Examples of walking orbits seen in studies of Lorentz channels by Sanders et al., for triangular scatterers placed along the upper and lower walls of the channel. These walking trajectories generally cause the motion of particles to be super-diffusive.*
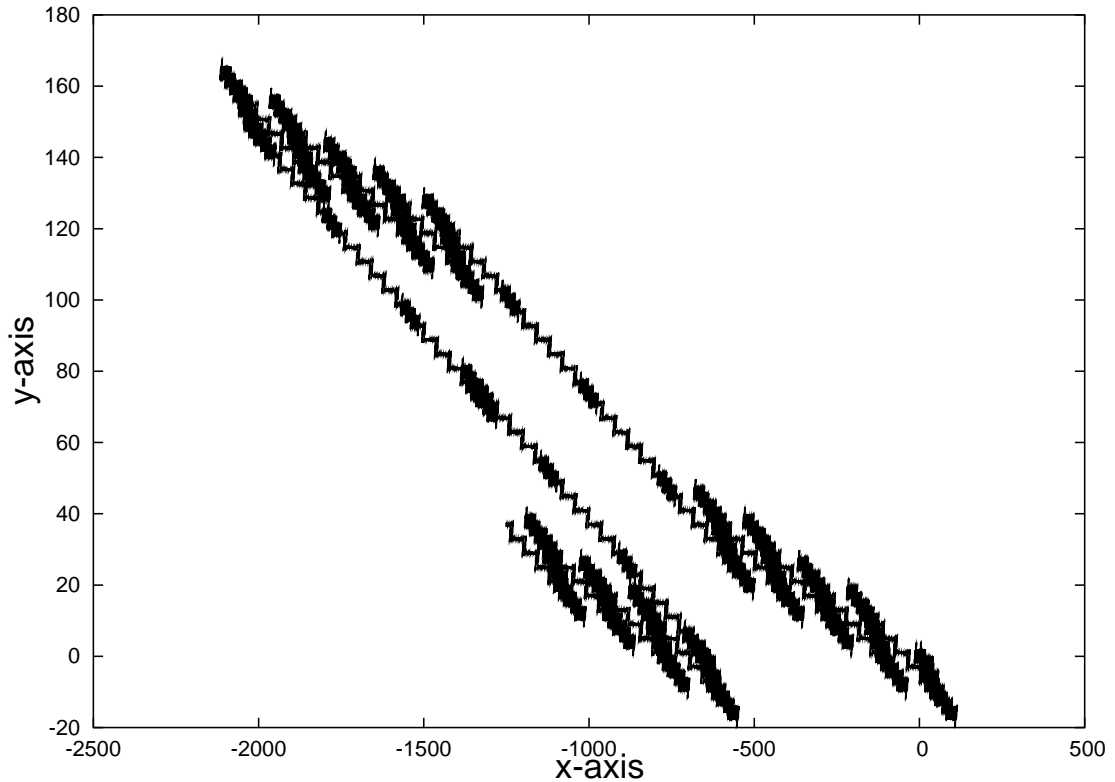
Figure 5.7: *An example of a walking trajectory of a particle in a periodic polygonal Lorentz gas with square scatterers. The axes are given in the same units as those shown in figure (5.1), but cover many cells. Each cell contains two scatterers and is repeated periodically in the infinite plane. Here the particle "walks" for long intervals, and the transport in this system is super-diffusive.*

have a system where the scatterers are placed on a lattice, and the overall system has a periodic nature. Then one can use a fundamental cell to describe the dynamics of the system. Dettmann and Cohen also studied such systems, one such system as previously shown, was a system containing a few randomly oriented and randomly placed scatterers in a unit cell and then the cell is repeated periodically on the plane. Dettmann and Cohen used unit cells that contain four randomly placed and randomly oriented scatterers, subsequently repeating these cells to tile the plane.

110

This system is diffusive. However this system contains many stable periodic orbits that confine, or localize, particles, leading to a smaller diffusion coefficient than that for a fully random system at the same scatterer density.

We wish to construct a simple system which would allow us to isolate and then determine the effects of different features of polygonal Lorentz gases upon the motion of particles in the system. The goal is to determine, as fully as we can, which features of such systems are responsible for normal diffusion and which features are not so crucial. We construct a pseudo-one-dimensional billiard system with one "free" scatterer in each unit cell that can be rotated or even moved within the cell. With such systems one can study a wide range of systems, from fully periodic to fully random by varying the orientation and position of the free scatterer. We wish to observe the minimum number of randomly oriented scatterers that are necessary in order to provide a diffusive system. To do this we first start with a periodic gas with square scatterers of Chapter 4 as shown in fig. (5.7).

The unit cell contains 5 scatterers - one at each corner and one in the center, which will be the free scatterer. We repeat this cell to form the channel. If all of the free scatterers have the same orientation, we find that the transport exponent is 1.72, as to be expected for a periodic system.

Next consider two neighboring cells and select random orientations for each of the two free scatterers. Then merge these two cells into a unit cell containing 8 scatterers as shown in fig. (5.9 and 5.10). Then we repeat this configuration along the line of the channel.

We find that this system is also super-diffusive with a transport exponent that

111
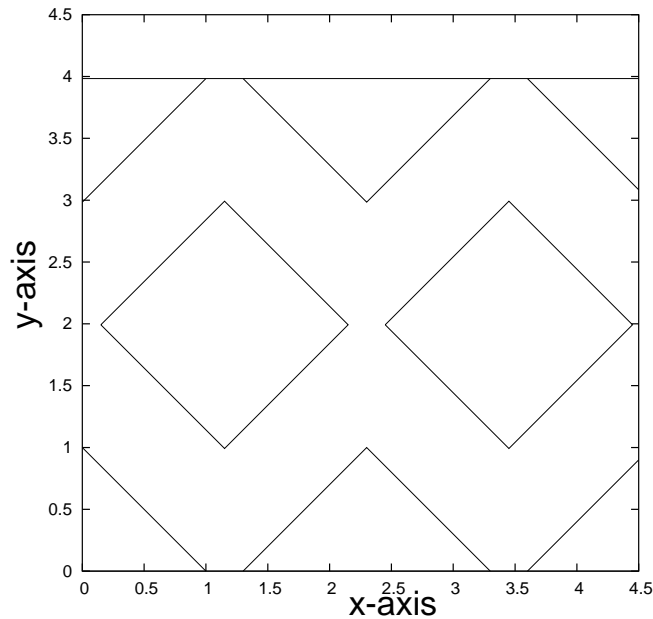
Figure 5.8: *Two unit cells of the Lorentz channel with square central scatterers, with diagonals aligned with the axes of the channel. One can vary the orientation, the location, and the type of scatterer in each cell.*

varies depending on the orientation. In all cases the transport exponent is super-diffusive with $\mu > 1.1$ with the largest value being 1.76, which is the same as that for the non-random case shown in fig. (5.1). Considering that the errors in determining these exponents are on the order $\pm 0.01$, we conclude that for two random cells the system is super-diffusive.

However, if we add a third cell to our merged cell and randomize its center scatterer we find a very interesting behavior. Sometimes the system appears to diffusive and sometimes super-diffusive depending on the angle of rotation of the scatterers. Moreover it is unclear which is more common the diffusive or the super-

112
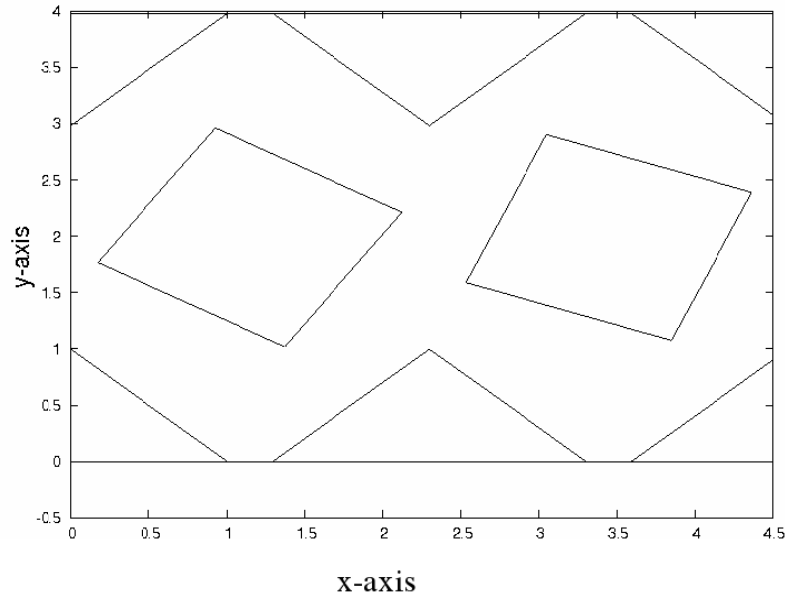
Figure 5.9: *A Lorentz channel with two randomly oriented scatterers in a unit cell. The cell is repeated periodically along the channel. In this system the center scatterers of the cell are each rotated about an axis perpendicular to the plane by a random angle between* $[0, 2\pi)$.

diffusive orientations.

If we add a fourth cell to our merged cell the same behavior is found as with the 3 cell system. Sometimes the system is diffusive and sometimes the system is super-diffusive depending one the exact orientation angles of the center scatters. However we also find that the diffusive orientations appear to be more frequent then the super-diffusive orientations.

Now if we add a fifth random center scatterer the frequency of the diffusive orientation becomes even more frequent and by the sixth random center scatterer
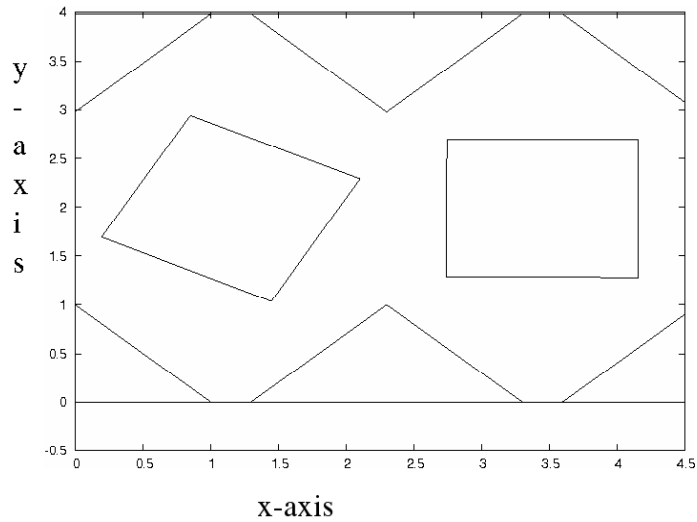
Figure 5.10: *Another example of a billiard containing* 2 *randomly oriented scatterer. The system is the same as that shown in fig. (5.9) but the scatterers are oriented by different angles.*

the system appears diffusive for any orientation except for the trivial orientations where the scatterers are all oriented in the same direction.

Further if we also considered the stability of the four random scatterer system by varying the orientation of center scatterer of the first cell by up to 0.1 radians we found that these variations have no affect on the transport properties of the system. Thus it appears the configuration is fairly stable.

A list of orientations that were found to be diffusive is found in Appendix A of the thesis.

It is not clear if there exist certain orientations that are super-diffusive in each case where we find only diffusive behavior. The surprising fact is that the particular orientations matter at all when the systems exhibit different behaviors. It is unclear why certain orientations are diffusive and others are diffusive. None of the diffusive

114

orientation contain irrational ratios of $\pi$, and all the orientations appear to be fairly stable. The super-diffusive systems also have a short time period in which they appear diffusive as shown in figs. (5.11) and (5.12).
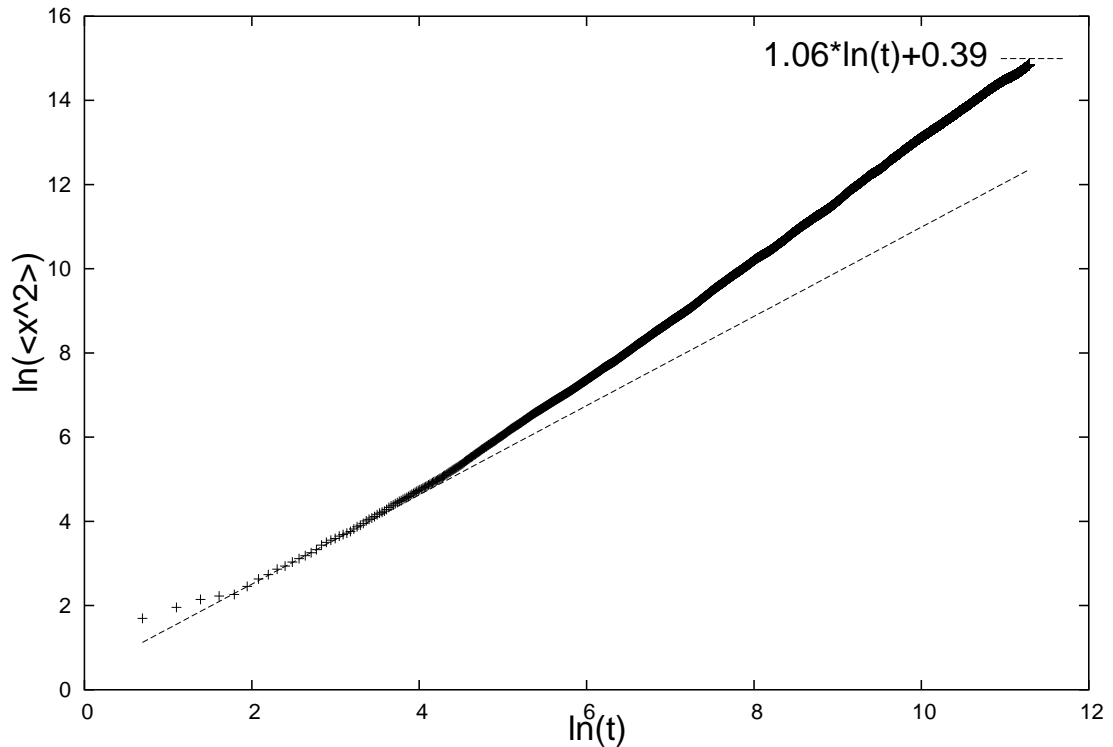


Figure 5.11: *The mean square displacement for a particle moving in the system containing two randomized center scatterers, as illustrated in fig. (5.9). This curve shows a long-time super-diffusive behavior, but for short times the system appears to have a diffusive regime, similar the irrational rhombi system of Lepri et al. [66]. The dotted line indicates diffusive behavior. The equation for the best fit line is given by* $1.06 \ln(t) + 0.39$

These results raise the question as to whether we are actually seeing diffusion in these periodic systems. One possibility reason is that these periodic systems eventually become super-diffusive, but we have not run the system for long enough
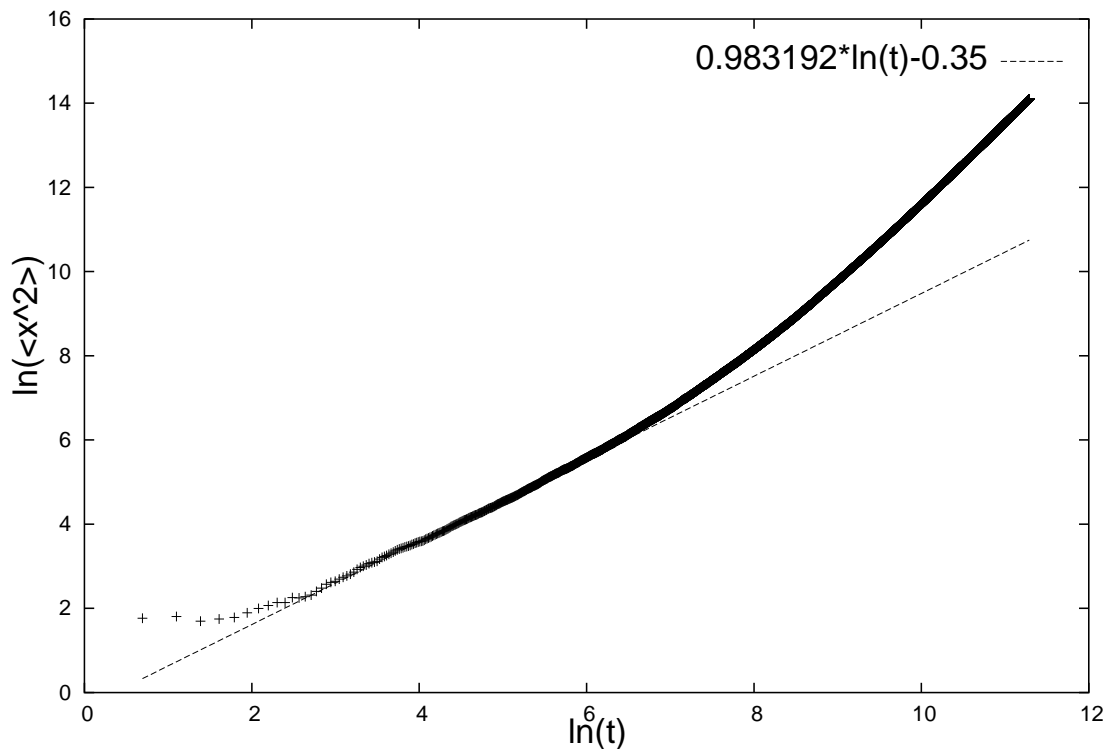
Figure 5.12: *The mean square displacement for a particle in a periodic system with a unit cell consisting of 3 center scatterers, rotated by random angles. As is the case with the system with two randomized scatterers in a unit cell, this system shows a long-time super-diffusive region and a short-time diffusive regime, similar to that illustrated in fig. (5.9). The dotted line indicates diffusive behavior given by* $0.98192 * \ln(t) - 0.35$

times. To check this possibility, we have lengthened the time of the simulations by factors of 10 and 100, and the behavior still persists. Therefore, at least for times studied here, the systems are diffusive. Another possibility is that some randomness creeps into the systems by means of computer round-off error. This possibility might be checked by following trajectories over the length of a run to see if they begin to deviate from the strictly mechanical predictions over the course of the

116

run. Since the motion is not chaotic, there is no exponentially rapid growth rate of errors, and we have found no evidence for round-off error influencing the motion of the point particles. Further it should be noted that all the trajectories are double precision values in conjunction with an integer value (winding number) to store the cell number. Therefore it is nearly impossible to increase the precision of the actual trajectories. We can verify that the trajectory is behaving as expected by looking at a portion of it, as illustrated in fig. (5.13).
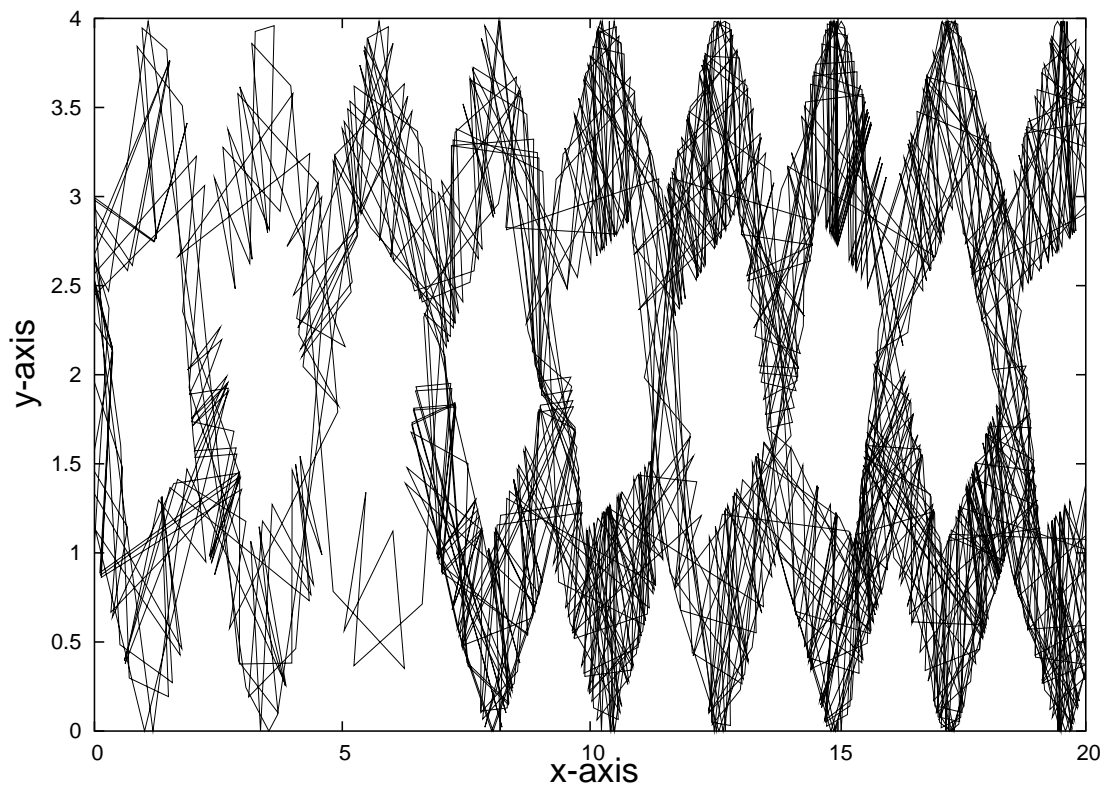


Figure 5.13: *An example of a trajectory of a particle in a Lorentz channel with square scatterers. The particles are reflected at the boundaries of the scatterers. The boundary of a scatterer becomes visible if the particle collides with it a sufficiently large number of times.*

In fig. (5.13) we illustrate a typical trajectory, and in figs. (5.14)-(5.15) we

117

show the mean square displacement as a function of time for two different period 4 systems. We find similar results for longer times.
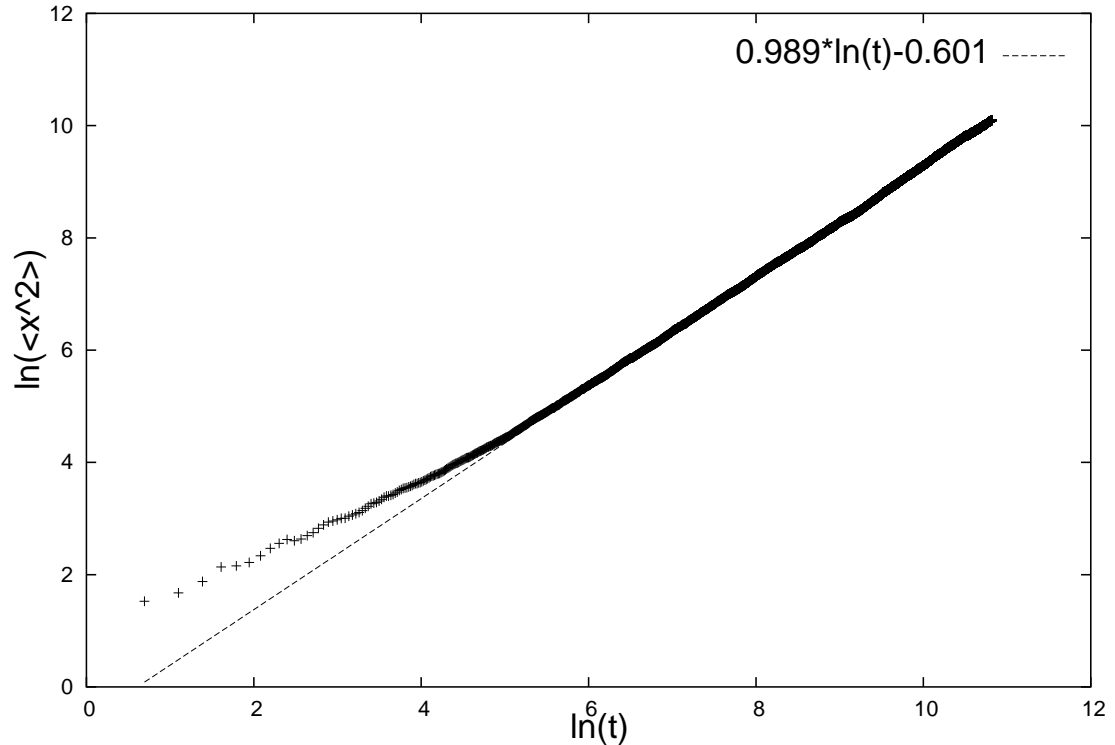


Figure 5.14: *The mean square displacement for a particle moving in a periodic system with a unit cell consisting of four randomized center scatterers. This system appears to be diffusive, within the error bars of the computations with a best fit given by* $0.989 \ln(t) - 0.601$

We point out that for diffusive systems the mean square displacement shows a stable, linear growth after about 10 collisions and does not deviate from that behavior over the course of a run. However, super-diffusive systems take a much longer time, on the order of several hundred collisions, to exhibit a stable time dependence of the mean square displacement. There is also a large difference between the values of the transport exponents for the two types of systems. The super-diffusive trans-
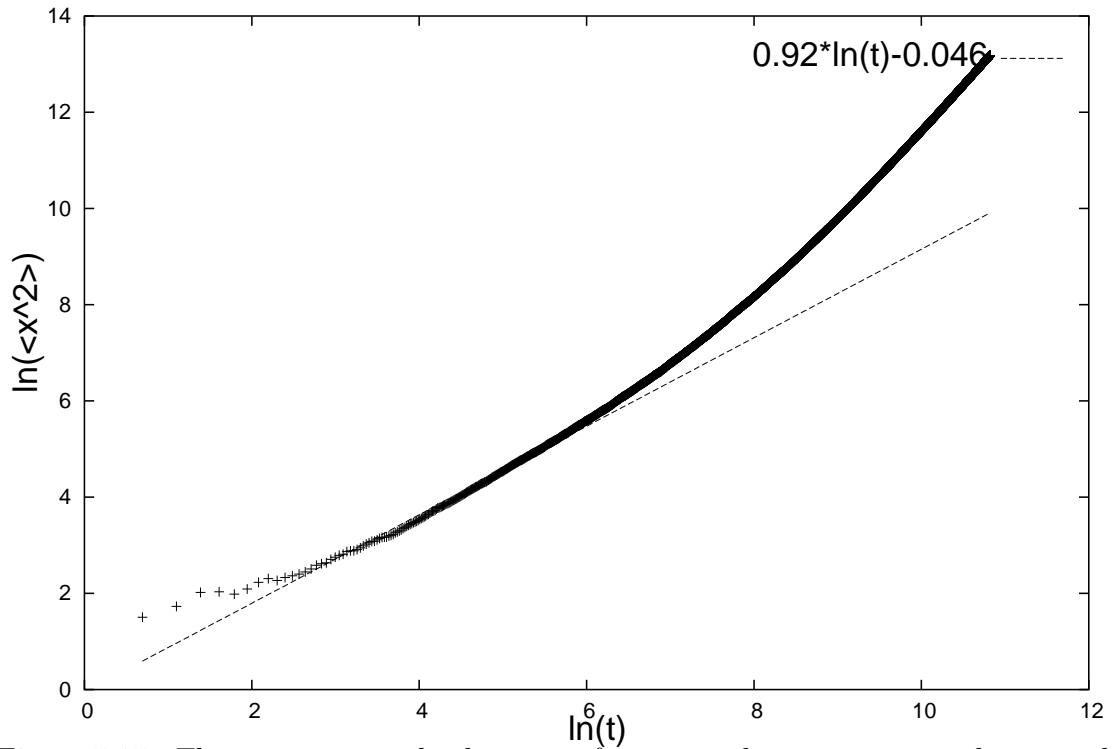
Figure 5.15: *The mean square displacement for a particle moving in another periodic system with unit cell consisting of four randomized center scatterers. In contrast to the results illustrated in figure (5.14), this orientation of scatterers leads to a long-time super-diffusive behavior. However, for short time periods the system appears to be diffusive.*

port exponents are about 1.72 while those for diffusive systems are in a range of about $1.02 - 0.98$. In each case the errors are about $\pm 0.02$. Thus one would expect if round-off errors were strongly influencing the trajectories, all systems would eventually either be super-diffusive or diffusive. We do not see this behavior. Instead we see for both short times and long times, diffusive systems are diffusive. Super-diffusive are diffusive for a short time period and become super-diffusive after 400 collisions. Our runs typically last for about $10^4$ collisions.

119

We conclude this section with the observation that the source of the randomness in the periodic but diffusive systems is subtle and elusive. That one expects to find randomness in some form is a consequence of identifying a linear growth of the mean square displacement as the result of some form of random walk. One might suspect that the sharp corners on the scatterers may be responsible for this linear growth, through a weak form of chaotic-like motion that we identified as resulting from *vertex splitting* in previous chapters. This possibility was studied by Lepri *et al.* [66] who looked at diffusion in arrays of rhombi with smoothed corners. These authors found that for short periods of time billiard consisting of rhombi with irrational internal angles would exhibit a diffusive behavior.

## 5.2   Particle Transport in Systems with Irrational Angles

The systems described above are not the only models with simple polygonal scatterers that have been found to be diffusive. Many authors have described diffusion in arrays of polygonal scatterers, particularly triangles, with internal angles that are irrational fractions of $\pi$. Such systems have the interesting property that no sequence of collisions can restore the velocity direction of a moving particle to any previous direction. This follows from the observation that each collision of the particle with a scatterer rotates the velocity direction by an irrational fraction of $\pi$. This property is not shared by systems with scatterers that are regular polygons, which all have interior angles that are rational fractions of $\pi$. Casati *et al.* [18] first showed that a channel consisting of triangles with irrational internal angles will

exhibit diffusive behavior [95].

Alonso, Ruiz, Vega and Sanders [2, 3, 86] constructed Lorentz channels with scatterers with irrational angles that was able to exhibit a wide range of behavior. Their systems are illustrated in fig. (5.16). Their systems are defined by two angles
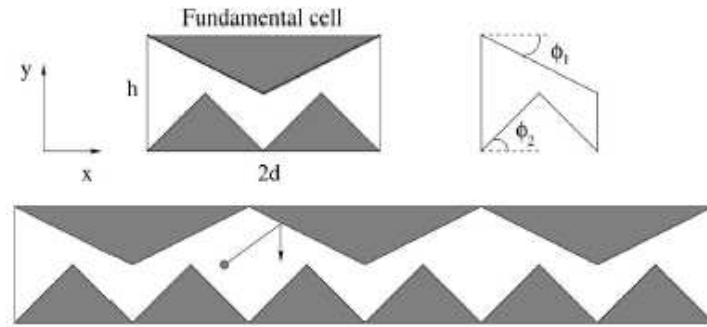


Figure 5.16: *The Lorentz channel system studied by Alonso et al., which consists of three triangular scatterers in a unit cell. The largest triangle contains at least two irrational internal angles.*

$\phi_1$ and $\phi_2$. The angle $\phi_1$ is chosen to be a fraction of the golden ratio times $\pi$ or more specifically $\frac{5^{1/2}-1}{4} * \pi$. The value of $\phi_2$ is allowed to vary over several rational values of $\pi$.

In this case the system takes on several different transport exponents depending on the angles of the system. Depending on the value of $\phi_2$ the system can be sub-diffusive, diffusive, and super-diffusive. Table (5.1) show a list of the angles $\phi_2$ and the corresponding transport exponents $\mu$ for the system.

Sanders *et al.* studied systems similar to those of Alonso and co-workers. Sanders *et al.* proposed that the super-diffusive behavior seen by Alonso *et al.* is caused by the existence of parallel sides of scatterers in these systems. Sanders *et al.*

Table 5.1: *This table shows that by varying $\phi_2$ in fig. (5.16) we find systems exhibiting sub-diffusive, or diffusive, or super-diffusive motion.*

| $\phi_2$ in radians | $\mu$ |
|---|---|
| $\pi/3$ | 1.3 |
| $\pi/4$ | 0.86 |
| $\pi/5$ | 1.03 |
| $\pi/6$ | 1.04 |
| $\pi/7$ | 1.06 |
| $\pi/8$ | 1.01 |
| $\pi/9$ | 1.01 |

use a system shown in fig. (5.17). They showed systems that contain parallel sides allow particles to travel down the channel in a nearly ballistic fashion as shown in fig. (5.18) [86]:
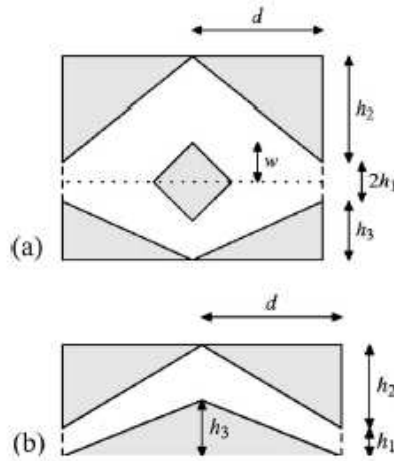


Figure 5.17: *A fundamental cell for a periodic system with triangular scatterers, with irrational angles.*
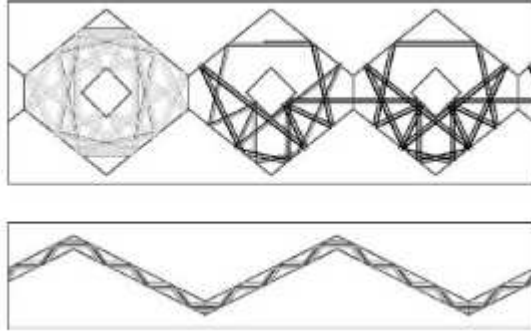
Figure 5.18: *Examples of ballistic-like motion of a particle in a Lorentz channel with unit cell illustrated in fig. (5.17). The parallel sides of the scatterers allow the particles to move quickly through the system. These "walking orbits" appear to lead to a super-diffusive behavior [86].*

Sanders *et al.* studied systems where there were no parallel sides, and thus eliminated the resulting ballistic trajectories. These systems will be diffusive, provided that:

1. The system is in a finite horizon regime.

2. All the angles within the cell are irrational fractions of $\pi$.

3. There are no parallel sides within the cell.

These models allow us to identify the source of randomness needed for diffusion with the irrational angles of the scatterers [2, 3, 86].

## 5.2.1   Studies of Polygonal Scatterers with Irrational Internal Angles

This work suggests that we should find diffusive behavior in *any* system where the scatterers have irrational internal angles and no parallel sides . We checked this

idea using the channel model similar to that shown in fig. (5.1) described in this chapter and in chapter 4. We will use two different irrational angles. One irrational angle for the edge polygons, and a different irrational angle for the center scatterer. All the edge polygons in the cell are constructed having 3 irrational internal angles having a value of:

$$\frac{\sqrt{2}}{8} * \pi \tag{5.1}$$

$$2\pi - 3\frac{\sqrt{2}}{8} * \pi \tag{5.2}$$

For the center scatterer 3 of the angles are

$$\frac{3 - \sqrt{5}}{4} * \pi \tag{5.3}$$

and one internal angle of

$$2\pi - 3\frac{3 - \sqrt{5}}{4} * \pi \tag{5.4}$$

A system with a four sided, "irrational" polygon is illustrated in fig. (5.19).

The transport exponent for this system is $\mu = 1.02$ indicating that, within the error bars of this computation, the system is diffusive. To ensure that we remove any possibility of walking orbits taking place in these systems, we will further rotate the center polygon by $\pi/4$:

Eliminating the possibility of walking orbits results in a diffusive system with a transport exponent of $\mu = 1.00$. Lastly we considered a four sided system where all the scatterers had the same arrangement and values of irrational angles, and are symmetrically placed, as illustrated in figs. (5.20 and 5.21)

We form the polygons as shown in fig. (5.19) but we rotate the center polygon by $0.7 * \pi$. Calculating the transport exponent for this system we find the transport
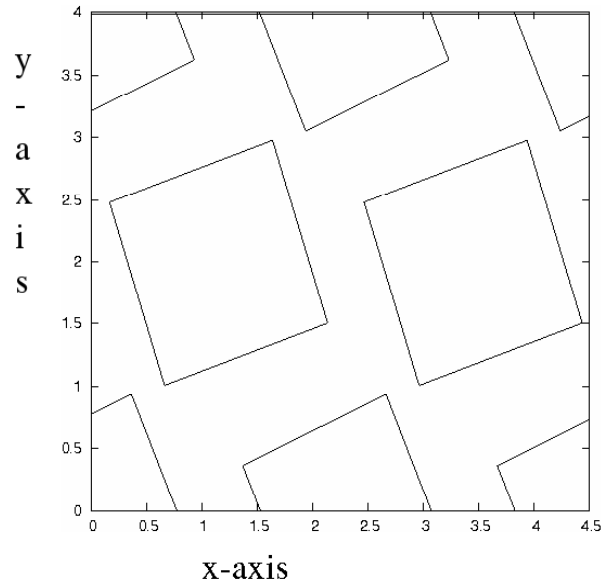
Figure 5.19: An example of an irrational set of scatterers. The location of the scatterers is identical to that in figure (5.1). The edge polygons have three internal angles equal to $\frac{\sqrt{2}}{8} * \pi$, and the center scatterer having three irrational angles of $\frac{3-\sqrt{5}}{4} * \pi$.

exponent is 1.00. We conclude this chapter by noting that we have constructed a Lorentz channel model that allows us to test various ideas about the origin of diffusion in pseudo-chaotic systems by examining each of the possible sources in isolation from the others. Nevertheless riddles still remain. Diffusion is a very subtle phenomenon!
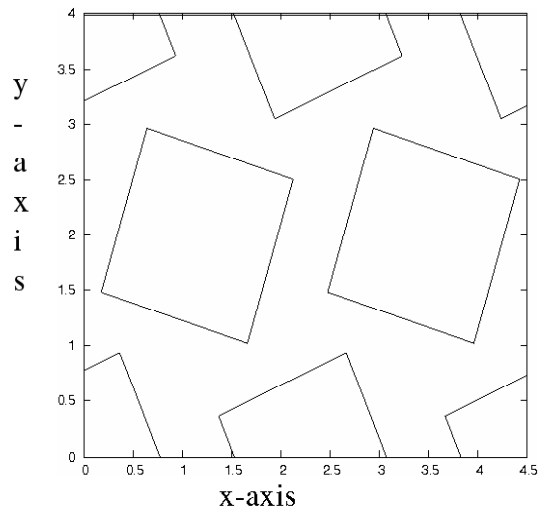
Figure 5.20: Another example of an irrational set of scatterers. The scatterers are identical to those in fig. (5.19), except for the middle scatterer being rotated by $.7\pi$

126
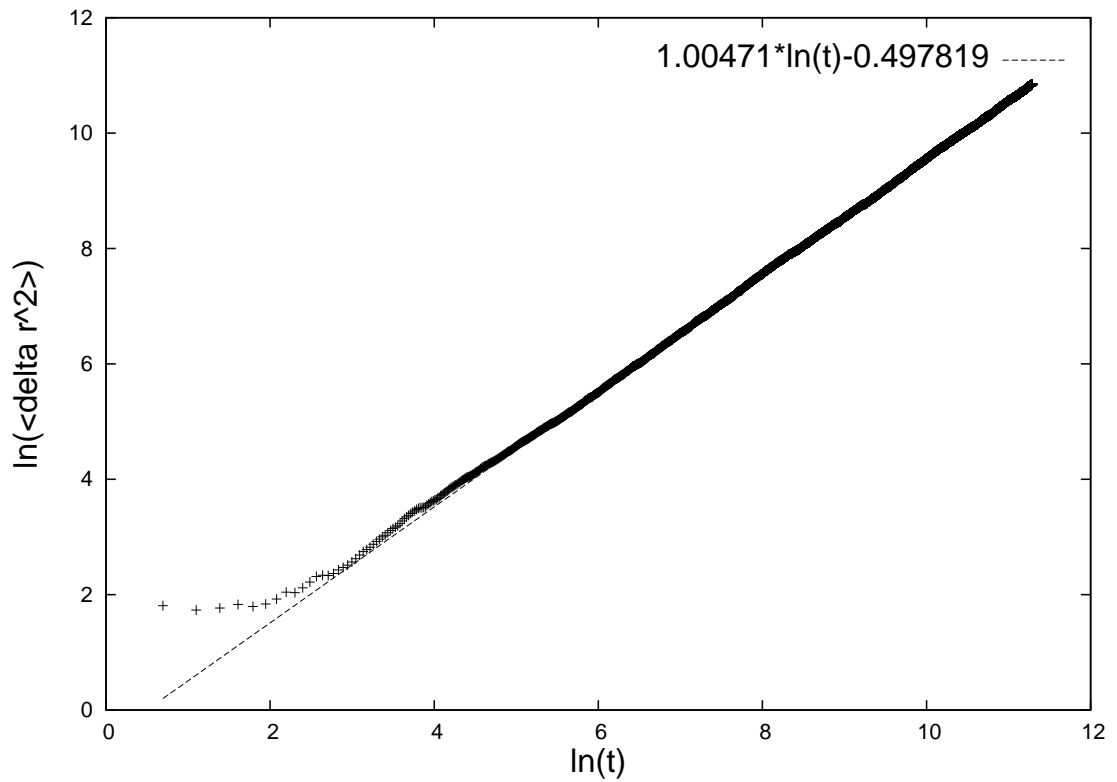
Figure 5.21: *The mean square displacement for a particle moving in the system containing irrational angled scatterers, as illustrated in fig. (5.20). The dotted line indicates diffusive behavior. The equation for the best fit line is given by the dotted line.*

Chapter 6

Conclusion

## 6.1   Transport

In this dissertation we considered particle transport in each of four different types of pseudo-chaotic systems, all of which are Lorentz gases with *convex*, polygonal scatterers. Our goal was to discover the differences between transport in chaotic systems and in pseudo-chaotic systems. We focused our attention on the contrast between particle transport in pseudo-chaotic systems with polygonal scatterers and that in chaotic systems where the scatterers are hard disks in a plane with no infinite horizons. In the chaotic system, transport is diffusive, with, among other properties, a mean square displacement of the moving particles that grows linearly with time. In the non-chaotic systems, one finds a range of behaviors for the mean square displacement including all the possibilities - sub-diffusive, diffusive, and super-diffusive behaviors. The four types of systems we studied are:

1. Periodic Lorentz gases with scatterers that are regular polygons with many sides. These systems were studied in Chapter 3.

2. Periodic Lorentz gases with scatterers that are regular polygons with few sides. These systems were studied in Chapter 4.

3. Lorentz gases with polygonal scatterers that are placed in some random way on the lattice. These systems were studied in Chapter 5

4. Periodic Lorenz gases with polygonal scatterers with at least two irrational, central angles. These systems were also studied in Chapter 5

We studied Lorentz gases with many-sided scatterers in order to gain a better understanding of the transition of properties of a non-chaotic system to those a chaotic one. It is clear from the work described in Chapter 3 that, as the number of sides of the polygons increases without bound and the polygons approach circles, the properties of these systems smoothly approach those of Lorentz gases with circular scatterers. Many sided polygons may be said to have *effective Lyapunov exponents*, whenever nearby trajectories separated by distances on the order of the length of the side of a polygon, but not infinitesimally close, collide with different faces of the same polygons for a number of collisions and thereby mimic the mechanism that produces exponential separation of trajectories for chaotic systems. This exponential separation obtains as long as the two trajectories encounter exactly the same sequence of scatterers, but encounter different faces of these scatterers. In this case the two adjacent trajectories are reflected at different angles from the same scatterer. As long as the polygons are convex, this is a perfectly adequate de-focusing mechanism for generating exponential separations of trajectories. In this connection it is worth pointing out that this is exactly the mechanism that produces exponential separations of trajectories for circular scatterers in any computational study like those carried out here. On a computer circles are actually polygons, but with

number of sides on the order of $10^{24}$. Since the polygons considered in Chapter 3 have on the order of $10^2$ to $10^4$ sides it is not difficult to consider nearby trajectories that are much closer than the length of the side of a polygon. Since the sides are straight lines, one must say that in principle the de-focusing mechanism needed for the divergence of infinitesimally close trajectories is absent when the trajectories are very close and, as a result, the Lyapunov exponents are strictly zero

Something very similar happens when we turn our attention to the transport properties of these periodic polygonal systems. If we sample a large number of trajectories we find that the transport exponent for the mean square displacement is greater than unity. In other words, the motion of the moving particle is, to the best of our ability to measure it, super-diffusive. However if we reduce the number of trajectories in the sample by restricting the initial distance between any two trajectories to be on the order of the length of a side of the scatterers, we find diffusive motion! Not only is the motion diffusive, the diffusion coefficient is nearly equal to that of that for diffusion of a particle $0.24 \pm 0.04$ vs. $0.24$, respectively as obtained by replacing each polygon in the system by a circle. Since diffusion is a property of trajectories considered singly, and not a property of trajectory pairs, we must conclude that taking a coarse grained sample of initial points eliminates a sufficient number of ballistic-like trajectories to affect the sample average of the square displacement. Figure (4.6) in Chapter 4 showing the formation of trajectory "jets" is good evidence to support this conclusion [87].

## 6.2   Partial Van Hove function

We next considered the partial Van Hove function for systems with periodic arrangements of scatterers. The object was to see what remains of the fractal properties of this function when the diffusion process is not based upon chaotic dynamics. It is important to mention again that the derivation of the formula for the Hausdorff dimension depends heavily of the chaotic nature of the underlying dynamics. As an indication of the role of the chaotic dynamics, the Lyapunov exponent appears in the dimension formula. For chaotic systems, such as the Lorentz gas with circular scatterers, one can generate a fractal structure by plotting the imaginary part *vs. Re* the real part of the partial Van Hove function. Remarkably we found the same kind of structure for the partial Van Hove function for the case where the scatterers are many sided polygons. This function has nearly identical fractal properties as a circular scatterer/hard disk system. This was observed in both the infinitesimal scale and the coarse grained scale. The fractal further appears stable over time for these many-sided polygons just as in a hard disk system. We observed that the Hausdorff dimension for this fractal satisfies the dimension formula if one uses the effective Lyapunov exponent and the diffusion coefficient. However, it remains unclear whether one can rigorously justify this relation mathematically. In fact there is probably no valid dimension formula for few-sided polygons because of the zero Lyapunov exponent and the self-intersection partial Van Hove function. We do not know if the validity of the formula is due to the mechanism whereby trajectory pairs hit different sides of the same scatterers for a number of successive

collisions or to a different mechanism that is due to the splitting of trajectory pairs due to the sharp corners of the polygons. One might also gain insight into this issue by studying the fractal properties as a function of the number of sides of the scatterers. Another option is considering the fractal properties over different lengths of time. If polygons less than 500 sides are any indication at some point, very long times, the partial Van Hove function should cease being a fractal much like the partial Van Hove function for square scatterers. However, one would need to be able to run the system for extremely long times and for long times round-off errors will become an issue. In each case, however, the effects are subtle and our results are inconclusive.

## 6.3 Dynamics

This issue was studied previously by Uzer, Ford, and Mantica, who concluded [96], for reasons discussed several times in this dissertation, that there is very little practical difference between chaotic and non-chaotic billiards. The problem with their approach in our context is that we do know rigorously that polygonal scatterers are not chaotic. Furthermore, our most careful numerical studies indicate that the motion of a particle in a periodic array of many-sided polygons is super-diffusive, not diffusive. All that we can conclude at the moment is that the properties of diffusion in the polygonal systems studied here are quite subtle and we are far from a complete understanding of them. However, from our observations of diffusion in systems of many sided polygons we conclude that under certain circumstances one should make

a distinction between mathematical chaos/Lyapunov chaos and *physical chaos*. At the moment we have only some intuitions about the precise circumstances for which this distinction is relevant.

Our studies of many-sided polygons led us naturally to a consideration of few-sided polygons. As we decrease the number of sides of the polygons, we observe that there appears to exist a lower limit on the number of sides of polygons for which one can get any useful information by coarse graining the trajectories used in the simulations to form averages. In Chapter 4 we considered polygons with fewer sides than this lower limit of about 500 sides. We studied Lyapunov exponents, fractal dimensions of the Van Hove functions, transport properties, and the properties of diffusion using fractional kinetics. We observed the Lyapunov exponent was zero for these systems, we saw that lattice properties prevented one from defining an effective/coarse grained Lyapunov exponents for these systems. This is a due to the fact as one increases the exterior angle the separation angle between two nearby trajectories increases. For example for square scatterers, two trajectories where particles hit adjacent sides travel, after collision, at almost 180 degrees to one another: It is physically impossible for the trajectories to hit the same scatterer during the next collision. In order to define an effective Lyapunov exponent one needs about 15 consecutive collisions with same scatterers. This appears to occur first when the polygons have about 500 sides. Further we considered the partial Van Hove function for particle motion in periodic, few-sided polygonal systems. This function appeared to have fractal properties for short times with a dimension proportional to $k^2$. However we discovered that the partial Van Hove function was

not stable for longer times and exhibited loops, etc, which means that it could not be considered to be a function. We observed that these systems are super-diffusive and that for the few sided polygons normal diffusion was not observed in these lattice periodic systems. However we were able to construct diffusive models with periodic properties, based upon some models considered by Dettmann and Cohen[30]. We discuss these models below.

We also considered transport properties in periodic systems with few-sided scatterers, in terms fractional kinetics, as discussed by Zaslavsky and co-workers. We were able to check Zaslavsky's result that shows that the even moments of the displacement of the moving particles in these systems satisfy a simple scaling formula, of the form $< \Delta r^{2n} >=< \Delta r^n >^2$ for all $n$ that we studied. Zaslavsky's work using fractional kinetics appears to be able to provide a useful method for studying diffusion in systems few-sided polygonal scatterers [101, 102, 104, 105, 106]. It would be beneficial and constructive to be able extend Zaslavsky approach to polygons with an arbitrary number of sides. This would enable one to decide if it is possible to derive a functional relationship between the number of sides and the transport exponent.

Since we could not find a regime in which the motion of a particle in a periodic array of few-sided polygons appears to be diffusive, we next considered, disordering the polygonal systems. We constructed a one dimensional array of scatterers with finite horizon, known in the literature as a *Lorentz channel*. The array was nearly periodic, but we allowed one scatterer to be placed in a random orientation with respect to the other scatterers. In fact, we could make a wide variety of structures

134

in order to test some ideas about diffusion in these systems. We found that if the orientation of the central scatterer is randomized and then fixed, but all the cells in the channel are identical to it, the motion is purely super-diffusive, and if one randomizes the central scatterers in all of the cells, the motion is purely diffusive. We also constructed some arrangements based upon ideas of Dettmann and Cohen [30] where we allowed three or four consecutive cells to have randomly oriented central scatterers, but then repeated the three or four cell structure throughout the channel. Under these circumstances, we would sometimes observe diffusive behavior, and other times super-diffusive behavior depending on the orientation of the scatterers. It further appears that each of these orientations is stable in the sense that their transport properties do not change when the central scatterers are rotated by an angle of 0.1 radians. This diffusive behavior did not disappear for longer runs or a narrower graining. This behavior is surprising and appears to indicate that certain orientations favor diffusive behavior and certain orientation favor super-diffusive behavior. This raises several, so far unanswered, questions about which orientations actually provide a diffusive behavior and exactly how stable the transport properties are for these orientations. It would also be informative to extend this process to two dimensional systems. Further, it would informative to study these systems using the fractional kinetics of Zaslavsky . Lastly it would informative to study these systems for longer times and for finer scales to see if there are an long time effects for these systems.

The last system considered was that of polygonal scatterers with some vertex angles that are irrational fractions of $\pi$. We considered several models including

135

systems where all the angles are irrational, where all the angles are irrational and the center scatterer rotated and finally an irrational rhombus scatterer. As suggested by Alonso and Sanders [2, 3, 86], we also find that as long the arrangements of scatterers have only finite horizon, and, at the same time, the scatterers have at least two irrational vertex angles, and no two scatterers in a unit cell have parallel sides, the systems appears to exhibit diffusive transport. This appears to always occur; however, there may be exceptions to this rule. It would be useful to learn what if any relation exists between these systems and the randomly rotated systems discussed earlier. Does the irrational angle or the angle of rotation cause the system to be at least weakly mixing. If so, is there is a connection between mixing and diffusive transport? This too requires further study.

While these systems are not the only non-chaotic models to be studied [15, 17, 85], the systems we studied provide us with a great number of intriguing and challenging problems, some insights into the transition from non-chaotic systems and their transport behavior to that for chaotic systems.

In conclusion, polygonal systems appear to be of great interest for understanding the transport properties of a system, based on the simplicity of the dynamics. However this simplicity is very deceptive, and diffusion in these systems is very subtle. It appears much research remains to be done on these systems. We hope that future research will provide answers to some of the questions raised here about mechanisms for diffusion.

136

# Appendix A

## Appendix

In chapter 5 we found that the transport properties of the system depended on the angular orientation of the center scatterers of the system. In this Appendix we list the periodicity and the orientation of the angles as well as their tranport properties.

| Angles of center scatterers in radians |
| --- |
| Four randomized center scatterers |
| 0.7439802024609051 |
| 3.66132852282568 |
| 1.746487930582959 |
| 1.6702164997593452 |
| Adding 0.1 radians to the first scatterer listed above |
| 0.8439802024609051 |
| 3.66132852282568 |
| 1.746487930582959 |
| 1.6702164997593452 |
| 4.318064961112611 |
| 1.6359643359670528 |
| 3.958172999685392 |
| 3.105918190350991 |
| 4.823396344491143 |

| Angles of center scatterers in radians |
| --- |
| Five randomized center scatterers |
| 4.318064961112611 |
| 1.6359643359670528 |
| 3.958172999685392 |
| 3.105918190350991 |
| 4.823396344491143 |

| Angles of center scatterers in radians |
| --- |
| Six randomized center scatterers |
| 0.8122743913930374 |
| 0.25621825942551457 |
| 0.8206779395349731 |
| 5.103670521398973 |
| 1.6098668030535206 |
| 5.15647157161256 |
| 0.2969766186664319 |
| 0.0732792087064511 |
| 0.286708470248064 |
| 1.8659591269807996 |
| 0.46042684746612 |
| 1.8014424477065714 |
| 0.30854948592645726 |
| 0.8185071436039721 |
| 0.07967608042851371 |
| 1.9386735965109307 |
| 5.142832058514009 |
| 0.5006195778820963 |

| Angles of center scatterers in radians |
|---|
| Eight Randomized scatterers |
| 0.9137995543828611 |
| 0.11688704548072448 |
| 0.5748582812706159 |
| 0.40887318912752646 |
| 5.741571933805646 |
| 0.7344229667641201 |
| 3.6119411065900437 |
| 2.5690260144257344 |
| 0.12838137269649363 |
| 0.6659421800273666 |
| 0.10102593145429717 |
| 0.4827129590362429 |
| 0.8066439546421553 |
| 4.184238120979093 |
| 0.634764648157772 |
| 3.032974971801703 |

For the four randomize center scatterer system the following are found to be super-diffusive

| Angles provided in radians |
| --- |
| 3.7062643243482913 |
| 1.7343357243656132 |
| 4.316475010758053 |
| 3.9282764045589835 |
| 2.9409244385912787 |
| 2.976821091426946 |
| 1.7308677179415064 |
| 1.9817522042131828 |

# Bibliography

[1] D. Alonso, R. Artuso, G. Casati and I. Guarneri, "Heat conductivity and dynamical instability," Phys. Rev. Lett. **82** 1859-1862 (1999).

[2] D. Alonso, A. Ruiz, and I. de Vega, "Polygonal billiards and transport: Diffusion and heat conduction," Physical Review E **66**, (2002).

[3] D. Alonso, A. Ruiz and I. de Vega, "Transport in polygonal billiards," Physica D **187**, 184-199 (2004).

[4] V.I. Arnold and A. Avez, *Ergodic problems of classical mechanics* (W.A. Benjamin, New York, 1968).

[5] R. Artuso, G. Casati and I. Guarneri, "Numerical study on ergodic properties of triangular billiards," Phys Rev. E **55**, 6384-6390 (1997).

[6] R. Artuso, I Guarneri and L. Rebuzzini, "Spectral properties and anomalous transport in a polygonal billiard," Chaos **10**, 189-194 (2000).

[7] R. Artuso and G. Cristadoro, "Anomalous deterministic transport," Chaos **15**, 015116/1-7 (2005).

[8] P. Balint and S. Troubetzkoy, "Rotor interaction in the annulus billiard," J. Stat. Phys. **117** 681-702 (2004).

[9] C. Beck, and F. Schögl, *Thermodynamics of Chaotic Systems: An Introduction* (Cambridge Press., 1995).

[10] S. Benkadda, S. Kassibrakis, R.B. White and, G.M. Zaslavsky, "Reply to 'Comment on *Self-similarity and transport in the standard map*,'" Phys. Rev. E **59**,3761-3764 (1999).

[11] P. M. Bleher, "Statistical properties of a two dimensional periodic Lorentz gas with infinite horizon," J. Stat. Phys. **66**, 316-373 (1991).

[12] J. Boon and S. Yip *Molecular Hydrodynamics* (Reprint, Dover publications, 1991).

[13] M.E. Briggs, J.V. Sengers, M.K. Francis, P. Gaspard, R.W. Gammon, J.R. Dorfman, and R.V. Calabrese, "Tracking a colloidal particle for the measurement of dynamics entropies," Physica A **296**, 42-59 (2001).

[14] L. Bunimovich and Y. Sinai, "Statistical properties of Lorentz gas with periodic configurations of scatterers." Comm. in Math. Phys. **78** 479 (1981).

[15] L.A. Bunimovich, "Mushrooms and other billiards with divided phase space," Chaos **11**, 802-808 (2001).

[16] L.A. Bunimovich and M.A. Khlabystova, "One-dimensional Lorentz gas with rotating scatterers: Exact solutions," J. Stat. Phys. **112** 1207-1218 (2003).

[17] L.A. Bunimovich and Dettmann, "Open circular billiards and the Riemann hypothesis," Phys. Rev. Lett. **94**, 100201/1-4 (2005).

[18] G. Casati and T. Prosen, "Mixing property of triangular billiards," Phys. Rev. Lett **83** 4729-4732 (1999).

[19] F. Cecconi, "The origin of diffusion: the case of non chaotic systems," Phys. D: Non. Phenom. **180**, 129-139 2002

[20] F. Cecconi, M. Cencini, M. Falcioni and A. Vulpiani, "Brownian motion and diffusion: From stochastic process to chaos and beyond," Chaos **15**, 026102/1-9 (2005).

[21] M. Cencini, M. Falcioni, E. Olbrich, H. Kantz, and A. Vulpiani, "Chaos or noise: Difficulties of a distinction," Phys. Rev. E **62**, 427-437 (2000).

[22] S. Chapman and T Cowling *The mathematical theory of non-uniform gases: an account of the kinetic theory of viscosity, thermal conduction and diffusion in gases* (Cambridge Universty Press., 1970).

[23] T. Cheon and Thomas Cohen, "Quantum level statistics of pseudointegrable billiards." Phys. Rev. Lett. **62**, 2769-2772 (1989).

[24] E.D.G Cohen and L. Rondoni, "Note on phase space contraction and entropy production in thermostatted Hamiltonian systems," Chaos **8**, 357-365 (1998).

[25] E.D.G Cohen and L. Rondoni, "Particles maps and irreversible thermodynamics," Physica A **306**, 117-128 (2002).

[26] I.P. Cornfeild, S.V. Formin and Ya. G. Sinai, *Ergodic Theory* (Springer, New York, 1982).

[27] R. Creswick, H. Farach, and C. Poole, *Introduction to Renormalization Group Methods in Physics* (John Wiley & Sons, 1991)

[28] S. Denisov, J. Klafter and M. Urbakh, "Dynamical heat channels," Phys. Rev. Lett. 91, 194301/1-4 (2003).

[29] C.P. Dettmann and E.D.G. Cohen and H. van Bejheren. "Microscopic chaos from Brownian motion." Nature **401**, 875-875 (1999).

[30] C.P. Dettmann and E.D.G. Cohen, "Microscopic Chaos and Diffusion," Journal of Statistical Physics **101**,775-817, 2000.

[31] R.L. Devaney, *An introduction to chaotic dynamical systems* (Addison-Wesley, Reading, second edition, 1989).

[32] J.R. Dorfman *An Introduction to Chaos in Non equilibrium Statistical Mechanics* (Cambridge University Press, 1999).

[33] J.R. Dorfman, P. Gaspard, and T. Gilbert, "Entropy production of diffusion in spatially periodic deterministic systems," Phys. Rev. E **66** (2002).

[34] D. Durr and H. Spohn, "Brownian motion and microscopic chaos," Nature **394**, 831-833 (1998).

[35] J.P. Eckmann and L.-S. Young, "Temperature profile in Hamiltonian heat conduction," Europhys. Lett. **68**, 790-796 (2004).

[36] J.P. Eckmann, C. Meija-Monasterio and E. Zabey, "Memory effects in nonequilibrium transport for deterministic Hamiltonian systems," J. Stat. Phys **123**, 1339-1360 (2006).

[37] J.P. Eckmann and L.-S. Young, "Nonequilibrium energy profiles for a class of 1-D models," Comm. Math. Phys. **262** 237-267 (2006).

[38] P. Ehrenfest and T. Ehrenfest, *The conceptual foundations of statistical approach in mechanics* (Cornell Univ. Press, Ithaca, 1959).

[39] S. Galatolo, "Complexity, initial condition sensitivity, dimension and weak chaos in dynamical systems," Nonlinearity **16**, 1219-1238 (2003).

[40] G. Gallavotti and E.D.G. Cohen, "Dynamical Ensembles in Nonequilibrium Statistical Mechanics," Phys. Rev. Lett **74**,2694-2697 (1995).

[41] P. Gaspard and X.-J. Wang, "Sporadicity: Between periodic and chaotic dynamical behaviors," Proc. Nat. Acad. Sci. USA **85**, 4591-4595 (1988).

[42] P. Gaspard, "What is the role of chaotic scattering in irreversible processes ?," Chaos **3**,427-442 (1993).

[43] P. Gaspard, *Chaos, Scattering and Statistical Mechanics* (Cambridge University Press., 1998).

[44] P. Gaspard, M.E. Briggs, M.K. Fancis, J.V. Senger, R.W. Gammons, J.R. Dorfman and R.V. Calabrese, "Experimental evidence for microscopic chaos," Nature **394**, 865 (1998).

[45] P. Gaspard, I. Claus, I., T. Gilbert and J.R. Dorfman, "Fractality of Hydrodynamics Modes of Diffusion," Physical Review Letters **86** 1506-1509 (2001).

[46] P. Gaspard, "Dynamical Theory of Relaxation in classical and quantum systems," in: *Dynamics of dissipation*, p. 111-163, Springer Berlin (2002).

[47] P. Gaspard, G. Nicolis, and J.R. Dorfman, "Diffusive Lorentz gases and multi baker maps are compatible with irreversible thermodynamics," Physica A **323**, 294-322 (2003).

[48] E. Glasner and B. Weiss, "Sensitive dependence on initial conditions," Nonlinearity **6**, 1067-1075 (1993).

[49] T. Gilbert C.D. Ferguson and J.R. Dorfman, "Field driven thermostated systems: A nonlinear multibaker map." Phys. Rev. E **59** 364-371 (1999).

[50] T. Gilbert and J.R. Dorfman, "Entropy production in a persistent random walk." Physica A **282**, 427-449 (2000)

[51] T. Gilbert, J.R. Dorfman and P. Gaspard, "Entropy production, fractals and relaxation to equilibrium." Phys. Rev. Lett **85** 1606-1609 (2000).

[52] T. Gilbert, J.R. Dorfman and P. Gaspard, "Fractal dimensions of hydrodynamics modes of diffusion." Nonlinearity **14**, 339-358 (2001).

[53] G.A Gottwald and I. Melbourne, "A new test for chaos in deterministic systems," Proc. Roy. Soc. London **460** , 603-611 (2004).

[54] G.A. Gottwald and I. Melbourne, "Testing for chaos in deterministic system with noise," Physica D **212**, 100-110 (2005).

[55] P. Grassberger and T. Schreiber, "Microscopic chaos from Brownian motion?," Nature **401**, 875-876 (1999).

146

[56] E. Gutkin, "Billiards in polygons: Survey of recent results," J. Stat. Phys. **83** 7-26 (1996).

[57] J.H. Hannay and R.J. McCraw, "Barrier billiards: simple pseudo-integrable system," J. Phys. A: Math. Gen **23**, 887-900 (1990).

[58] E.H. Hauge and E.G.D. Cohen, "Normal and abnormal diffusion in Ehrenfest's wind-tree model," Phys. Lett. A **25** 78-79 (1967).

[59] O.G. Jepps and L. Rondoni, "Thermodynamics and complexity of simple transport phenomena," J. Phys. A: Math. Gen. **39**, 1311-1338 (2006).

[60] R. Klages, *Microscopic Chaos, Fractals and Transport in Nonequilibrium Statistical Mechanics* (World Scientific Publishing, 2007).

[61] V. Kokshenev, "On Chaotic Dynamics in Rational Polygonal Billiards," arXiv:math-ph/0511076v1

[62] S. Kolyada and L'Ubomir Snoha, "Some aspects of topological transitivity a survey," Grazer Mathematische Berichte **334**, 3-35 (1997).

[63] N. Korabel, "Deterministic Transport: From normal to anomalous diffusion," PhD thesis Technische Universitat Dresden, 2004.

[64] H. Larralde, F. Leyvraz and C. Mejia-Monasterio, "Transport properties of a modified Lorentz gas," J. Stat. Phys. **113** 197-231 (2003).

[65] J. Lebowitz, and Spohn, "Transport properties of the Lorentz gas: Fouriers law," J. Stat. Phys. **19** 633-654 (1978).

[66] S. Lepri, L. Rondoni, and G. Benettin. "The Gallavotti-Cohen Fluctuation Theorem for a Nonchaotic Model" J. Stat. Phys. **99**, 857-872 (2000).

[67] B. Li, L. Wang, and B. Hu, "Finite thermal conductivity in 1d models having zero Lyapunov exponent," Phys. Rev. Lett. **88**, 223901/1-4 (2002).

[68] B. Li, G. Casati and J. Wang, "Heat conductivity in linear mixing systems," Phys. Rev. E **67**, 021204/1-4 (2003).

[69] B. Li and J. Wang, "Anomalous heat conduction and anomalous diffusion in one-dimensional systems," Phys. Rev. Lett. **91**, 044301/1-4 (2003).

[70] B. Li, J. Wang, L. Wang, and G. Zhang, "Anomalous heat conduction and anomalous diffusion in nonlinear lattices, single walled nanotubes, and billiard gas channels," Chaos **15**, 015121/1-13 (2005).

[71] H.A. Lorentz, "The motion of electrons in metallic bodies." Proc. Roy. Acad. Amst. **7**, 438-453 (1905).

[72] C. Mejia-Monasterio, H. Larralde and F. Leyvraz, "Coupled normal heat and matter transport in a simple model system," Phys. Rev. Lett. **86**, 5417-5420 (2001).

[73] R. Metzler and I.M. Sokolov, "Comment on 'Anomalous heat conduction and and anomalous diffusion in one-dimensional systems,'" Phys. Rev. Lett. **92**, 089401/1 (2004).

[74] B. Moran, W. Hoover, and S. Bestiale, "Diffusion in a Periodic Lorentz Gas," J. Stat. Phys. **48** 709-726 (1987).

[75] G. Morriss and L. Rondoni, "Periodic Orbit Expansions for the Lorentz Gas," J. Stat. Phys. **75**, 553-584 (1994).

[76] E. Ott, *Chaos in Dynamical Systems* (Cambridge Press, 1994).

[77] J.B. Perrin, "Movement brownien et realite moleculaire," Ann. Chim. Phys. **19**, 5-104 (1909).

[78] T. Prosen and D.K, Campbell, "Normal and anomalous heat transport in one-dimensional lattices," Chaos **15**, 015117/1-17 (2005).

[79] K. Rateitschak, R. Klages and G. Nicolis, "Thermostatting by deterministic scattering: The periodic Lorentz gas," J. Stat. Phys. **99**, 1339-1364 (2000).

[80] P.J. Richens and M.V. Berry, "Pseudointegrable systems in classical and quantum mechanics," Physica D **2**, 495-512 (1981).

[81] L. Reichl, *A Modern Course in Statistical Physics* (Wiley Interscience, 1998).

[82] C. Robinson, *Dynamical Systems* (CRC Press, London, 1995).

[83] L. Rondoni and E.G.D. Cohen, "Gibbs entropy and irreversible thermodynamics," Nonlinearity **13**, 1905-1924 (2000).

[84] L. Rondoni, T. Tel and J. Vollmer, "Fluctuation theorems for entropy production in open systems," Phys. Rev. E **61**, R4679-R4682 (2000).

[85] S. Russ, S. Zschiegner, A. Bunde and J. Krger, "Lambert diffusion in porous media in the Knudsen regime: Equivalence of self-diffusion and transport diffusion," Phys. Rev. E **72**, 030101(R)/1-4 (2005).

[86] D. Sanders, and H. Larralde, "Occurrence of Normal and Anomalous diffusion in Polygonal billiard channels," Phys. Rev. E **73** 026205 (2006).

[87] M. Schmiedeberg and H. Stark, "Superdiffusion in a honeycomb billiard," Phys. Rev. E. **73** 031113 (2006).

[88] M.F. Shlesinger, G.M. Zaslavsky and J. Klafter, "Strange kinetics," Nature **363**, 31-37 (1993).

[89] S. Tabachnikov, *Billiards and geometry*, volume 30 of Student Mathematical Library (American Mathematical Society, Providence, 2005).

[90] S. Tasaki and P. Gaspard, "Fractal distribution and Ficks law in a reversible chaotic system." in M. Yamaguti Eds., *Towards the Hastening of Chaos*, 273-288 (Elsevier, Amsterdam, 1994)

[91] S. Tasaki and P. Gasspard, "Ficks law and fractality of nonequilibrium stationary states in a reversible multibaker map." J. Stat. Phys. **81**, 935-987 (1995).

[92] T. Tel, J. Volmmer and L. Matyas, "Comments on the paper 'Particles, maps, and irreversible thermodynamics'" by E.G.D. Cohen and L. Rondoni, Physica A **306** (2002) 117," Physica A **323**, 323-326 (2002).

[93] C. Tricot, *Curves and Fractal Dimension* (Springer, 1994).

[94] H. van Beijeren, "Generalized dynamical entropies in weakly chaotic system," Physica D **193**, 90-95 (2004).

[95] F. Vivaldi and J.H. Lowenstein, "Arithmetical properties of a family of irrational piecewise rotations," J. Phys. A: Mat. Gen. **19**, 1069-1097 (2006).

[96] J. Vega, T. Uzer, and J. Ford, "Chaotic billiards with neutral boundaries," Physical Review E **48** (1993).

[97] William M. Visscher, "Transport process in solids and linear response theory," Phys. Rev. A **10** 2461-2472 (1974).

[98] J. Vollmer, "Chaos, spatial extension, transport, and non-equilibrium thermo-dynamics," Phys. Rep. **372** 131-267 (2002).

[99] B. West, M. Bologna, and P. Grigolini, *Physics of Fractal Operators* (Springer, 2003).

[100] J. Wiersig, "Hexagonal dielectric resonators and microcrystal lasers," Phys. Rev. A **67**, 023807/1-12 (2003).

[101] G.M. Zaslavsky and M. Eldelman, "Weak mixing and anomalous kinetics along filamented surfaces," Chaos **11**, 295-305 (2001).

[102] G.M. Zaslavsky and D.A. Usikov, *"Weak chaos and quasi-regular patterns"*, *Cambridge Nonlinear Science Series* (Cambridge University Press, Cambridge, 2001).

[103] G.M. Zaslavsky, "Chaos, Fractional Kinetics, and Anomalous Transport," Physics Reports **371**, 461-580 (2002).

[104] G.M. Zaslavsky and M. Edelman, "Pseudochaos," in E. Kaplan and J.E. Marsden, Eds., *Perspective and problems in nonlinear science*, pages 431-443, Springer, New York (2003).

[105] G.M. Zaslavsky, B.A. Carreras, V.E. Lynch, L. Garcia and M. Eldelman, "Topological instability along invariant surfaces and pseudochaotic transport," Phys. Rev. E **72**, 026227/1-11 (2005).

[106] G.M. Zaslavsky, *Hamiltonian Chaos and Fractional Dynamics* (Oxford University Press, 2005).

[107] G.M. Zaslavsky, *The physics of chaos in Hamiltonian systems* (Imperial College Press, 2007).

[108] G. Zumofen and J. Klafter, "Comment on 'Self-similarity and transport in the standard map,'" Phys. Rev. E **59**, 3756-3760 (1999).

[109] R. Zwanzig, "From classical dynamics to continuous time random walk," J. Stat. Phys. **30**, 255-262 (1983).